Energy & Environmental Science

ROYAL SOCIETY OF CHEMISTRY

REVIEW

View Article Online
View Journal

Cite this: DOI: 10.1039/d2ee01590k

Human body IoT systems based on the triboelectrification effect: energy harvesting, sensing, interfacing and communication

Qin Zhang,[a] Chuanfu Xin,[a] Fan Shen,[a] Ying Gong,[a] YunLong Zi,[b] Hengyu Guo,[c] Zhongjie Li,†*[ade] Yan Peng,†*[ad] Quan Zhang†*[ade] and Zhong Lin Wang †*[f]

In recent years, the internet of things (IoT) has been progressing rapidly with the integration of technologies in various fields. At this stage, triboelectric nanogenerator (TENG) technology based on the triboelectrification effect and electrostatic induction has revealed great potential in various fields, including energy harvesting and sensing. Due to the improvements of configurations and materials, TENGs offer flexibility, compatibility, and stability, enabling novel auxiliary applications by harvesting and converting human mechanical energy. In this review, we first propose a concept of the TENG-based human body IoT system, consisting of energy harvesting, sensing, and interfacing, to effectively obtain, monitor and manage human motion and physical status information. Then, we present a comprehensive overview of such an IoT system from the three aforementioned focuses. Firstly, studies on human body energy harvesting are categorized according to the configurations and materials of TENGs. Secondly, based on the high sensitivity of TENGs, wearable and implantable sensors are investigated to develop the potential of human motion or physiological signal monitoring. Thirdly, the representative studies on TENG-based interfacing between human body and external electronics by using a microcontroller (MCU) are investigated based on various interactive types. Furthermore, we statistically discuss the developmental trend of TENGs in the above focused fields, and the materials suitable for TENGs to offer inspirational angles for future research. We also elaborate the proposed TENG-based human body IoT system by introducing various integrated modules with multi-functions. Finally, we systematically present promising prospects for future research directions and challenges from the perspectives of materials, power management, and communication. This review is dedicated to offering critical insights into the development of TENG-based human body IoT systems.

Received 17th May 2022,
Accepted 14th July 2022

DOI: 10.1039/d2ee01590k

rsc.li/ees

Broader context

Triboelectric nanogenerators (TENGs) have demonstrated the capability of converting diverse types of mechanical energy into electrical energy, featured with the advantages of simple fabrication, lightweight, low cost, and high conversion efficiency. Recent years have witnessed the prosperous development of TENGs, which have been widely distributed in various fields, such as energy harvesting, sensing, and interaction. Yet, a comprehensive system consisting of the aforementioned advantages and multi-functions has not been discussed so far. Herein, a concept of the human body IoT system is first proposed with technologies of TENGs, biosensing, data acquisition, and wireless communication. Such an IoT system, consisting of a self-powered data acquisition module, a data processing center, and user terminals, can be employed to systematically monitor and manage human body status information. It also offers promising insights towards the development of smart health management and healthcare systems.

[a] School of Mechatronic Engineering and Automation, Shanghai University, Shanghai, 200444, China. E-mail: lizhongjie@shu.edu.cn, pengyan@shu.edu.cn, lincolnquan@shu.edu.cn
[b] Thrust of Sustainable Energy and Environment, The Hong Kong University of Science and Technology (Guangzhou), Nansha, Guangzhou, Guangdong, 511400, China
[c] Department of Applied Physics, Chongqing University, Chongqing, 400044, China
[d] School of Artificial Intelligence, Shanghai University, Shanghai, 200444, China
[e] Engineering Research Center of Unmanned Intelligent Marine Equipment, Shanghai University, Shanghai, 200444, China
[f] Beijing Institute of Nanoenergy and Nanosystems, Chinese Academy of Sciences, Beijing, 100083, China. E-mail: zlwang@gatech.edu
† These authors contributed equally to this work and should be considered co-corresponding authors.

1. Introduction

As the world is marching into the era of 5G telecommunication technology, studies in various fields have tended toward the integration of big data, cloud computing, artificial intelligence (AI) and the internet of things (IoT).[1] The combination of these technologies has completely enhanced productivity and changed lifestyles. The concept of the IoT is defined as the internet-connecting things or people *via* multi-functional nodes, so that real-world objects possess communicative and analytic capability to collect information from themselves or their surroundings by using smart devices.[2] This concept has been extended to all aspects of various fields, including transportation, industrial manufacturing, social services, smart city or smart home, as well as mobile and electronic devices.[3–5] It is predicted that 75.44 billion IoT devices will be connected to the Internet by 2025.[6]

A simple IoT system mainly consists of power supply units, sensor units, signal processing units, and a data transmission system.[7] Such systems are widely distributed in various fields, including the monitoring of ocean and forest fire. A battery, as one of the typical power supply units, requires frequent replacement and presents a high replacement cost. Moreover, batteries featured with a limited lifespan cannot provide a reliable and sustainable power energy, which is the major factor restricting their future potential applications.[8–10] Due to the recent progress in low-power technology, the power consumption of microelectronic devices has come to the level of micro-/nanowatts. Meanwhile, portable wireless electronics are undergoing explosive advancement, with the total number increasing tremendously and power consumption decreasing significantly.[11] Converting various energy, such as solar,[12] wind,[13] electromagnetic,[14–16] and mechanical[17–19] energy, into electricity is a practical strategy. Among these energy sources, the mechanical energy generated by human motion displays distinct advantages of high density, wide distribution, and convenient acquisition, which makes it a premier choice for portable energy supply units.[20,21] However, significant dissipation of mechanical energy often occurs in human daily life. Different types of energy transducing mechanisms and energy harvesters have been developed to scavenge the dissipated energy.[22–25] Moreover, the energy supply units should possess the characteristics of portability, sustainability, miniaturization, wearability, or even implantability.[26–28]

The triboelectrification effect (TE), as one of the major energy transducing mechanisms, was first utilized to construct triboelectric nanogenerators (TENGs) in 2012 by Prof. Wang and his team.[29] The working principles of TENGs are the TE effect and electrostatic induction, through which certain materials become electrically charged after contact or rubbing against a different material. Such principles have been extensively explored for mechanical energy harvesting with the advantages of versatile operation modes, broad material availability, simple fabrication, and low cost.[30,31] Replacing batteries as the power source, TENGs have been widely applied to harvest human motion energy for low-power electronics.[32–36] Furthermore, owing to the high stability and sensitivity, TENGs have been employed as self-powered sensors for real-time monitoring of human motion and physiological signals such as walking and running,[37,38] finger touch,[39,40] joint movement,[41–44] heart rate,[45,46] and breathing.[45,47] Meanwhile, TENGs with such excellent capabilities have also been employed as tools for interfacing between human body and external electronics.[48]

In this review, we first propose a concept of the human body IoT system based on the technologies of TENGs, biosensing, data acquisition, and wireless communication. Compared with the traditional IoT system, the TENG-based human body IoT system, which is mediated by the human body, can efficiently monitor and manage the human motion and health status without external power supply. (i) The energy harvesting module based on TENGs in the human body IoT system enables the low-power sensors to work powered by electricity converted from human motions, while the traditional IoT system is mostly powered by electrochemical batteries or the national grid. (ii) TENG-based sensors in the human body IoT system display the advantages of light weight, low cost, and high sensitivity, while the traditional IoT system usually consists of stiff sensors with significant weight and relatively low wearability. (iii) The TENG-based human–machine interface in the human body IoT system can exhibit higher reliability and faster response due to its high performance synthetic materials, than that of the interaction in the traditional IoT system. By integrating various TENG-based sensors for monitoring human body motion and health status, it will promote the intellectualization and integration of human medical health. Fig. 1 shows an extension from a simple IoT system to a TENG-based human body IoT system. Meanwhile, we present a comprehensive overview of the proposed IoT system, which is powered or sensed by TENG technology and mainly includes energy harvesting,[49–51] sensing,[52–54] interfacing,[55] and communication. Starting with the brief concept of human body IoT systems and the working principle of TENGs, the detailed studies related to TENG-based human body IoT systems are introduced. We mainly focus on three aspects. Firstly, the TENG, through harvesting human energy, is implemented as the power source for low-power electronic devices. Secondly, the TENG functions as a sensor for monitoring human body status, including motion and physiological activities. Thirdly, the TENG is utilized as the key technology for electronics to interact with external objects. Moreover, we statistically discuss the output of recent papers on TENGs and the materials suitable for TENGs in the above research points to observe the development trends. We also elaborate the proposed TENG-based human body IoT system by introducing various integrated modules with multi-functions. Finally, we present promising prospects for future research directions and challenges on focused aspects, such as properties of materials for different research areas, TENG packaging, power management and energy storage, communication and networking, AI technology, as well as fundamental theory of TENGs.

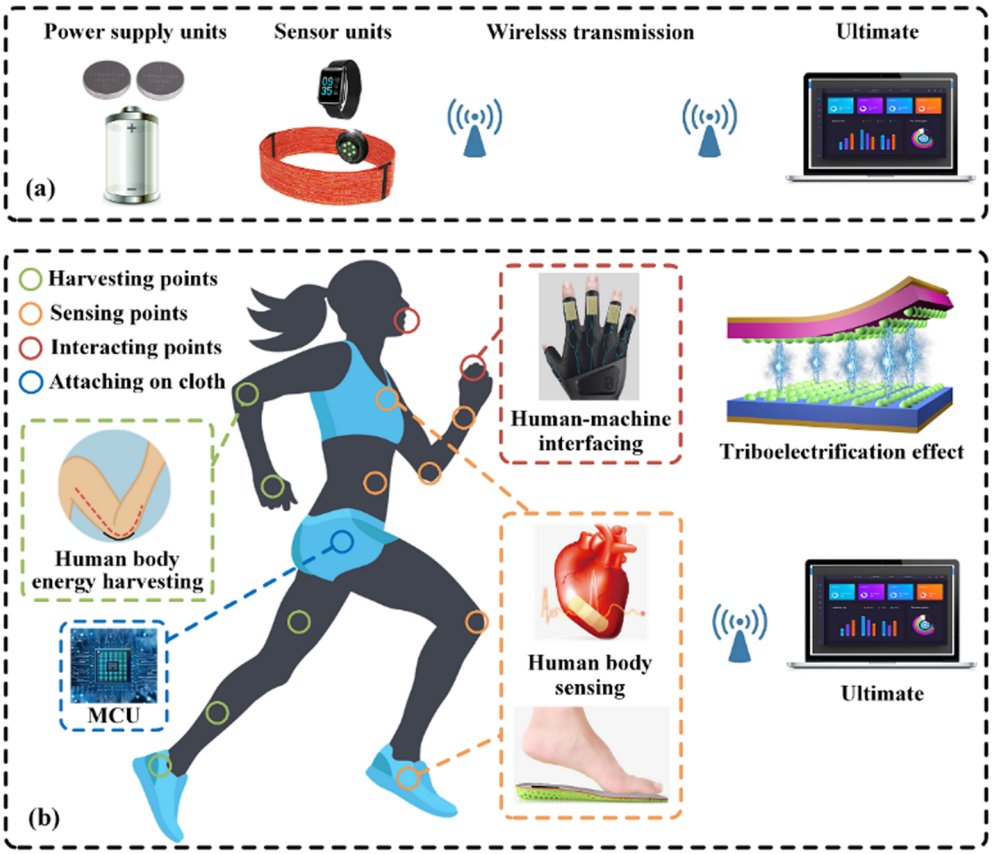

Fig. 1 Schematic illustrations of (a) a simple IoT system composition and (b) a human body IoT system based on the triboelectrification effect.

2. Fundamental theory and mechanism

2.1 Triboelectrification effect

The triboelectrification effect, as a basic effect of electricity, is usually elaborated as a phenomenon whereby two different materials can be electrically charged when they are brought into contact and separated (Fig. 2a).[56] The understanding of its mechanism has been controversial and requires further studies. Recently, Prof. Wang proposed an electron-cloud overlap model,[56] which could explain the TE effect occurring in solid–solid and liquid–solid interfaces generally. The TE effect, which commonly creates electric fires and discharge, and leads to energy dissipation in our daily life, has always been deemed as a negative effect.[57] With the invention of Kelvin probe force microscopy (a tool for detection of nano TE), the positive effect of TE was gradually developed and utilized, such as TENGs.[58,59] Using the electrostatic charges created on the surfaces of two different materials brought in contact, separation of the two surfaces under an external force promotes the contact-induced triboelectric charges to generate a potential drop, which can drive electrons to flow between the two electrodes fabricated on the top and bottom surfaces of the two materials.[60] Accordingly, the four basic modes of TENGs (vertical contact–separation mode,[61,62] contact-sliding mode,[63,64] single-electrode mode,[65,66] and free-standing mode[67,68]) are developed as illustrated in Fig. 2c.

2.2 Maxwell's displacement current

Maxwell's equations,[69] as some of the top 10 equations in physics, have presented huge significance in modern fundamental science and technologies. The specific expressions are as follows:

$$\nabla \cdot \boldsymbol{D} = \rho_f \quad \text{(Gauss's law)} \tag{1}$$

$$\nabla \cdot \boldsymbol{B} = 0 \quad \text{(Gauss's law for magnetism)} \tag{2}$$

$$\nabla \times \boldsymbol{E} = \frac{\partial \boldsymbol{B}}{\partial t} \quad \text{(Faraday's law)} \tag{3}$$

$$\nabla \times \boldsymbol{H} = \boldsymbol{J}_f + \frac{\partial \boldsymbol{D}}{\partial t} \quad \text{(Maxwell} - \text{Ampere's law)} \tag{4}$$

where $\boldsymbol{E}$ denotes the electric field, $\boldsymbol{B}$ denotes the magnetic field, $\boldsymbol{H}$ denotes the magnetizing field, ρ_f denotes the free electric charge density, $\boldsymbol{J}_f$ denotes the free electric current density, and $\boldsymbol{D}$ denotes the displacement field.

In addition, the relationship between $\boldsymbol{D}$ and $\boldsymbol{P}$ is expressed as

$$\boldsymbol{D} = \varepsilon_0 \boldsymbol{E} + \boldsymbol{P} \tag{5}$$

where $\boldsymbol{P}$ denotes the polarization field and ε_0 denotes the permittivity in vacuum. For isotropic media, eqn (5) is defined as

$$\boldsymbol{D} = \varepsilon \boldsymbol{E} \tag{6}$$

where ε denotes the permittivity of the dielectrics.

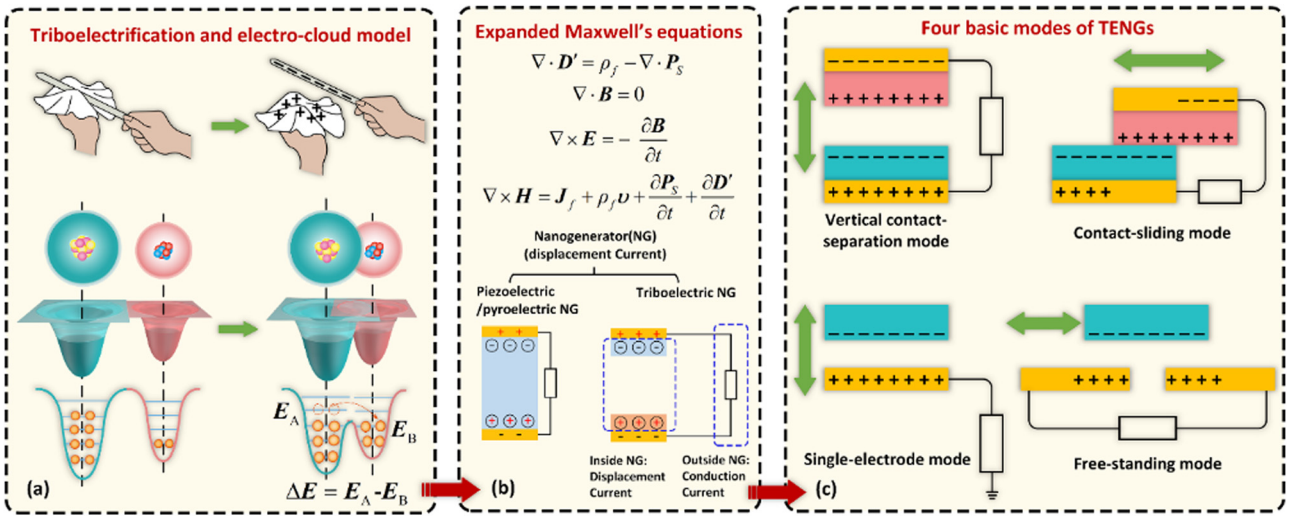

Fig. 2 Triboelectrification effect and its extension. (a) Triboelectrification and the atomic potential energy model and electronic states. $\Delta \boldsymbol{E}$ is the potential barrier between the two atoms. $\boldsymbol{E}_A$ and $\boldsymbol{E}_B$ are the two atoms belonging to two materials A and B, respectively. (b) The expanded Maxwell's equations, and the mechanism of NGs. (c) Four basic modes of TENGs.

The second term in eqn (4) is the Maxwell's displacement current, which is defined as

$$\boldsymbol{J}_D = \frac{\partial \boldsymbol{D}}{\partial t} = \varepsilon_0 \frac{\partial \boldsymbol{E}}{\partial t} + \frac{\partial \boldsymbol{P}}{\partial t} \tag{7}$$

The second term in eqn (7) has been demonstrated to be related to the outputs of TENGs in 2017 by Prof Wang.[60] Furthermore, Wang has derived the expanded Maxwell's equations, which can be employed to explain the general theory of TENGs.[70] The specific expression is as follows:

$$\nabla \cdot \boldsymbol{D}' = \rho_f - \nabla \cdot \boldsymbol{P}_S \tag{8}$$

$$\nabla \cdot \boldsymbol{B} = 0 \tag{9}$$

$$\nabla \times \boldsymbol{E} = -\frac{\partial \boldsymbol{B}}{\partial t} \tag{10}$$

$$\nabla \times \boldsymbol{H} = \boldsymbol{J}_f + \frac{\partial \boldsymbol{D}'}{\partial t} + \frac{\partial \boldsymbol{P}_S}{\partial t} \tag{11}$$

where $\boldsymbol{D} = \boldsymbol{D}' + \boldsymbol{P}_S = \varepsilon_0 \boldsymbol{E} + \boldsymbol{P} + \boldsymbol{P}_S$, with the term $\boldsymbol{P}_S$ denoting the mechano-driving created polarization owing to the relative movement of the charged media surfaces by mechanical triggering,[56] which is different from the electric field induced medium polarization $\boldsymbol{P}$. Such charges on the surfaces are created from physical contact among the moving media due to the TE effect.

Moreover, for a mechano-driven, shape-deformable, charged-media system,[71] slowly moving at an arbitrary velocity field $\boldsymbol{\nu}(\boldsymbol{r}, t)$, eqn (8)–(11) can be expressed as

$$\nabla \cdot \boldsymbol{D}'(\boldsymbol{r}, t) = \rho_f(\boldsymbol{r}, t) - \nabla \cdot \boldsymbol{P}_S(\boldsymbol{r}, t) \tag{12}$$

$$\nabla \cdot \boldsymbol{B}(\boldsymbol{r}, \boldsymbol{t}) = 0 \tag{13}$$

$$\nabla \times (\boldsymbol{E}(\boldsymbol{r}, t) - \nu(\boldsymbol{r}, t) \times \boldsymbol{B}(\boldsymbol{r}, t)) = -\frac{\partial}{\partial t} \boldsymbol{B}(\boldsymbol{r}, t) \tag{14}$$

$$\begin{aligned} &\nabla \times [\boldsymbol{H}(\boldsymbol{r}, t) + \nu(\boldsymbol{r}, t) \times (\boldsymbol{D}'(\boldsymbol{r}, t) + \boldsymbol{P}_S(\boldsymbol{r}, t))] \\ &= \boldsymbol{J}_f(\boldsymbol{r}, t) + \rho_f(\boldsymbol{r}, t) \nu(\boldsymbol{r}, t) + \frac{\partial}{\partial t} [\boldsymbol{D}'(\boldsymbol{r}, t) + \boldsymbol{P}_S(\boldsymbol{r}, t)] \end{aligned} \tag{15}$$

where all the quantities in eqn (12)–(15) are a function of $(\boldsymbol{r}, t)$ in the Lab frame. The term $\nu \times \boldsymbol{B}$ in eqn (14) is the contribution of the Lorentz force to the local electric field. The term $\nu \times (\boldsymbol{D}' + \boldsymbol{P}_S)$ in eqn (15) is the local induced electric current due to the movement of medium to the local electric field.

Summarily, mechanical energy can be converted into electricity by employing the displacement current generated from such external force *via* the triboelectrification effect as the driving force, which is also referred to as the fundamental theory of TENGs.[72]

3. Harvesting human mechanical energy with TENGs for power supply

As power generators, TENGs can serve as highly customizable, flexible, and low-cost power sources for wearable devices.[73] Humans' adaptable and complex daily activities such as joint motion, hand motion, walking, and running can generate large amounts of mechanical energy. By converting these energies, milliwatts of power can be obtained to supply power for portable low-power electronics. Traditional wearable electronics are powered by batteries with regular power replenishment or replacement. Hence, cost-effective TENGs, which possess unique advantages for harvesting the waste energy efficiently, have been proved as a reliable and stable energy harvester for powering next-generation wearable IoT devices.[74,75] However, the challenges in exploring triboelectric materials with low cost and high performance still exist and have aroused the interests

of many researchers.[76,77] Furthermore, various approaches, such as energy extraction enhancement circuit,[78] have been reported to significantly enhance the energy conversion efficiency.[79–82] In 2019, Lee *et al.* reported an overview of harvesting mechanical energy *via* TENG technology, which focused on the surface modification methods beyond the limitations of structural parameters and materials.[83] A more recent overview of studies related to human mechanical energy harvesting is illustrated in this section from the angles of more sophisticated configuration design, and material synthesis and interface processing for performance enhancement of TENGs.

3.1 Configurations

Based on the principle of the triboelectrification effect, researchers have designed many intriguing configurations for mechanical energy harvesting from different human body parts, such as fold,[84] nanowire,[85,86] ball,[87] sandwich,[88] origami,[89] honeycomb,[90] and woven[91] configurations. The relevant representative work is illustrated in Fig. 3.

Researchers have proposed a few configurations to harvest subtle human mechanical energy for power supply of commonly used low-power electronics. Rana *et al.* designed a hybridized biomechanical nanogenerator (HBNG) combining an electromagnetic generator and a TENG.[85] The output performance of the TENG was enhanced by a PTFE film with a nanowire structure. The output power density reached 185 W m^{-2} at a frequency of 5 Hz. By harvesting the human mechanical energy, HBNG simultaneously supplied power for a Bluetooth mouse, a smart watch and other electronics for 3 minutes. Similarly, to harvest human-induced vibrations, Rahman *et al.* constructed a miniature TENG that adopted the nanowire and micro–nano hierarchical structure to further enhance the energy harvesting efficiency.[86] As shown in Fig. 3a, the proposed TENG was able to supply power for miniature low-power electronics such as smart watches and thermo-hygrometers by harvesting human mechanical energy. Ren *et al.* integrated a groove-shaped micro-structured haze thin film (GHF) into an autonomous single-electrode TENG (AS-TENG) to harvest human mechanical energy (Fig. 3b).[92] The GHF was employed as a triboelectric layer to enhance the surface charge density of the AS-TENG. The output voltage and current of AS-TENG exhibited 120 and 105% improvements, respectively.

Some different configurations were presented to harvest human mechanical energy from large amplitude human motion, such as walking. Jung *et al.* developed a hybrid organic photovoltaic cell TENG system consisting of a non-fullerene organic photovoltaic cell and a Cu ball.[87] The Cu ball-based TENG of the hybrid device was able to effectively harvest human mechanical energy through processive and regular contact–separation of the Cu balls during human motion. Tan *et al.* reported a fully energy-autonomous temperature-to-time converter (TTC) based on the TENG for biomedical applications.[93] The proposed TTC was attached to the arm to be driven by the low frequency (<1 Hz) of human arm motion. After the storage capacitor collected a voltage of 0.6 V, the low-power TTC, which performed one-shot conversion of temperature to pulse width, was activated by the power management unit. Yun *et al.* utilized a bi-directional gearbox to construct an exo-shoe TENG, which enhanced the energy conversion efficiency.[94] As shown in Fig. 3c, the key of the structure was converting the low frequency (1 Hz) walking into uni-directional rotation with a high speed of 700 rpm.

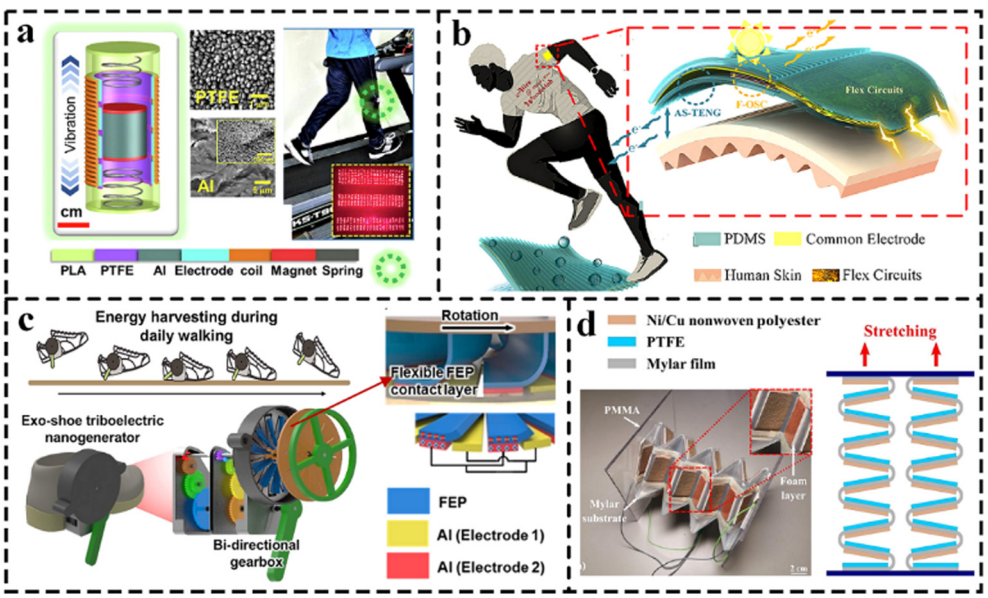

Fig. 3 Harvesting human mechanical energy with various configurations of TENGs. (a) Schematic illustration of the miniaturized TENG with micro–nano hierarchical configuration. Reproduced with permission from ref. 86, Copyright 2020, Elsevier. (b) Schematic illustration of the TENG based on a micro-nano haze film. Reproduced with permission from ref. 92, Copyright 2019, Elsevier. (c) Structural design of the exo-shoe TENG based on the sliding mode for high frequency stepping motion energy harvesting. Reproduced with permission from ref. 94, Copyright 2020, Elsevier. (d) Structural design of the Mylar-based TENG with a novel origami configuration. Reproduced with permission from ref. 89, Copyright 2021, Elsevier.

To further improve the human mechanical energy conversion efficiency, many other diverse novel configurations of TENGs were developed. Li *et al.* reported a sandwich-structured TENG (S-TENG) with silicone rubber and silver-coated glass microspheres.[88] The S-TENG with a high stretchability of 300% exhibited robustness when placed on various parts of the human body to harvest human motion energy. It yielded an open-circuit voltage (V_{oc}) of 370 V and a short-circuit current (I_{sc}) of 9.5 μA *via* optimized parameters. By contrast, based on an innovative origami structure, Zargari *et al.* firstly utilized a Mylar film to fabricate the origami TENG, which operated continuously without any external power sources (Fig. 3d).[89] Similarly, the honeycomb structure was extended and stacked along a certain direction in a limited space. Accordingly, Yang *et al.* proposed a honeycomb-shaped TENG (H-TENG) with high structural density and flexibility.[90] It generated an open-circuit voltage of 1500 V and a power density of 10.79 W m^{-2}. Furthermore, human walking motion powered an electronic watch and pedometer through the H-TENG. Considering the challenges of wearable TENGs from the aspects of flexibility, breathability and washability, Guan *et al.* designed a novel woven-structured TENG (WS-TENG) that generated an open-circuit voltage of 166 V, a short-circuit current of 8.5 μA, and a power density of 93 mW m^{-2}.[91] The high output of the WS-TENG made it suitable for driving portable and wearable electronics.

3.2 Material synthesis and interface processing

Considering the significance of materials in implementing the triboelectrification effect, many researchers attempted to conduct material synthesis and interface processing to improve the output performance of TENGs.[95,96] The related representative work is illustrated in Fig. 4.

Numerous novel composite materials for the triboelectric layers have been tested in TENGs for human mechanical energy harvesting. Chen *et al.* constructed a TENG with a chitosan-silk fibroin-airlaid paper composite film (CSA film).[97] The CSA-based dual-electrode TENG was able to efficiently harvest human motion energy due to the excellent electron donating ability of the CSA film. It was successfully applied to harvest energy from hand clapping and trampolining. Similarly, Kim *et al.* developed a TENG with outstanding electric performances, which was sufficient to illuminate 117 light-emitting diodes and drive several low-power electronics.[98] You *et al.* fabricated an organic semiconductor-based TENG by using poly(3,4-ethylene dioxythiophene):poly(styrene sulfonate) (PEDOT:PSS) as the triboelectric layer (Fig. 4a).[99] The proposed TENG achieved an open-circuit voltage of 1 V and a short-circuit current of 309 μA. Its internal resistance was measured to be 208 Ω, and the power density reached up to 11.67 mW m^{-2}. The charging ability of the fabricated TENG was experimentally tested for further potential applications. In addition, Zhang

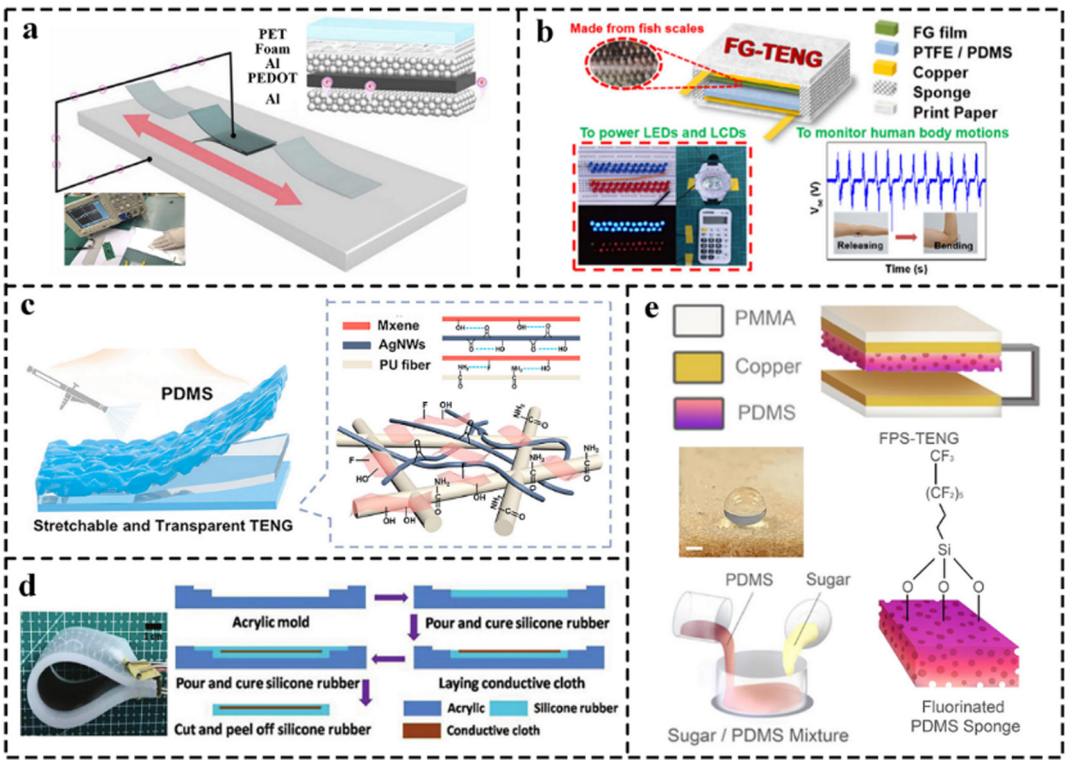

Fig. 4 Harvesting human mechanical energy based on TENGs with various materials. (a) Configuration of the semiconductor-based TENG. Reproduced with permission from ref. 99, Copyright 2021, Elsevier. (b) Schematic illustration of the eco-friendly TENG based on a fish gelatin film and a PTFE/PDMS composite film. Reproduced with permission from ref. 101, Copyright 2020, American Chemical Society. (c) Configuration of the MAMP electrode-based TENG. Reproduced with permission from ref. 102, Copyright 2020, Elsevier. (d) Configuration of the single-electrode TENG based on polyester conductive cloth. Reproduced with permission from ref. 104, Copyright 2021, The Royal Society of Chemistry. (e) Configuration and fabrication process of the humidity-resistant TENG based on a fluorinated polymer sponge. Reproduced with permission from ref. 105, Copyright 2021, Elsevier.

et al. reported a unique wearable TENG (W-TENG) which employed a PTFE film and cotton fabric as the materials of the triboelectric pair.[100] By converting the low-frequency human mechanical energy into electricity, the W-TENG generated an open-circuit voltage of 556 V, a short-circuit current of 26 μA, and a power density of 0.66 mW cm^{-2}. As shown in Fig. 4b, Han *et al.* designed a flexible and versatile TENG based on a fish gelatin film and a PTFE/PDMS composite film.[101] It exhibited high performance with an open circuit voltage of 130 V, a short circuit current of 0.35 μA, and a power density of 45.8 mW cm^{-2}, which was sufficient to activate 50 light-emitting diodes.

Additionally, various materials are available for fabrication of electrodes. Considering the stretchability of TENGs, Liu *et al.* utilized an Mxene–AgNWs–Mxene–polyurethane nanofiber (MAMP) electrode to construct a TENG (Fig. 4c).[102] It generated a voltage of 38 V and a current density of 1.67 mA m^{-2} only by tapping. Su *et al.* developed a simply structured wearable TENG which included a tribo-material of silk and an electrode material of carbon nanotubes.[103] By combining both materials in liquid phase bio-conductivity could be achieved. This specially designed TENG showed great potential to supply power for low-power devices by attaching it to a glove and harvesting the energy of various human movements. As depicted in Fig. 4d, Zhao *et al.* used polyester conductive cloth that was wrapped in a flexible elastomer to develop a flexible and extendable single-electrode TENG (S-TENG).[104] The 40 × 100 mm^2 S-TENG exhibited a high output performance with an open-circuit voltage and power density of up to 534 V and 230 mW m^{-2}, respectively. Moreover, the S-TENG was employed to drive various low-power electronics by converting mechanical energy from various human motions, including joint movement, walking and hand tapping.

The output performance of TENGs has been proved to decrease in humid environments. Therefore, it is essential to synthesize novel humidity-resistant materials to construct TENGs with stable performance in humidity. As shown in Fig. 4e, Peng *et al.* designed a novel TENG based on a fluorinated polymer sponge (FPS-TENG).[105] The voltage output of FPS-TENG was three times higher than that of the TENG based on a pristine polymer film. The FPS-TENG maintained almost 90% electrical output performance under 20–85% relative humidity, which made it a stable and viable power source for low-power devices in humid environments. Zheng *et al.* presented a multi-functional wheat starch TENG (S-TENG) through an eco-friendly method, which generated an open-circuit voltage of 151.4 V and a short-circuit current of 47.1 μA.[106] The proposed S-TENG was used to harvest mechanical energy from human motion, the performance of which was less affected in humidity than in dryness. To better harvest the mechanical energy of human motion, Mariello *et al.* developed a flexible TENG based on the combination of a polysiloxane elastomer and poly(*para*-xylylene) as a power source for low-power wearable electronics.[107] Particularly, the proposed TENG was composed of a PDMS substrate made *via* a steam-curing step. Then, a layer with metallized titanium and gold was deposited on the surface of PDMS. Finally, the metallized layer was covered with a film of parylene C as the friction layer. The inertness and barrier properties of the material made the device resistant to humidity.

Different from the traditional methods based on the modification of the interface, novel interface processing methods were proposed to increase the surface contact area for performance enhancement. Pyo *et al.* utilized a textile made of pile-embroidered fibres as one of the contact surfaces to develop a flexible wearable TENG.[108] The key point was to significantly promote the contact area through the deformability of the fibres originating from the suspended structure. The prepared TENG exhibited a high output power, which was 24 times higher than that of traditional TENGs. Liang *et al.* executed a specialized welding to ensure a AgNW electrode-based TENG with high conductivity.[109] Under a frequency of 2 Hz, the open-circuit voltage, short-circuit current and power density reached up to 66 V, 8.6 μA and 446 mW m^{-2}, respectively.

Summarily, large amounts of dissipated human mechanical energy can be harvested and converted into electricity for power supply of low-power electronics by TENGs. Moreover, the energy conversion efficiency is distinctly improved by designing innovative configurations and synthesizing various materials, which demonstrates the great potential of high-performance TENGs in harvesting human mechanical energy, as summarized in Table 1.

4. Sensing human motion and physiological activities based on TENGs

Decades of progress in the miniaturization of electronics and advances of materials are paving the way for the continuous development of wearable and implantable devices. Various miniature low-power sensing devices have been applied for the monitoring of human motion signals and health-related physiological signals.[110–114] Humans are experiencing greater and greater conveniences which are brought by diverse sensing devices, including smartwatches, glasses, shoes, gloves, pacemakers, and necklaces. Considering the advantages of TENGs with high sensitivity, flexibility, and stretchability, many researchers have developed diverse TENGs to construct sensors for supporting continuous monitoring of human motion and health.[115,116] Designing these kinds of sensors to function as wearable and implantable devices usually requires materials to be sensitive to human activities while maintaining the comfort of the user and meeting the requirements of biocompatibility. Consequently, material sensitivity is the main focus for device fabrication. This section summarizes the recent studies from the angles of sensing motion/physiological signals *via* TENG-based wearable/implantable sensors.

4.1 Sensing human motion signals *via* TENG-based wearable sensors

Detecting changes in the motion of different body parts is crucial for real-time monitoring of physical conditions, which

Table 1 Summary of human mechanical energy harvesters based on TENGs

Material	Configuration	V_{oc} (V)	I_{sc} (μA)	Power density	Excitation	Year	Ref.
PTFE, nylon, Al	Nanowire-like	215	25	185 W m^{-2}	5 Hz	2020	85
PTFE, Al	Nanograss-like	92.2	21	16.16 W m^{-3}	5 Hz	2020	86
Cu, PDMS	Double-layer	7	0.7	0.99 mW m^{-2}	Walking 4.0 m s^{-1}	2020	87
Silicone rubber, Ag	Sandwich	370	9.5	54.9 μW cm^{-2}	2.5 Hz	2021	88
Mylar film, Ni/Cu, PTFE	Origami	1050	131	—	Walking	2021	89
TPU, Al, PBAT film	Honeycomb	1500	183	10.79 W m^{-2}	Tapping	2021	90
P(VDF-TrFE), PA66, SSY	Textile	166	8.5	93 mW m^{-2}	3 Hz	2021	91
Ni-PFA, Ni	Sandwich	4	0.5	1 μW cm^{-2}	<1 Hz	2021	93
Sandpaper, carbon paper	Fold	330	18.6	32.2 mW m^{-2}	2.5 Hz	2018	95
Silicone rubber, nylon	Spiral winding	19	0.43	11 W m^{-3}	5 Hz	2018	96
CSA film, PTFE, Al	Sandwich	135	5	268.8 mW m^{-2}	3 Hz	2021	97
PI/PVDF-TrFE, PET, Al	Sandwich	364	17.2	2.56 W m^{-2}	2 Hz	2021	98
PTFE, cotton	Fold	556	26	0.66 mW cm^{-2}	10 Hz	2021	100
PTFE/PDMS, FG, Cu	Sandwich	130	0.35	45.8 μW cm^{-2}	4 Hz	2020	101
MAMP, PDMS	Sandwich	38	1.67	7.22 mW m^{-2}	Tapping	2020	102
CNT, PET, ITO	Arch-shape	262	8.73	2.86 W m^{-2}	Patting	2020	103
Silicone rubber, cloth	Sandwich	534	3.8	230 mW m^{-2}	3 Hz	2021	104
PDMS, PMMA, Cu	Sandwich	184	9.5	0.89 W m^{-2}	8 Hz	2021	105
PMMA, Al, starch, FEP	Sandwich	151.4	47.1	113.2 μW cm^{-2}	4 Hz	2022	106
PDMS, Au, parylene-C	Sandwich	1.6	0.15	2.24 mW m^{-2}	5 Hz	2020	107
Ni, pile	Deformable	113	0.17	2.44 mW m^{-2}	1 Hz	2020	108
AgNW, PDMS	Welded	66	8.6	446 mW m^{-2}	2 Hz	2019	109

can in turn be leveraged for self-assessments and interventions. Various wearable sensors have been widely applied in human body movement monitoring and play an increasingly significant role in daily life, especially for health training[117,118] and medical rehabilitation.[119,120] In these distinct applications, sensors equipped with the properties of flexibility, ductility, and shape-adaptability are essential to ensure device availability and reliability.[121–123] Meanwhile, the application of TENGs as human wearable sensors has made significant progress due to the availability of novel flexible, stretchable, durable, and waterproof materials.[124,125] As users pay more and more attention to physical movement, TENG-based wearable sensors, which can be attached to various human body parts, have been widely applied in monitoring physical motions, such as joint motions,[126,127] hand gestures,[116,128] and gaits.[129]

4.1.1 Joint motions. Bending and stretching are two of the most common activities of human extremities. Accordingly, many researchers focused on these biomechanical movements for monitoring joint motions *via* signal acquisition.[130,131] The relevant state-of-the-art work is illustrated in Fig. 5.

Researchers have developed various TENG-based sensors to sensitively obtain the bending angle of joint motions. Wen *et al.* coated a poly(3,4-ethylenedioxythiophene):poly(4-styrenesulfonate) (PEDOT:PSS) thin film onto the stretched PDMS plate to construct a novel TENG which exhibited high stretchability and transparency.[132] As shown in Fig. 5a, with the bending of the human elbow joint, the fabricated TENG recorded the bending angle and the motion frequency by analysing the peak value of voltage and counting the peak number. As shown in Fig. 5b, He *et al.* designed a novel strain/pressure sensor using a stretchable, soft, and compressible hydrogel based on a mix of silk fibroin, polyacrylamide, graphene oxide, and PEDOT:PSS.[133] It exhibited a wide sensing range with a strain of 2–600% and a pressure of 0.5–119.4 kPa. Particularly, the hydrogel-based sensor was non-allergenic on human skin and possessed superior biocompatibility, which made it suitable as a motion monitor for human physical activity such as joint bending. Huang *et al.* developed a TENG-based active pressure sensor with a premier exhibition of stability and sensitivity.[134] The biomass-based bacterial cellulose/chitosan (BC/CS) composites and PDMS/Cu film were used as positive and negative triboelectric layers, respectively. The proposed sensor with a sensitivity of 0.24 V kPa^{-1} in the range of 10.5–96.25 kPa was convenient for human joint motion detection through attaching it to the elbow, knee, wrist and other body parts.

Various materials and configurations were also proposed to effectively enhance the output performance of TENGs. As shown in Fig. 5c, Yang *et al.* employed azobisisobutyronitrile (AIBN) as a self-reactive agent to modify PDMS and form a self-assembled porous structure through the difference in temperature between PDMS pre-curing and AIBN decomposition.[135] The proposed TENG exhibited 2.5- and 2.7-fold enhancement in output voltage and current compared with that without modification respectively. It was also implemented as a sensor for monitoring the bending motion of joints. Researchers have focused on multifunctional ink-based patterned circuits for sensing in printed and flexible devices. As shown in Fig. 5d, Sun *et al.* presented a novel TENG-based sensor for human motion monitoring on fireground by employing designed patterned MXene ink electrodes printed directly onto the triboelectric materials.[136] A TENG with a rectangular electrode was attached to the elbow to sense the bending of the joint by sensing simple emergency hand signals. By using the double needle bed flat knitting machine technology, Chen *et al.* fabricated a 3D double faced interlock fabric TENG that was implemented as a stretchable wearable TENG-based sensor to monitor the bending of the arm joint (Fig. 5e).[137] This novel,

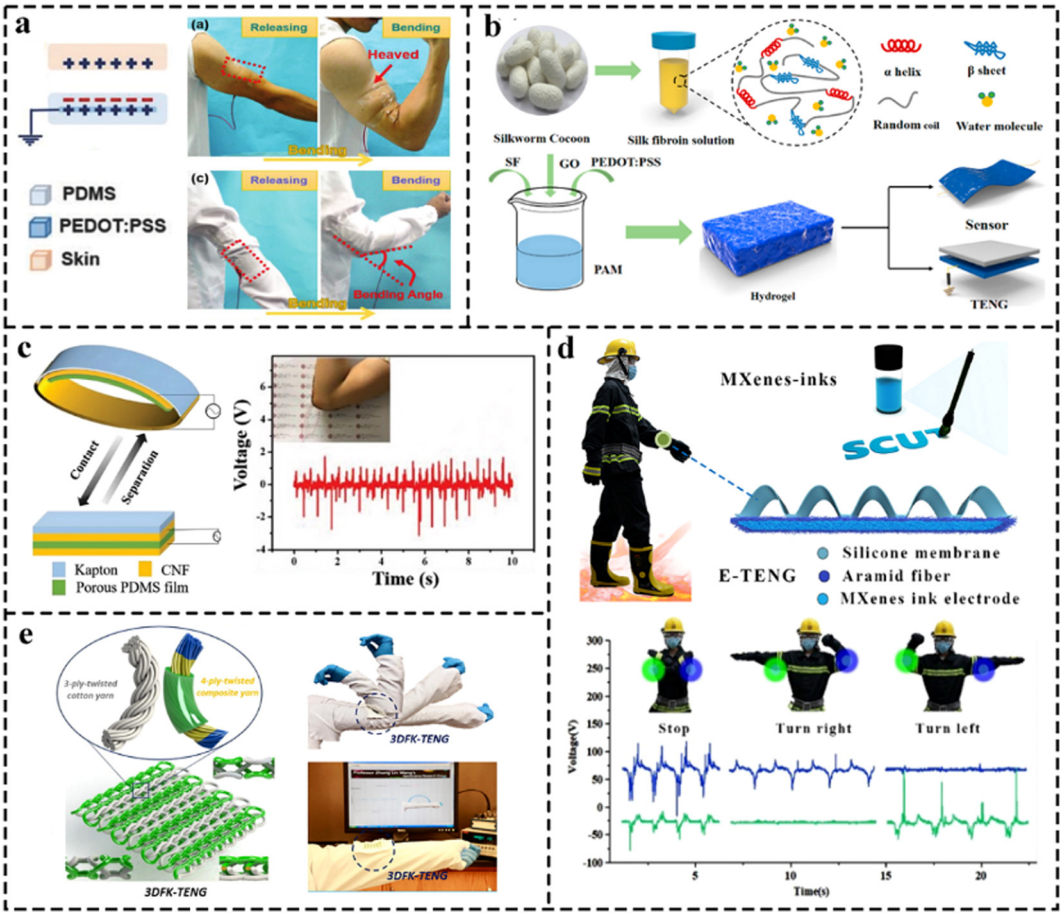

Fig. 5 Sensing joint motions *via* TENG-based wearable sensors. (a) Schematic illustration of the proposed TENG, and bending monitoring of human arm joint motion. Reproduced with permission from ref. 132, Copyright 2018, Wiley-VCH. (b) Schematic illustration and fabrication process of the TENG-based sensor. Reproduced with permission from ref. 133, Copyright 2020, American Chemical Society. (c) Voltage output and schematic illustration of the proposed TENGs for monitoring human joint motion. Reproduced with permission from ref. 135, Copyright 2020, Wiley-VCH. (d) Schematic illustration and voltage outputs of the proposed TENG for monitoring human motion on fireground. Reproduced with permission from ref. 136, Copyright 2021, Elsevier. (e) Schematic illustration of the proposed TENGs. Reproduced with permission from ref. 137, Copyright 2019, Elsevier.

subtle, and modifiable 3D structure provided a promising direction for wearable devices.

Besides the sensitivity and stretchability of TENGs, other studies have also paid substantial attention to the requirements of stability, humidity-resistance, and high conductivity simultaneously. Sheng *et al.* used a double-network polymer ionic conductor sodium alginate/zinc sulfate/poly acrylic-acrylamide (SA-Zn) hydrogel to fabricate a novel TENG with outstanding stretchability (>10 000%), high transparency (>95%), and good conductivity (0.34 S m^{-1}).[138] Ma *et al.* reported a flexible sensor based on a TENG with a simple integrated structure of chitosan film as the positive triboelectric layer, PDMS film as the negative triboelectric layer, conductive fabric as the electrode, and polyurethane foam as the flexible substrate.[139] The test results confirmed that the proposed sensor with significant flexibility and stability was convenient for real-time monitoring of human joint motion, such as elbow bending and foot contact. Different from conventional TENG-based sensors, Liu *et al.* developed a switchable textile-TENG (S-TENG) to achieve self-powered capacitive sensing, which offered many unique advantages, including decreasing the influence of temperature and humidity.[140] The S-TENG was demonstrated to work as a bending angle sensor when the device was attached to the elbow.

4.1.2 Hand gestures. Besides the monitoring of joint motions, researchers have sought to provide an alternative method of communication using hand gesture recognition and interpretation.[131,141–143] The relevant representative work is illustrated in Fig. 6.

As a communication medium, sign languages are crucial for the deaf-mute.[144] Researchers have achieved accurate gesture recognition by sensing gesture signals. Zhou *et al.* developed a wearable sign-to-speech translation system, which consists of yarn-based stretchable sensor arrays and a wireless printed circuit board.[145] This device can accurately translate the hand gestures of American Sign Language into speech with the assistance of machine learning. By analysing 660 acquired sign language hand gesture recognition patterns, the device exhibited a recognition rate of up to 98.63% and a recognition time of less than 1 s. Similarly, Chiu *et al.* developed a TENG-based

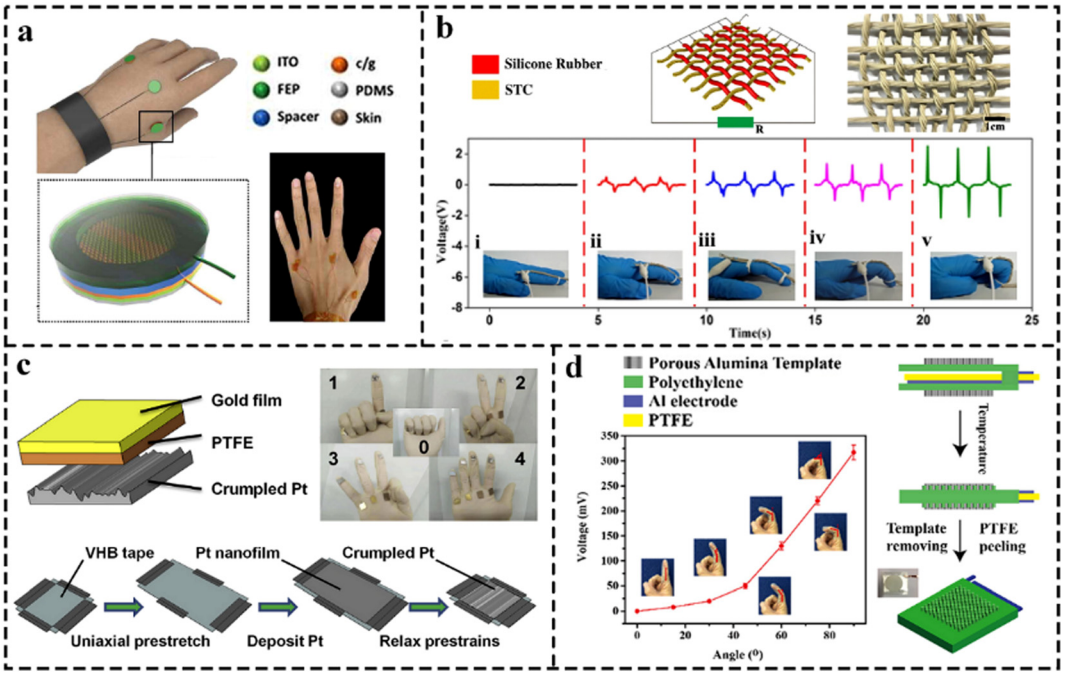

Fig. 6 Sensing hand gesture *via* TENG-based wearable sensors. (a) Schematic illustration of the TENG-based gesture sensors. Reproduced with permission from ref. 146, Copyright 2019, Taylor & Francis Group. (b) Schematic illustration and structure of the proposed TENG, and voltages of different bending angles. Reproduced with permission from ref. 147, Copyright 2019, Springer. (c) Schematic illustration and fabrication process of the TENG, and photographs of the gesture motion. Reproduced with permission from ref. 150, Copyright 2020, Elsevier. (d) Fabrication process of the dual-mode TENG and the output voltage at different bending angles. Reproduced with permission from ref. 151, Copyright 2020, American Chemical Society.

gesture-sensing system, which was attached to the back of the hand.[146] As shown in Fig. 6a, it distinguished hand gestures by measuring changes of the TENG output signal caused by the displacement of tendons. Furthermore, this system was integrated into gloves to enhance its viability in the field of sensing.

High sensitivity is essential for a fast response to finger motions. As shown in Fig. 6b, Zhu *et al.* reported a novel stretchable rubber-based thread-shaped TENG composed of silver-coated silicone rubber as one stretchable conductive thread (SCT) and silicone rubber-coated SCT as the other triboelectric thread.[147] The proposed TENG presented a fast response to different finger motions. Sukumaran *et al.* developed a flexion-based TENG, which converted the mechanical energy of the human finger joint motion into electrical signals that were further programmed by using a microcontroller to actuate robotic devices.[148] Wang *et al.* integrated a magnetorheological elastomer, Cu foil and metal wires into a TENG with tuneable performance, which was implemented as a self-powered sensor for human motion monitoring.[149] Different from various contact materials, it perceived external magnetic fields *via* its fast response and high flexibility.

Environmental corrosion of materials still remains an obstacle for TENG-based sensors. Lu *et al.* developed a crumpled platinum-based TENG with high corrosion resistance (Fig. 6c).[150] The device exhibited a voltage of 175.2 V, a current of 11.03 μA and an output power density of 0.518 mW cm^{-2}. It also showed great reliability under harsh environmental conditions and corrosion resistance. Furthermore, the proposed TENG can be easily integrated into gloves to collect human body energy and perform motion detection. Based on the polymer melt wetting technique, Huang *et al.* constructed polymer nanotubes on the surface of a TENG featured with self-cleaning and hydrophobic properties (Fig. 6d).[151] It reached up to a maximum output power of 0.025 mW and an open-circuit voltage of 41 V. The dual-mode TENG with designed dimensions was used as a self-powered sensor to detect human body motions, which offered critical insights for artificial intelligent prosthetics and human kinematics.

Conventional TENG electrodes are usually non-stretchable. To tackle this issue, researchers have developed novel stretchable TENGs that can be easily integrated into gloves. Deng *et al.* developed a carbon nanotube (CNT)–silicone rubber liquid composite to fabricate a super-stretchable TENG (SS-TENG) capable of withstanding 900% stretching deformation.[152] It realized the detection of dynamic motions of joints *via* electrical signals related to gestures. Moreover, a wearable keyboard based on SS-TENG arrays with outstanding conformability on curved surfaces was demonstrated, which exhibited promising potential for wearable electronics. Ren *et al.* reported a functional TENG consisting of foam and polyvinyl chloride (PVC) as the materials of the triboelectric layer.[153] The output power, open-circuit voltage, and short-circuit current of F-TENG reached up to 183 μW, 224.26 V, and 2.74 μA, respectively. Moreover, it was demonstrated to function as a self-powered sensor for hand gesture detection.

Using TENGs for upper body motion sensing has been shown to be effective and comfortable to record movement data. Additionally, many of these devices allow for a wide range of data interpretation, from measuring bending angles to converting finger gestures into spoken words, offering a unique and sustainable modality for relaying information about the body back to the user. Moreover, these TENG applications have even provided a means of non-verbal communication between individuals.[154,155] Thus, future research can focus on providing warnings or feedback signals to inform the wearer of the biomechanical status of their body.

4.1.3 Gaits. Human gaits can reveal a wealth of information, including personal identification and health status.[156,157] Gait monitoring also provides another metric for step counting and other daily fitness goals of users, as seen with modern smartphones and smartwatches. However, these sensing technologies are often limited by inaccuracies or lack comfort and breathability for everyday use. Additionally, considering that gait sensing is based on high loads, textiles can better fulfill this need compared to other traditional materials while maintaining high biocompatibility. Textiles are typically in contact with the knee and foot, which are two integral device locations for gait sensing, making TENGs a more intuitive choice for this application. The development of TENG-based sensors makes it possible for the direct implementation of sensors onto the lower extremities for accurate and comfortable real-time gait monitoring. The representative work is illustrated in Fig. 7.

Researchers have applied TENGs into shoes for better gait sensing. Dong *et al.* integrated the three-dimensional five-directional braided (3DB) structure to develop a TENG-based e-textile with the features of high flexibility, shape adaptability, washability, and superior mechanical stability for power and sensing (Fig. 7a).[158] Due to the spatial frame column structure formed between the outer braided yarn and the inner axial yarn, the 3DB-TENG was also endowed with high compression strength and sensitivity, and it responded to tiny force variations. An intelligent shoe and an identity recognition carpet were constructed to demonstrate its performance. As shown in Fig. 7b, Zhou *et al.* designed a novel shock-resistant TENG with high-speed impact energy-harvesting and safeguarding properties by assembling Kevlar fibre and a conductive shear-stiffening gel.[159] The proposed TENG generated a maximum power density of 5.3 mW m^{-2} with a voltage of 13.1 V under oscillator compression. Functionalized as a self-powered sensor, a wearable sole array with high sensitivity and a fast response was fabricated to distinguish toe in/out motions. By integrating a portable TENG-based sensor into a commercial sport shoe, Mao *et al.* achieved the monitoring of human gait

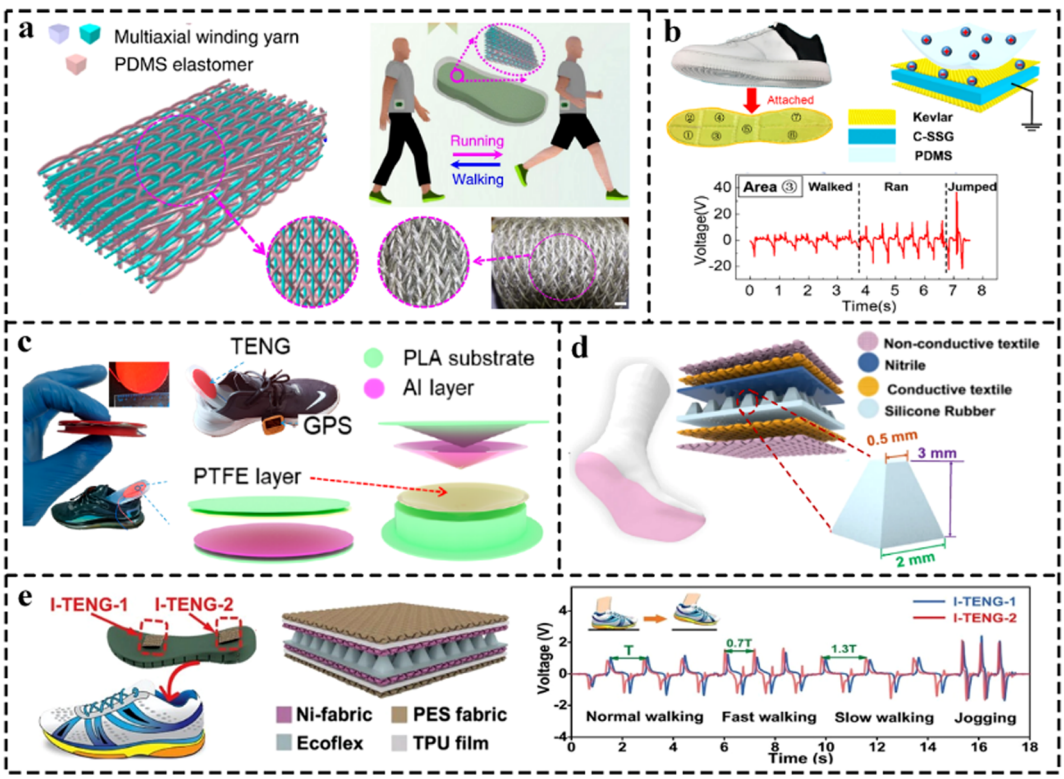

Fig. 7 Sensing human gaits *via* TENG-based wearable sensors. (a) Structural design of the 3DB-TENG. Reproduced with permission from ref. 158, Copyright 2020, Springer Nature. (b) Schematic illustration of the SS-TENG, the sole array based on the SS-TENG, and its output voltage on gait monitoring. Reproduced with permission from ref. 159, Copyright 2021, American Chemical Society. (c) Schematic illustration of the TENG and its installation position on shoes. Reproduced with permission from ref. 160, Copyright 2021, MDPI. (d) Structural design of the textile-based TENG on socks. Reproduced with permission from ref. 161, Copyright 2020, Springer Nature. (e) Structural design of the TENG, the TENG-based smart insole for gait monitoring, and the voltage signals of the TENG under different walking speed. Reproduced with permission from ref. 165, Copyright 2021, Wiley-VCH.

and stability.[160] As shown in Fig. 7c, the materials involved are common PTFE and aluminum (Al) foil, acting as a triboelectric layer, which generated electrical signals based on the triboelectric effect. Moreover, 3D printing technology was applied to fabricate the optimized structure of the TENG, which significantly improved its performance.

Moreover, many novel TENGs were developed for integration into socks for gait sensing. As shown in Fig. 7d, Zhang *et al.* designed low-cost intelligent triboelectric socks equipped with a self-powered functionality that were implemented as wearable sensors to deliver information on the identity, activity, and health status of individuals.[161] To further address the issue of ineffective analysis methods, an optimized deep learning model with an end-to-end structure on the socks signals for the gait analysis was proposed to detect five different human activities with a high accuracy of 96.67%. Aiming at practical application, the physical signals collected through the socks were mapped in virtual space to establish a digital human system for sports monitoring, healthcare, and future smart home applications. Zhang *et al.* developed a novel sock-cloth-based TENG (SC-TENG) which consisted of a PTFE film as the triboelectric layer and copper foil as the conductive electrode.[162] The proposed SC-TENG was implemented as a self-powered sensor in the field of intelligent sports. The open-circuit voltage, short-circuit current, and output power of SC-TENG reached up to 267 V, 3.4 μA, and 225.6 μW, respectively. As a lightweight, flexible and wearable TENG device, such design promoted the development of TENG devices in intelligent sports.

Additionally, monitoring thigh movement is also a practical strategy for gait sensing. To achieve significant monitoring functions during human balance control processes, Liu *et al.* designed a hybrid electromagnetic–triboelectric nanogenerator (HETNG), which consisted of a symmetrical pendulum structure and a cylinder magnet rolling inside.[163] The proposed HETNG was positioned on the thigh and foot of an artificial limb, for monitoring the actions of squatting and standing up, as well as moving the leg up and down. For the elderly who walk slowly with a walking aid, a HETNG on the walking aid was used to record the motions of moving forward and unexpected falling, which is useful for calling for help. This work showed the potential of the biomechanical energy-driven HETNG for powering portable electronics and monitoring human motions, offering great promise for individuals with impaired mobility or other disabilities.

Monitoring the motion of lower-limb, waist, and foot is significant for lower-limb rehabilitation.[164] Zhang *et al.* developed a wearable TENG-based device for gait analysis and waist motion capture (Fig. 7e).[165] Four triboelectric sensors were equidistantly sewed onto a fabric belt to recognize the waist motion, enabling the real-time robotic manipulation and virtual games for immersion-enhanced waist training. The insole equipped with two TENG sensors was designed for walking status detection, offering 98.4% identification accuracy for five different humans aiming at rehabilitation plan selection. This was achieved by leveraging machine learning technology to further analyse the signals. Through a lower-limb rehabilitation robot, the authors demonstrated that the sensory system performed well in user recognition, motion monitoring, as well as robot and gaming-aided training, showing its potential for IoT-based smart healthcare applications.

Recent studies have been proposed with novel methods to provide cost-effective, comfortable, and accurate alternatives to current gait monitoring devices. The use of strong and readily available materials with facile fabrication processes has enabled the mass distribution of these durable monitoring devices to help provide continuous gait monitoring for the public.[166,167] Additionally, choosing footwear that provides heightened comfortability is a priority for many people, so that TENG integration for foot pressure monitoring can be a more practical choice for human daily life. Future research may be aimed to improve the monitoring of unhealthy joint and walking angles to prevent further joint degradation and improve long-term joint health.

4.1.4 Other physical motions. In addition to the sensors in the above-mentioned studies, TENG-based wearable sensors powered by other physical motions can also be applied in special circumstances, exemplified by eye blinks. Anaya *et al.* developed an orbicularis oculi muscle motion sensor to monitor eye blinks for remote control, such as hands-free remote car and drone control, or monitoring of driving behaviour.[168] Fu *et al.* developed a double helix TENG (DH-TENG) with high space efficiency and charge utilization for application as a self-powered weight sensor.[169] The open-circuit voltage and short-circuit current of the fabricated DH-TENG reached up to 42.9 V and 1.8 μA, respectively. The corresponding peak power density was 8.87 μW cm^{-3}. Zhao *et al.* designed a new wave-shaped TENG (W-TENG), which yielded an open-circuit voltage of 224.26 V and a short-circuit current of 2.74 μA.[170] Its maximum output power reached up to 184 μW. The described W-TENG can work as a self-powered human walking counter for promotion of sensor applications.

Among these studies, some devices were designed for general purposes, whereas other designs focused on specific scenarios to bring forward optimal designs, which jointly promote the development of wearable human motion sensors. The aforementioned studies are summarized in Table 2.

4.2 Sensing physiological signals *via* TENG-based wearable/implantable sensors

Recent years have witnessed an upsurge of energy harvesting from the biomechanical energy of heartbeats, blood pressure, and other physiological activities for power supply of wearable/implantable electronic devices.[171,172] Human health conditions can be assessed on the basis of typical physiological signals, which mainly include the cardiovascular system with heart rate[173] and wrist pulse,[174–176] and the respiration system with respiration.[177,178] Conventional health monitoring devices with large size and heavy weight are not convenient to carry. By contrast, TENG-based sensors, which can convert human biomechanical energy from the above vibrations into electrical outputs, provide new insights into physiological condition monitoring. On the one hand, TENG-based wearable bioelectronics

Table 2 Summary of wearable TENG sensors based on human motion signals

Type	Material	V_{oc} (V)	I_{sc} (μA)	Sensitivity	Detection range	Year	Ref.
Joint	PEDOT:PSS, Al	180	22.6	8–80 Pa^{-1}	—	2018	132
	PEDOT:PSS, PAM	12	0.4	0.1 V kPa^{-1}	0.5–119.4 kPa	2020	133
	PDMS, AIBN	119	2.32	—	—	2020	134
	Silicone, aramid	—	—	0.11 V deg^{-1}	0°–140°	2021	135
	BC/CS, PDMS/Cu	23	0.5	0.24 V kPa^{-1}	10.5–96.25 kPa	2021	136
	PA yarn, Ag	50	0.15	12.5 V kPa^{-1}	0.4–4 kPa	2020	137
	SA-Zn, PMMA	30	0.5	—	>10 000% stretchability	2021	138
Hand	SSE, Cu	20.99	55.07	0.24 V N^{-1}	30°–130°	2020	149
	PTFE, Pt film	175.2	11.03	1.6 V kPa^{-1}	0.04–0.11 MPa	2020	150
	PTFE, Al	41	1.4	0.46 V deg^{-1}	0°–90°	2020	151
	Silicone, CNT/SR	275	8.8	0.34 V deg^{-1}	0°–90°	2021	152
	Foam, PVC, Cu	224.3	2.74	—	—	2021	153
	PTFE, Cu, Foam	24	—	—	0–97% RH	2020	156
Foot	CNT, SSG	41.27	8.9	1.46 V kPa^{-1}	67 Pa–52 kPa	2020	157
	C-SSG, PDMS	13.1	1.71	0.04 V	2.6 kPa–0.3 MPa	2021	159
	PDMS, Cu	57	3.2	—	—	2021	162
	FEP, PET, PU, Al	234.9	8.03	—	—	2021	163
	TPU, Ni	20	0.26	66.67 mV N^{-1}	1–300 N	2022	165
Others	Teflon, nylon	42.9	1.8	—	—	2021	169
	$MgSiO_3$, PET, Cu	224.6	2.74	—	—	2021	170

offer flexibility, stretchability, durability, stability, and comfort, enabling the development of unobtrusive wearable biosensors.[179,180] On the other hand, the recent progress in the field of electronics has resulted in widespread acceptance for implantable TENG-based devices as helpful biomedical tools in clinical studies.[181–183] Self-powered implantable TENG devices with the advantage of biocompatibility and reliability are suitable for *in vivo* applications for continuous healthcare monitoring. Therefore, it is possible to monitor the health of individuals stably by using the wearable/implantable TENG-based devices to observe the crucial physiological signals. These flexible and light devices can assist humans to adjust their physical status better by monitoring the basic physiological signals from daily activities.[184–186] Yet, it still remains a great challenge to accurately monitor with a fast response. It is suggested that future research focus can be on the high sensitivity and accuracy of TENG-based wearable/implantable sensors for sensing physiological signals in real time. Additionally, the compatibility of materials with human body is still a key issue to better ensure human body comfort.

4.2.1 Heartbeat and pulse. The cardiovascular system, also known as the circulatory system, is composed of the heart, arteries, veins and capillaries. Wearable sensors have become increasingly popular for monitoring the state of the cardiovascular system. As one of the major indicators that directly reflect human cardiovascular health, the heart rate can be routinely measured by using TENG-based wearable cardiac sensors and pulse sensors.[187] The relevant representative work is illustrated in Fig. 8.

Heart-rate monitoring plays a central role in personal healthcare management. TENG-based cardiac sensors without any other auxiliary energy sources can detect the heart beat directly and provide feedbacks on the heart rhythm in real time. As shown in Fig. 8a, Lin *et al.* designed a self-powered wireless body sensor network (BSN) system for heart-rate monitoring by integrating a downy-structure-based TENG, a power management circuit, a signal processing unit, and a Bluetooth module.[188] The generated heart-rate signals in the signal processing circuit were sent to an external device *via* the Bluetooth module, and displayed on a personal cell phone in real time. This work presented a promising approach for personal heart-rate monitoring by using a self-powered, noninvasive, and user-friendly device.

Besides directly monitoring the beating of heart, the cardiovascular status can also be measured by pulse sensors which transform the wave motion of the pulse into a waveform of voltage. TENGs can be attached to different human body parts where arterial pulses can be conveniently detected, such as the radial artery at the wrist or the carotid artery on the neck,[189–191] which shall be addressed as follows.

TENGs can be easily attached to the skin close to the carotid artery, which can generate a subtle amplitude for pulse monitoring. Lou *et al.* developed a triboelectric sensing textile based on core–shell yarns.[192] In the woven structure, nylon and polytetrafluoroethylene filaments were selected as the positive and negative layers, respectively. The sensitivity of the sensing textile reached up to 1.33 V kPa^{-1} and 0.32 V kPa^{-1} in the pressure range of 1.95–3.13 kPa and 3.20–4.61 kPa, respectively. It exhibited superior mechanical stability and sensing capability even after continuous operation for 4200 working cycles or after 4 h continuous washing in water. Moreover, the sensing textile was demonstrated to monitor real-time pulse signals and reflect the current health status of users. Similarly, the authors utilized a facile electrospinning technique to construct an all-fibre structured pressure sensor.[193] As shown in Fig. 8b, the fabricated sensor textile consisted of a polyvinylidene fluoride/Ag nanowire nanofibrous membrane (NFM), an ethyl cellulose NFM, and two layers of conductive fabrics. The proposed wearable device with high shape adaptability exhibited excellent sensing capability, reaching up to 1.67 V kPa^{-1} and 0.20 V kPa^{-1} in the pressure range of 0–3 kPa and 3–32 kPa, respectively. The prepared sensor textile presented premier mechanical stability even after

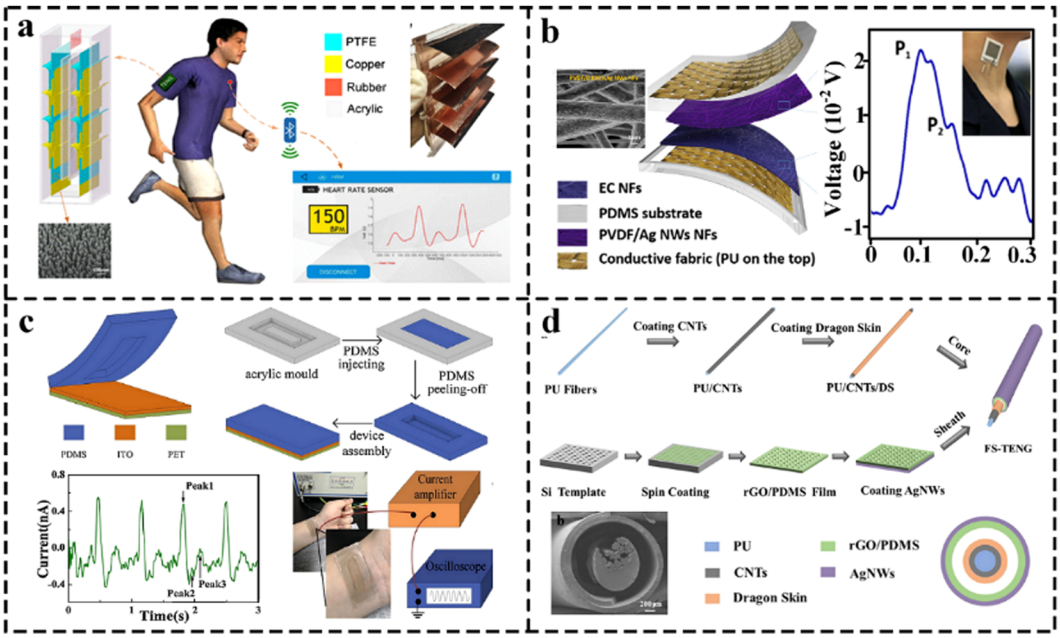

Fig. 8 TENG-based wearable sensors for monitoring the heartbeat and pulse. (a) A self-powered wireless body sensor network (BSN) system for heart-rate monitoring. Reproduced with permission from ref. 188, Copyright 2017, American Chemical Society. (b) Schematic illustration and microstructure of the TENG, and the voltage signal of the TENG-based pulse sensor at the neck. Reproduced with permission from ref. 193, Copyright 2020, American Chemical Society. (c) Schematic illustration and fabrication process of the single-electrode TENG, and the voltage signals of the TENG-based pulse sensor at the wrist. Reproduced with permission from ref. 196, Copyright 2018, American Chemical Society. (d) Structural design and fabrication process of the FS-TENG-based sensor for pulse monitoring. Reproduced with permission from ref. 199, Copyright 2021, Elsevier.

7200 cycles of continuous operation. It was demonstrated to be placed on the carotid artery to capture pulse signals, serving as a reliable device that reflected the state of health. These two studies offered promising insights into multifunctional pressure sensors with broad applications in the fields of smart textiles and personalized healthcare.

Besides the carotid artery with a subtle pulse amplitude, another human body part effectively available is the radial artery at the wrist for TENG-based cardiovascular monitoring. Maharjan *et al.* fabricated an innovative curve-shaped wearable hybridized electromagnetic-TENG powered by human motion.[194] It was demonstrated to function as a self-powered pulse sensor for health monitoring. Lin *et al.* fabricated a capacitive pressure sensor based on core–shell nanofibers composed of PDMS ion gel/PVDF-HFP by incorporating a cross-linking agent during electrospinning.[195] The resulting sensor exhibited a high sensitivity of 0.43 kPa^{-1} in the low-pressure range from 0.01 kPa to 1.5 kPa. A wrist-based pulse sensor was constructed to further demonstrate its high sensitivity. As shown in Fig. 8c, Cui *et al.* presented a TENG-based pulse sensor composed of a PET film and a thin PDMS film.[196] The output human pulse signal was implemented as a typical indicator of human health. The radial artery augmentation index AIr and the time difference between two peaks for arterial stiffness diagnosis were successfully obtained, which were highly consistent with the normalized medical values. Many researchers have attempted to improve the sensitivity of TENGs from the perspective of materials, enabling TENGs to be more sensitive to pulse beat for more precise monitoring.[197] As one of the commonly used polymers for biomedical applications, polyvinyl alcohol (PVA) presents promising prospects due to its biocompatibility. Wang *et al.* firstly fabricated a device based on the optimized PVA–gelatin composite films with high robustness.[198] The device accurately captured the cardiovascular information encoded in the pulse signals. Fu *et al.* designed a fibrous stretchable TENG-based sensor with a core–sheath structure (Fig. 8d).[199] The fabricated sensor achieved a sensitivity of 26.75 V N^{-1} at low pressure (0.02 N). By using the chargeable carbon black (CB)/thermoplastic polyurethane (TPU) composite material, Zhang *et al.* fabricated an ultrathin stretchable TENG with good stretchability ($\approx$646%), ultralow thickness ($\approx$50 μm), and a low weight ($\approx$62 mg) for the monitoring of physiological signals.[200]

High blood pressure, also called hypertension, has been well known as a key indicator for people with chronic heart and cerebrovascular diseases. Blood pressure (BP) usually increases with age, and should be monitored regularly in the elderly.[201] The early diagnosis and assessment of such diseases are possible *via* blood pressure monitoring. TENG-based sensors can be used to monitor blood pressure by converting the vibration signals from the pulse into electrical signals. Yet, it still remains a great challenge to accurately measure blood pressure *via* the pulse wave for continuous and noninvasive diagnosis of a disease associated with hypertension. Meng *et al.* developed a flexible weave constructed self-powered pressure sensor (WCSPS) for measuring of the pulse wave and BP in a noninvasive manner.[202] The WCSPS exhibited an ultra-sensitivity of 45.7 mV Pa^{-1} with an ultrafast response time of

less than 5 ms. After 40 000 motion cycles, the device showed no performance degradation. The discrepancy between the blood pressure measured using the WCSPS and that provided by the commercial cuff-based device was 0.87–3.65%. By combining the advantages of carbon materials with high conductivity and organic electrodes with high stretchability, Chen *et al.* fabricated a stretchable electrode with a rough surface.[203] As the carbon concentration increased, it exhibited high output performance with the maximum voltage performance further increased under a large strain (100%), which is suitable for wearable systems.

Besides the TENG-based wearable sensors mentioned above, implantable TENGs have been applied for auxiliary monitoring by implanting into human organs.[204] TENG-based implantable cardiological sensors have provided a self-powered alternative solution to conventional cardiological biomedical sensing, while maintaining a minimally invasive approach.[205] Fig. 9 shows the feasibility of various healthcare implantable devices based on TENGs for monitoring the parameters associated with the cardiovascular system, such as heartbeat.

Similar to the traditional electrocardiogram, flexible and biosafe TENG-based sensors can provide complementary information about cardiovascular activity, which plays a significant role in preventing cardiovascular diseases. Moreover, TENG-based implantable cardiology sensors can monitor the heart beat status directly without any other energy sources.[206] They provide real-time feedbacks regarding the rhythmic conditions of the heart. Compared to other wearable sensors, such implantable sensors present a higher level of accuracy without significantly affecting the activities of patients. As shown in Fig. 9a, Zheng *et al.* proposed a novel implantable TENG which can be driven by the heartbeat of adult swine, and it showed a high improvement of the output voltage and the current.[207] Owing to its superior *in vivo* performance and implantation stability over 72 h, a self-powered wireless transmission system was designed for real-time cardiology monitoring for human based on the swine prototype.

TENG-based pacemakers have been employed as activators of heart muscles to regulate the heartbeat *via* the electrical impulse from TENGs, which present lightness and durability compared with commercial pacemakers.[208] Conventional surgeries cause great inconvenience to patients, which make the TENG-based implantable pacemaker more attractive for its miniaturization.[209] As shown in Fig. 9b, Ouyang *et al.* developed a TENG-based implantable symbiotic pacemaker, which achieved energy harvesting and storage as well as cardiac pacing on a large-animal scale.[210] The fabricated TENG exhibited an open-circuit voltage of 65.2 V. The energy harvested from each cardiac motion cycle was 0.495 μJ, which was higher than the required endocardial pacing threshold energy (0.377 μJ). Implantable medical devices, offering high outputs and good durability, are expected to be widely applied in the

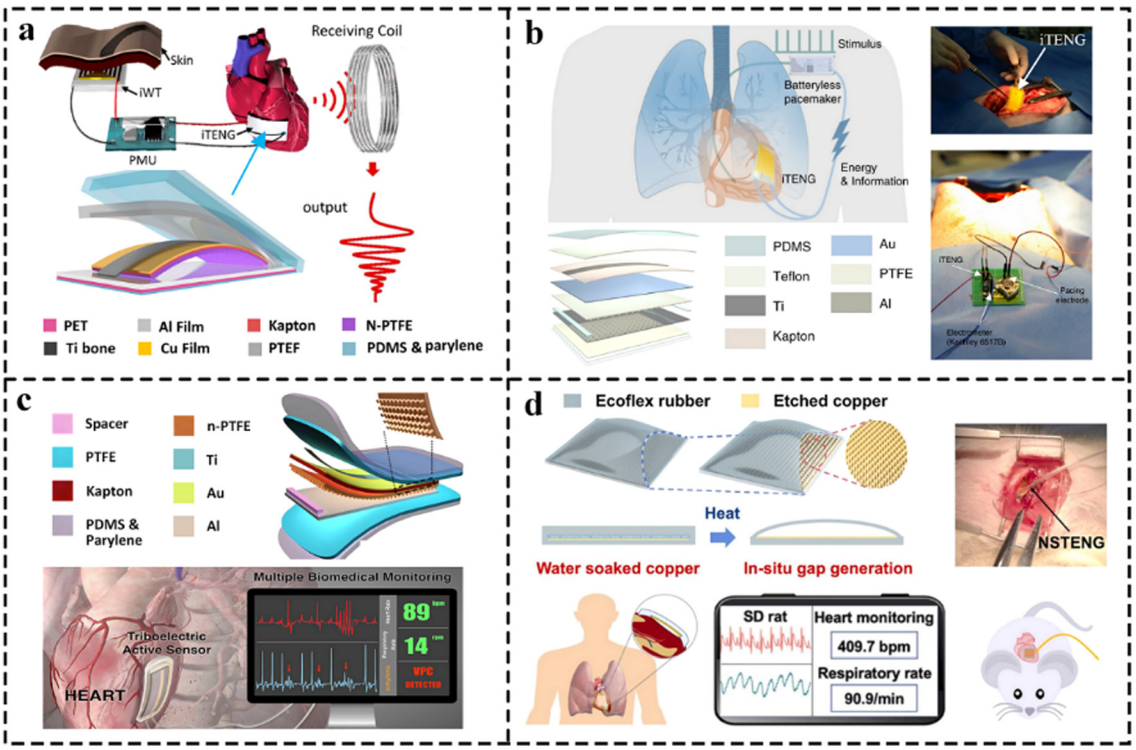

Fig. 9 TENG-based implantable sensors for monitoring the heartbeat. (a) Schematic illustration and working principle of the proposed TENG for heartbeat monitoring. Reproduced with permission from ref. 207, Copyright 2016, American Chemical Society. (b) Schematic illustration and working principle of the proposed TENG. Reproduced with permission from ref. 210, Copyright 2019, Springer Nature. (c) Configuration of the TENG and its responding voltage output. Reproduced with permission from ref. 212, Copyright 2016, American Chemical Society. (d) Structural design of the NSTENG and its *in vivo* heart monitoring in a rat. Reproduced with permission from ref. 213, Copyright 2021, Elsevier.

fields of treatment and diagnosis such as *in vivo* symbiotic bioelectronics.

Endocardial pressure, as an essential indicator for evaluating cardiac function, is generally monitored by invasive and costly cardiac catheterization, which is not suitable for continuous signal monitoring in a long term. Considering its clinical significance for patients with impaired cardiology function, Liu *et al.* integrated a self-powered endocardial pressure sensor (SEPS) into a surgical catheter for minimally invasive implantation.[211] In a porcine model, the SEPS was implanted into the left ventricle and the left atrium, achieving an ultrasensitivity of 1.195 mV $mmHg^{-1}$ *in vivo*. Moreover, it was employed for detecting cardiac arrhythmias such as ventricular fibrillation and ventricular premature contraction. As shown in Fig. 9c, Ma *et al.* reported a flexible and one-stop implantable triboelectric active sensor (iTEAS) for continuous monitoring of multiple physiological and pathological signs.[212] It can monitor the heart rates of human-scale animals with an accuracy of 99%. The *in vivo* biocompatibility was demonstrated after 2 weeks of implantation, which proved its suitability for practical applications. As shown in Fig. 9d, Zhao *et al.* designed an eco-friendly no-spacer TENG, which was utilized to monitor the heart rate with an accuracy of up to 99.73% by attaching to a rat's heart.[213] This work provided a new strategy that promoted the innovation of implantable biosafe sensors.

TENG-based wearable/implantable sensors mentioned above exhibit the feasibility of TENGs for monitoring the physiological signals related to the cardiovascular system. The high accuracy and sensitivity of the devices allow for a precise monitoring of cardiovascular diseases and offer another leading direction for monitoring *via* more lightweight and compatible TENGs, promoting the development of miniature implantable medical sensors. It is suggested that future research focus should be on the properties of higher sensitivity and faster response for monitoring in real time.

4.2.2 Respiration. Respiration, as one of the most principal physiological activities, reflects the physical health condition of individuals.[214,215] Recently, TENGs have been broadly investigated in respiration monitoring due to their intriguing features, including wearing comfort and delicate biocompatibility. Meanwhile, TENG-based sensors can sensitively convert slight amplitude motion from human respiration activities into electrical signals for further respiration status monitoring, compared with commercial respiration monitoring devices.[216–219] Air-flown exhaled chemicals can be continuously monitored by TENG-based sensors for personalized physical health.[220,221] Real-time monitoring of the respiratory status can provide early warning and diagnosis, for further appropriate treatment suggestions. Fig. 10 shows the representative work of TENG-based wearable/implantable respiration sensors for human health monitoring.

The sensitivity and wearing comfort of TENG-based sensors are two hotspots that users pay attention to. Researchers have developed novel materials of TENGs from the perspective of these two points for real-time monitoring of the subtle respiration activities. As shown in Fig. 10a, Zhang *et al.* designed a TENG-based waist-wearable wireless device to monitor the respiration status by sensing the variation of the abdomen circumference.[222] A series of real-time tests were performed on two volunteers with different waistlines and various breathing rhythms. The test results demonstrated the feasibility of the proposed device with high accuracy and sensitivity for real-time monitoring of respiration during various daily activities, including lying, standing and sitting. Considering the influence of the metal electrode without gas permeability on the personalized wearing comfort, Qiu *et al.* developed a fabric-based TENG with polymerized polyaniline as the electrode.[223] It yielded a voltage of 1000 V and a current of 200 μA under a frequency of 2.5 Hz. As shown in Fig. 10b, the proposed TENG with outstanding gas permeability was able to monitor the respiration conditions of patients in real time and sound an alarm when the individual's breathing stops.

Detection of gases from human respiration offers an effective and painless approach for the diagnosis of some diseases, such as prediabetes. Breathing gas flow-induced vibration can be converted into electrical signals *via* TENGs. Therefore, researchers have attempted to integrate TENGs into masks to fabricate sensors for respiration monitoring, which exhibit high accuracy and sensitivity. As shown in Fig. 10c, Su *et al.* utilized chitosan and reduced graphene oxide (RGO) to develop a wearable active acetone biosensor.[224] The proposed sensor exhibited a good sensing response of 27.89% to 10 ppm acetone in respiratory gases under 97.3% relative humidity, which was 5 times higher than that of pure chitosan film-based devices. This work offered a new insight into non-invasive prediabetes diagnosis. As shown in Fig. 10d, Araz *et al.* presented a diatom frustule (DF) as a biomaterial additive to improve the cellulose nanofibril (CNF)-based TENG.[225] The DF-CNF TENG exhibited an output voltage of 388 V and a time-averaged power of 85.5 mW m^{-2} under an area of 4.9 $cm.^2$ Moreover, the practical application of the DF-CNF TENG was demonstrated based on a smart mask designed for human respiration monitoring.

Respiration parameters, such as respiratory rate (RR), inhalation time, and exhalation time, are essential to clinically differentiate healthy people from those with respiratory diseases. Masks integrated with TENGs are also employed to monitor such parameters, which present excellent stability and high accuracy. As shown in Fig. 10e, He *et al.* developed a nanofibrous membrane-based respiration monitoring TENG (RM-TENG) which was used as a self-powered smart mask filter with high filtration efficiency.[226] The optimized RM-TENG accurately detected the aforementioned respiration parameters with excellent sensing stability for 40 h. Similarly, Wang *et al.* reported a poly(vinyl alcohol)/silver (PVA/Ag) nanofiber-based TENG for human respiration and harmful gas monitoring.[227] It exhibited a high output performance with an open-circuit voltage of 530 V and a power density of 359 mW m^{-2}. The proposed TENG was demonstrated to be driven by the gas exhaled from the nose to monitor human respiration parameters. Li *et al.* reported a novel TENG based on a multi-scale metal mesh electrode (MME) that was fabricated through an alloying–dealloying method to enhance the high specific

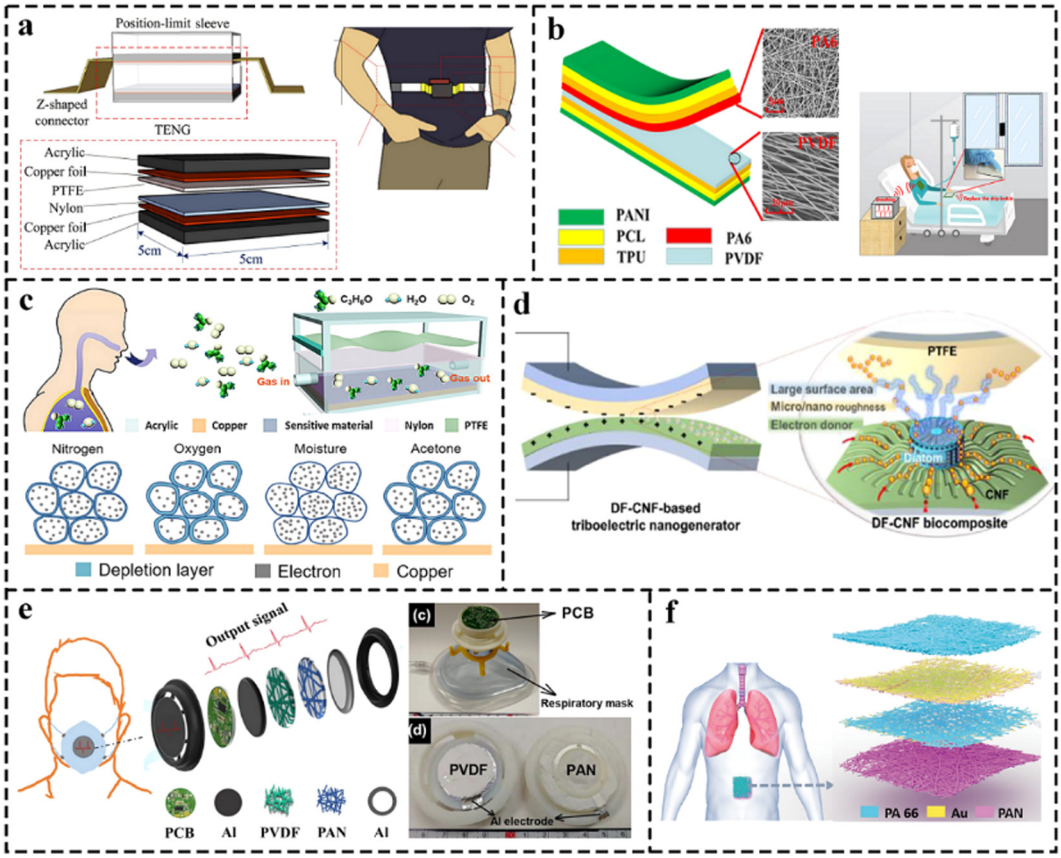

Fig. 10 Representative work on TENG-based sensors for monitoring respiration. (a) Structural design of the wearable TENG for respiration monitoring. Reproduced with permission from ref. 222, Copyright 2019, Elsevier. (b) Schematic illustration of the proposed TENG. Reproduced with permission from ref. 223, Copyright 2019, Elsevier. (c) Configurations and working principle of WSAS for detection of acetone in human respiration. Reproduced with permission from ref. 224, Copyright 2020, Elsevier. (d) Structural design of the TENG-based mask for respiration monitoring. Reproduced with permission from ref. 225, Copyright 2021, American Chemical Society. (e) Schematic illustration of the RM-TENG and its voltage signals at various walking speeds. Reproduced with permission from ref. 226, Copyright 2021, Elsevier. (f) Configurations of the TENG and its voltage signals during human respiration. Reproduced with permission from ref. 229, Copyright 2021, Wiley-VCH.

contacting surface.[228] Its output voltage reached up to 175.77 V at a frequency of 4 Hz, which was 4 times higher than that of the copper film electrode, while the corresponding power density was 0.85 W m^{-2}. A breathing valve mask integrating with the MME-based TENG was demonstrated to detect the real-time respiratory rate and respiration intensity under different conditions.

Sleep disorder, as a common health problem, has been bothering human beings. TENG-based wearable sensors with high sensitivity and stability can be employed for sleep quality diagnosis by monitoring the breathing movements of the thorax. As shown in Fig. 10f, Peng *et al.* developed a TENG-based e-skin with good permeability and high sensitivity for real-time human respiration monitoring and obstructive sleep apnea–hypopnea syndrome (OSAHS) diagnosis.[229] The e-skin was able to accurately monitor real-time subtle respiration due to its high-pressure sensitivity of 0.217 kPa^{-1}. Moreover, to prevent the occurrence of OSAHS and improve sleep quality, a self-powered diagnostic system was further developed for real-time detection and severity evaluation of obstructive sleep apnea–hypopnea syndrome. In another example, Song *et al.* integrated a patterned Al–plastic film and an entrapped cantilever spring leaf to develop a flexible TENG serving as a self-powered sensitive sensor for sleep-body movement monitoring.[230] The proposed device was demonstrated for diagnosis of sleep disorders due to its high sensitivity and excellent stability. Similarly, to monitor all-around physiological parameters during sleep, Zhou *et al.* reported a single-layered and ultra-soft textile with great stability and washability.[231] The proposed textile, exhibiting a high-pressure sensitivity of 10.79 mV Pa^{-1} and a wide working frequency bandwidth from 0 Hz to 40 Hz, was capable of real-time tracking of dynamic changes in sleep posture under subtle respiration.

Moreover, researchers have been paying more and more attention to monitor *in vivo* breathing activity. Li *et al.* developed an ultra-stretchable micro-grating implantable nanogenerator (i-NG) system, which was packaged by a cavity-designed soft silicone elastomer.[232] The i-NG system was demonstrated to convert the energy from slow diaphragm movement during normal respiration into an electrical output when implanted inside the abdominal cavity of adult rats.

Similarly, Ma *et al.* designed a TENG-based one-stop implantable triboelectric active sensor for stable monitoring of respiratory rates and phases by analyzing variations of the output peaks.[212] With the strategy of core–shell packaging, monitoring functionality remained precise during 72 h after closure of the chest. Moreover, it was proved to be practical as a self-powered multifunctional biomedical sensor by examining the *in vivo* biocompatibility after implantation over 2 weeks, revealing its great potential for healthcare applications.

With increasing studies on TENGs, implantable devices related to respiration monitoring have been a heated approach for monitoring the human health status. However, few studies have examined the *in vivo* lifetime of implantable TENGs. It still requires extensive research to further probe more stable and compatible TENGs for monitoring of respiration-related diseases.

4.2.3 Other physiological activities. Besides the above common physiological activities, researchers have also attempted to monitor the human health status by using TENG-based wearable/implantable sensors to monitor other health-related physiological signals.

Researchers have developed various lightweight and wearable TENGs for monitoring physiological activities, such as perspiration. Cai *et al.* integrated a novel TENG into an insole to detect the amount of perspiration on foot.[233] The open-circuit voltage and short-circuit current of the TENG reached up to 363 V and 42.38 μA, respectively. Yang *et al.* fabricated a multifunctional TENG (MF-TENG) with fast self-healing and photothermal properties.[234] The MF-TENG was adopted for the recovery of human joints *via* its photothermal properties under a near-infrared laser. Cai *et al.* utilized the facile ultraviolet ozone irradiation technique to fabricate a PDMS/MXene composite film, which was used as a tactile sensor.[235] It achieved a high sensitivity of 0.18 V Pa^{-1} during 10–80 Pa and 0.06 V Pa^{-1} during 80–800 Pa, showing promising prospects in monitoring human physiological signals.

In addition, monitoring other physiological signals *via* implantable TENGs has also attracted the attention of many researchers. Lee *et al.* performed *in vivo* experiments for delivering various beats per minute (BPM) to the nerves to explore the effect of stimulation frequency on mechano-neurostimulation and monitor changes in bladder pressure.[236] The test results demonstrated that implantation of the flexible clip interface could be potentially employed for self-powered mechano-neuromodulation for bladder function in the future. The implant-associated infections cause implant failure and suffering and increase the risk of infection death. Therefore, Shi *et al.* utilized a TENG to build a stable and reliable negatively charged implant surface, which effectively inhibited bacterial adhesion and reduced bacterial number.[237] Implanted neuro-prosthetic is a promising solution for restoring tactile sensation. Shlomy *et al.* developed an integrated tactile TENG that was implanted under the skin.[238] The electrical potential was delivered to healthy sensory nerves to mimic the tactile sensation by activating them. The current solutions developed for the purpose of in and on body electrical stimulation (ES) lack autonomous qualities necessary for comfortable, practical, and self-dependent use. Harnessing human biomechanical energy with TENGs to develop self-powered systems has allowed for the introduction of novel therapeutic ES solutions.[239]

Furthermore, increasingly integrated systems based on TENGs and medical techniques have been developed for human healthcare assistance.[240–242] Wang *et al.* reported a self-powered system by integrating a stacked-TENG and an epimysia electrode to stimulate the impaired muscles.[243] Summarily, applications of the implantable TENGs in the heart, stomach, and muscle demonstrated the ability of TENGs to tackle unknown medical diseases associated with other human internal organs. These promising results prompted further research to explore practical methods in which TENGs can be integrated into new implantable medical devices and systems. The aforementioned representative studies are summarized in Table 3.

5. Human–machine interfacing based on TENGs

The human–machine interface (HMI) is defined as information interaction between human body and external electronics *via* communication technology. Recent advances in electronics, materials, and mechanical designs have offered avenues toward related HMI devices which have been fully investigated. On the one hand, conventional HMI devices suffer from limitations such as the requirement of power sources and structure complexity. As a solution, the TENG-based HMI can be considered as an attractive alternative as the self-powered operation of the TENG-based HMI has been realized by using a microcontroller (MCU) to further process and analyze the generated electrical signals of TENGs which are used as the interaction media. Such technique is becoming increasingly intimate and inevitable, with broad application areas, including virtual reality/augmented reality (VR/AR),[244–246] healthcare,[247,248] and robotics.[249,250] On the other hand, communication, as an indispensable part of the IoT systems, also plays a significant role in the TENG-based human body IoT systems. Wireless communication technology has been widely employed for data transmission due to its convenience. A wireless body area network (WBAN), based on the IEEE 802.15.6 standard, was proposed for short-range wireless communication *via* the human body as a propagation medium with the advantages of low energy consumption.[251]

Yet, it still remains a challenge to realize interaction and communication with fast response, stability, and reliability. A user-friendly HMI also needs to be developed for convenient operations. Based on the common motions of the human body, researchers have attempted to develop innovative TENG-based HMI devices from the perspective of materials, which can be attached onto human body parts. Based on different human motion-induced interfaces, the HMI devices presented in this review are summarized into finger gesture-based interfaces, novel finger tactile-based interfaces, and other types of interfaces such as human body motion, voice, and breath.

Table 3 Summary of studies on various wearable/implantable TENGs for healthcare

Type	Monitoring	Material	Description	Indicator	Year	Ref.
Wearable	Heartbeat	PTFE, Cu	A self-powered wireless body sensor network (BSN) system	2.28 mW, 72–150 bpm	2017	188
Wearable	Neck pulse	PTFE, nylon	A triboelectric sensing textile constructed with core–shell yarns	1.33 V kPa^{-1}, 0.32 V kPa^{-1}	2020	192
Wearable	Neck pulse	PVDF, EC	A triboelectric all-fiber structured pressure sensor	1.67 V kPa^{-1} (0–3 kPa), 0.2 V kPa^{-1} (3–32 kPa)	2020	193
Wearable	Wrist pulse	PU/CNTs/DS, AgNWs	A fibrous stretchable TENG-based sensor with core–sheath structure	10 V, 0.6 μA, 0.02 N, 26.75 V N^{-1}	2021	199
Wearable	Wrist pulse	CB, TPU	A chargeable CB-TPU composite material TENG	4.95 mW m^{-2}, 646% strain	2021	200
Implantable	Heartbeat	PTFE, Cu, PET, Au	A novel implantable TENG driven by the heartbeat of adult swine	14 V, 5 μA, 60–120 bpm	2016	207
Implantable	Heartbeat	PFA, Cu, PVA-NH_2	A coin-sized TENG based on body motion and gravity driven by inertia	136 V 4.9 μW cm^{-3}, 60–150 bpm	2021	209
Implantable	Heartbeat	PTFE, Al, Cu, Teflon, Ti	A TENG-based implanted symbiotic pacemaker for cardiac pacing	65.2 V, 0.5 μA, 50–130 bpm	2019	210
Implantable	Endocardial pressure	PTFE, Au, Kapton, Al	A self-powered endocardial pressure sensor with a surgical catheter	70–350 mmHg, 1.195 mV $mmHg^{-1}$	2019	211
Implantable	Blood pressure	PTFE, Au, Al, Ti	An implantable triboelectric active sensor (iTEAS) for health monitoring	50–120 bpm, 17.8 mV $mmHg^{-1}$	2016	212
Implantable	Heartbeat	Etched Cu, rubber	An eco-friendly no-spacer TENG for heart rate monitoring	3.67 V, 51.7 nA, 99.73% accuracy	2021	213
Wearable	Respiration	Nylon, PTFE	Wearable active acetone biosensor employing chitosan and RGO	Response: 27.89% (10 ppm)	2020	224
Wearable	Respiration	PAN, PVDF	A TENG with nanofibrous membranes for respiration monitoring	RR = 24 BPM, 40 h (stability)	2021	226
Wearable	Respiration	PVA/Ag, FEP	A PVA/Ag nanofiber-based TENG for respiration and gas monitoring	Response: 510% (50 ppm)	2021	227
Wearable	Respiration	MME, PDMS/Al	A multi-scale metal mesh electrode TENG integrated in breathing mask	175.77 V, 0.85 W m^{-2}, 0.014 kPa^{-1}	2021	228
Wearable	Respiration	PAN, PA66	Breathable and highly sensitive self-powered e-skin based on the TENG	330 mW m^{-2}, 0.217 kPa^{-1}	2021	229
Wearable	Sleeping	Silicone, polyester	A textile for monitoring all-around physiological parameters during sleep	10.79 mV Pa^{-1}, 0–40 Hz	2020	231
Implantable	Respiration	PET, PTFE	A TENG-based ultra-stretchable micro-grating i-NG system	2.2 V, 45 kPa, 900% strain	2018	232
Wearable	Foot	PTFE, napkin, Cu	Integrating N-TENG into the insole to detect the perspiration of foot	363 V, 42.38 μA	2021	233
Wearable	Skin	PDMS-MXene, PET, ITO	A sensor can monitor physiological signals and imitate touch sensation	0.18 V Pa^{-1} (10–80 Pa), 0.06 V Pa^{-1} (80–800 Pa)	2021	235
Implantable	Bladder pressure	Polyimide, Au	*In vivo* experiments are performed for delivering various bpm to the nerves	25–150 BPM	2019	236
Implantable	Skin	PDMS, Kapton	An integrated tactile TENG device which is implanted under the skin	3 V, 1–20 kPa	2021	238

5.1 Gesture-based interface

Human fingers are dexterous, presenting complicated gestures containing abundant encoded information, which are convenient for intention expression. To decode such gesture information, the developed sensing interfaces are being embedded into integrated gesture-sensing gloves.[252] The representative work on HMIs based on gestures is illustrated in Fig. 11.

Researchers have attempted to attach TENGs on gloves to construct novel HMI gloves distinct from the commercial rigid and bulky HMIs with the advantages of flexibility, low cost, easy operation, and low power consumption. Luo *et al.* attached a bending-angle TENG (BA-TENG) on a simple glove to develop a multi-dimensional HMI device.[253] As shown in Fig. 11a, the device integrated with a customized print circuit board (PCB) exhibited high sensitivity and low crosstalk in real-time finger motion sensing with multi-channels. It has been widely applied for smart-home and robotic control by extracting and analysing the multi-dimensional signal features of the BA-TENG. Similarly, Sun *et al.* designed a haptic-feedback ring enabled glove-based HMI that used a ring-shaped TENG for finger bending sensing and a lead zirconate titanate (PZT) thin film for haptic sense simulation.[254] With the voltage integration method, the continuous motion of the finger was captured *via* a minimalistic design. The real sense of touch was successfully simulated by using PZT to stimulate the haptic feedback function, showing great potential in novel virtual reality applications. As shown in Fig. 11b, He *et al.* presented an intuitive glove-based HMI, which consisted of a PEDOT:PSS coated textile strip stitched onto the glove and a layer of silicone rubber thin film coated on the glove.[255] It was demonstrated to be applied for diversified HMI sceneries, such as wireless car and drone control.

Additionally, textile-based TENGs with excellent washability have been woven into gloves to fabricate HMI gloves for gesture interaction, which has realized more accurate intelligent clothing control due to the high outputs of TENGs. Xie *et al.*

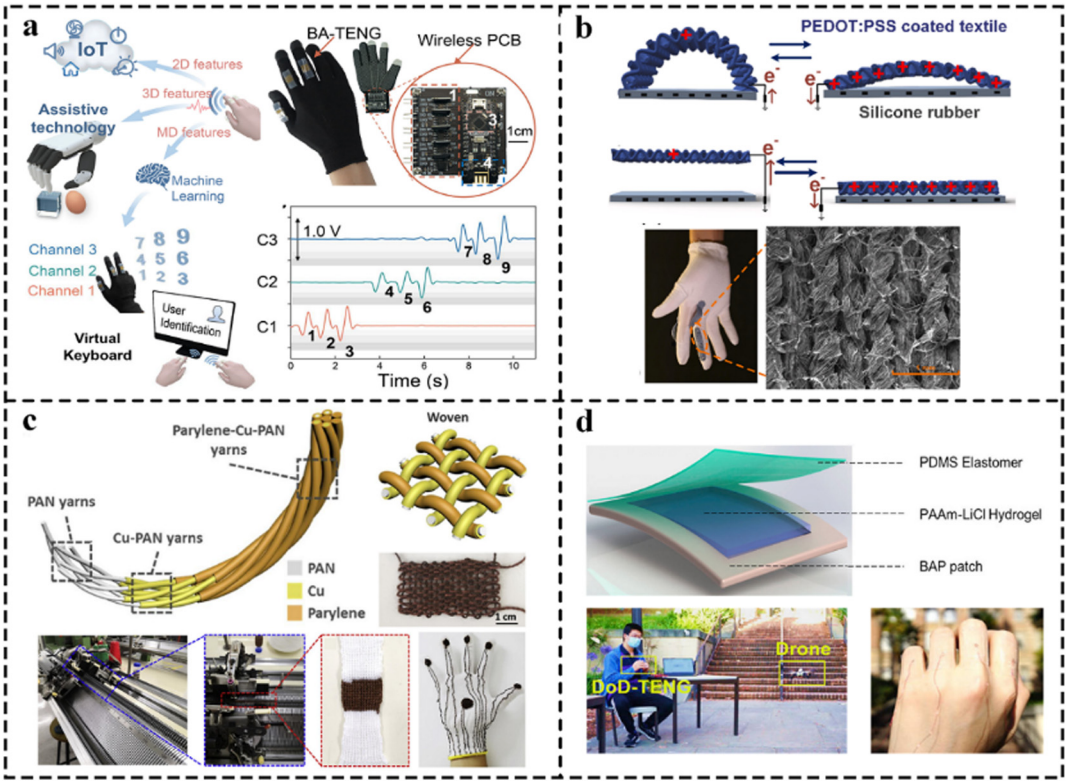

Fig. 11 Representative work on the HMI based on gestures. (a) A BA-TENG attached on a simple glove with a wireless PCB. Reproduced with permission from ref. 253, Copyright 2021, Elsevier. (b) Schematic illustration of the TENG-based glove. Reproduced with permission from ref. 255, Copyright 2019, Elsevier. (c) Structural design and fabrication process of the textile-based TENG and a smart woven glove. Reproduced with permission from ref. 257, Copyright 2020, Elsevier. (d) Configuration of the DoD-TENG and the navigation of the drone *via* the DoD-TENG on human fingers. Reproduced with permission from ref. 258, Copyright 2021, Elsevier.

constructed a fibre-shaped stretchable and tailorable TENG with high stability and continuous conductivity by using a geometric constructed steel wire as the electrode and selecting an ingenious silicone rubber as the triboelectric layer.[256] The fabricated device with a length of 6 cm and a diameter of 3 mm generated an open-circuit voltage of 59.7 V, a short-circuit current of 2.67 μA and an average power of 2.13 μW at a frequency of 2.5 Hz. It was also woven on gloves to monitor the motions of fingers, and it achieved the recognition of the bending angle of every single finger and numbers of bent fingers by analysing the collected signals. As shown in Fig. 11c, Zhao *et al.* firstly interweaved Cu-coated polyacrylonitrile (Cu-PAN) yarns and parylene coated Cu-PAN (parylene-Cu-PAN) yarns *via* machines to fabricate TENG-based textile pressure sensors with good breathability and washability.[257] The fact that the materials, processing circumstances, and manufacturing methods affected the sensitivity and washability of the designed sensors was demonstrated by experimenting different textile-structured TENG-based sensors under various fabrication conditions. Meanwhile, a textile glove with attached pressure sensors was fabricated to demonstrate posture detection.

Miniature electronics with biocompatible adhesion to skin surfaces are defined as electronic skins (E-skins). TENGs with compatibility, shape-adaptability, and adhesion have been employed to obtain accurate and reliable information by attaching TENGs on skins. Considering the damage of TENGs to the skin, Gao *et al.* proposed an innovative method to fabricate biocompatible bonding/debonding bistable adhesive polymers (BAPs) with skin temperature-triggered conformal adhesion (Fig. 11d).[258] They developed a debonding-on-demand TENG (DoD-TENG) which consisted of a BAP, a polydimethylsiloxane elastomer, and an ion-conductive elastomer. The DoD-TENG was used as a human–machine interface for a self-powered drone navigation system. Shan *et al.* designed a TENG-based artificial kinesthetic system with a field effect synaptic transistor which simulated the learning process of nerves.[259] The single-electrode TENG, with PDMS/MXene as the material of the triboelectric layer, exhibited a high sensitivity of 0.197 kPa^{-1} in the low-pressure region (6–30 kPa region). The proposed system achieved the assessment of fatigue driving risk by perceiving the motion state of muscles and joints.

5.2 Tactile-based interface

In addition to the above common gesture-based interfaces, other types of interfaces with novel designs have also received great research interest recently. A most extensive application for TENG-based HMI devices focuses on the monitoring of external pressure, which is exerted through human body touch.[260–263] Tactile interfaces, which are mainly developed based on the contact–separation mode[264,265] or the lateral-sliding

mode,[266] have been usually designed with sensing arrays consisting of a large number of sensing pixels.[40,267] This high structural complication brings extra difficulty in the layout design, transmission, and analysis. To address this issue, several dexterous designs have been constructed recently, aiming at fewer sensing electrodes for similar functions.[268–270] This section introduces tactile-based interfaces based on the contact–separation mode and sliding mode.

5.2.1 Contact–separation mode. Tactile-based interfaces based on the contact–separation (C–S) mode have been widely employed as HMI devices, such as keyboards and tactile switches.[271] Moreover, the recent representative work on HMIs based on the contact–separation mode is illustrated in Fig. 12.

Diversified self-powered keyboards have been developed *via* various TENGs with the advantages of flexibility, wearability, and portability, which can function *via* human finger tactile force.[272,273] He *et al.* designed a triboelectric vibration sensor (TVS) by simulating the ampulla in the lateral line of fish to perceive an external micro-vibration accurately.[274] The sensor achieved a high sensitivity of 0.97 V N^{-1} at a low force (<1 N). A TVS-based virtual digital keyboard was designed by sensing and locating the position of the keystroke for interactive input. As shown in Fig. 12a, Xia *et al.* presented a multifunctional alginate-metallic complex TENG, which demonstrated adaptable electrical output, by synthesizing the alginate complexes with different metal ions.[275] It was proved to be practical as a self-powered sensing array based on the binary-decimal conversion system, which offered a new insight for the development of HMI devices. Yi *et al.* developed a sandwich-structured fabric-TENG (F-TENG) with high flexibility for real-time biometric authentication.[276] A self-powered wearable keyboard was demonstrated to simultaneously trace and record physiological signals and identify the typing habits of individuals *via* the Haar wavelet by integrating large-area F-TENG sensor arrays. Ahmed *et al.* presented a flexible keyboard based on TENGs, which was employed for interacting with computers *via* wireless communication due to its self-powering mechanism.[264]

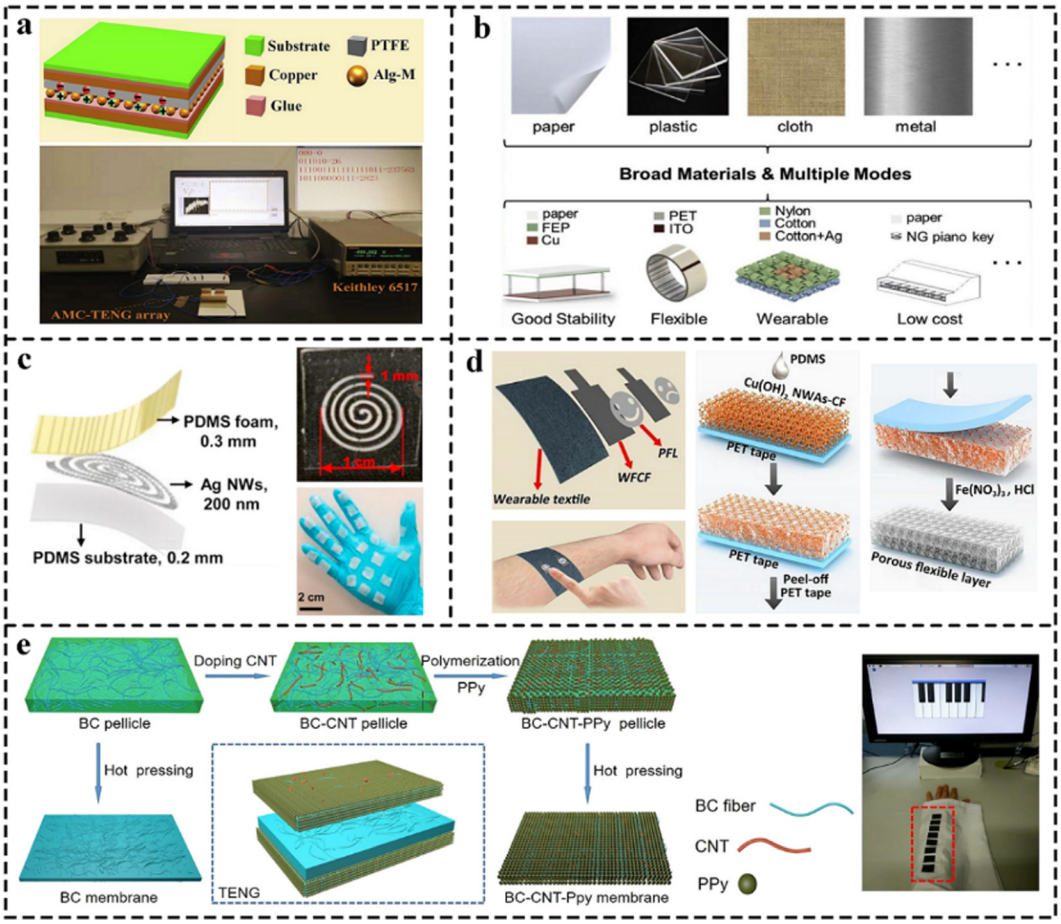

Fig. 12 Recent representative work on the HMI based on the contact–separation mode. (a) Schematic illustration of the TENG, and diagram of the TENG-based binary converter system. Reproduced with permission from ref. 275, Copyright 2020, Elsevier. (b) Various devices based on the tactile TENG with optional materials. Reproduced with permission from ref. 278, Copyright 2019, Elsevier. (c) Structural design of the foam-based TENG for tactile sensing. Reproduced with permission from ref. 280, Copyright 2021, Elsevier. (d) Fabrication process of the PEL and configuration of the PEL@WFCF-TENG. Reproduced with permission from ref. 281, Copyright 2021, Elsevier. (e) Fabrication process of the BC-TENG and schematic illustration of the wearable piano based on the BC-TENG. Reproduced with permission from ref. 282, Copyright 2021, Elsevier.

TENG-based HMI devices have been broadly applied in precise digital control and smart home applications due to the sensitivity and stability of TENGs.[277] Huang *et al.* designed a versatile tactile interactive system (TIS) through a self-powered optical communicator triggered by a TENG.[278] As shown in Fig. 12b, the developed TIS with a simple circuit design and low power consumption was applied to execute various applications, such as tactile switch and domestic wireless controller. Jiang *et al.* fabricated a stretchable composite electrode through synchronous electro-spinning of thermoplastic polyurethane (TPU) and electro-spraying of silver nanowires (AgNWs).[279] Meanwhile, with the optimized materials and structures, an ultrathin skin-inspired TENG with washability was constructed to conformally attach on human skin. As shown in Fig. 12c, Wu *et al.* developed an ultrathin TENG-based sensor with the integration of porous poly(dimethylsiloxane) foam and serpentine silver nanowires.[280] It generated an open circuit voltage of 78.7 V and a power density of 33.75 W m^{-2}, which was 20 times higher than that of the pure silicone-based TENG. The interactive capability of the TENG was demonstrated by integrating 24 sensors into a glove.

Various novel materials have been developed in specific tactile-interaction circumstances to overcome environmental factors such as humidity, and achieve eco-friendliness. Wang *et al.* used a porous flexible layer (PFL) and a waterproof flexible conductive fabric (WFCF) to construct a humidity-resistant TENG (PFL@WFCF-TENG).[281] It exhibited high outputs (135 V, 7.5 μA, 631.5 mW m^{-2}) and excellent humidity resistance (80% RH) with an area of 2 × 4 cm^2. A portable and wearable self-powered haptic controller was designed for various HMI devices *via* a microelectronic module (Fig. 12d). Biocompatible bacterial cellulose (BC) with good mechanical properties and a distinctive porous network has been proven to be suitable as the material of eco-friendly TENGs. Zhang *et al.* designed a recyclable interactive device based on a BC-TENG that consisted of pure BC and conductive BC (Fig. 12e).[282] It yielded an open-circuit voltage of 29 V and a short-circuit current of 0.6 μA.

5.2.2 Sliding mode. TENGs based on the lateral sliding mode can be employed for wireless controlling HMI applications, including writing pad,[283,284] tablet,[285] and touch pad.[286] The recent representative work on HMI applications based on the sliding mode is illustrated in Fig. 13.

Similar to gesture-based interfaces, e-skins have also been employed for tactile interfaces based on the sliding mode TENG. As shown in Fig. 13a, TENG-based e-skins have great potential in fine texture recognition. Zhao *et al.* designed a TENG-based fingerprint-inspired electronic skin (FE-skin) that exhibited a fast response to fine textures of the bionic-designed fingerprint.[287] The FE-skin detected the contact area between the fingerprint surface and the tested object surface with a minimum discerned texture size of 6.5 μm. Different textures were identified by using artificial neural networks to process

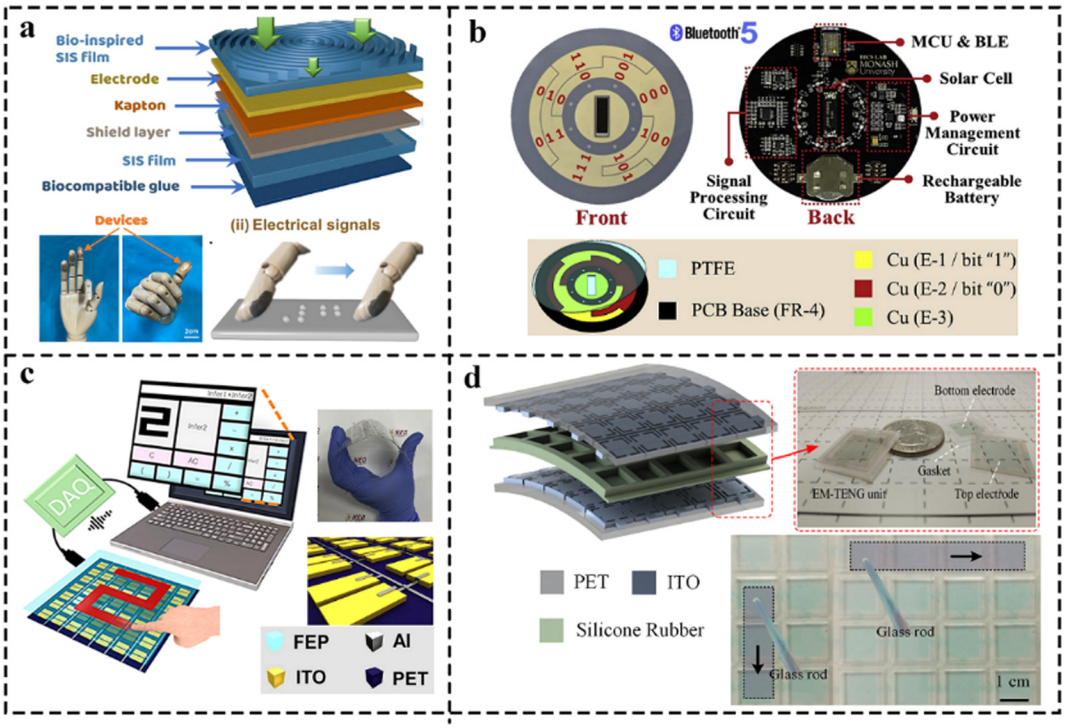

Fig. 13 Recent representative work on the HMI based on the sliding mode. (a) Configuration of the TENG-based FE-skin for sliding mode tactile sensing. Reproduced with permission from ref. 287, Copyright 2021, Elsevier. (b) Structural design and working principle of the TENG-based control disk interface. Reproduced with permission from ref. 290, Copyright 2020, Elsevier. (c) Schematic illustration of the TENG-based touchpad. Reproduced with permission from ref. 291, Copyright 2020, Elsevier. (d) Schematic illustration of the EM-TENG structure, and working principle of the device for the human–machine interface. Reproduced with permission from ref. 294, Copyright 2020, Elsevier.

the collected signals from TENGs. The test results demonstrated that disordered and ordered texture achieved accuracy rates of over 93.33% and 92.5%, respectively. It was proved to be superior in the field of bionic tactile perception, which was expected to be promising for HMI applications. Shi *et al.* designed a TENG-based electro-tactile (ET) system with high sensitivity *via* the ball-shaped electrode array to experience the real touch feeling.[288] The integrated ET system achieved touching position and motion trace on the TENG surface reappearing on the skin. To apply e-skin in the next generation of biomedicine and robotics, Yu *et al.* proposed an integrated perspiration-powered electronic skin (PPES) for human metabolic sensing *in situ*. The key metabolic analytes and the skin temperature during physical activities were monitored and wirelessly transmitted to the user terminal interface *via* Bluetooth.[289]

Additionally, TENGs with good flexibility and high sensitivity have been implemented as practical HMI devices by modelling the graphical user interface. Qiu *et al.* designed a control disk interface based on PTFE films and a photovoltaic cell (Fig. 13b).[290] It realized eight sensing transitions *via* the 3-bit BRGC encoding patterns. The fabricated control disk was utilized for wireless control of smart applications through a signal processing circuit and a Bluetooth transmitter. As shown in Fig. 13c, Yun *et al.* proposed a self-powered triboelectricity-based touchpad (TTP) with a TENG array (49 pixels) that was constructed of a thin and transparent substrate.[291] The designed TTP achieved recognition and classification of the digit patterns from '0' to '9' with an accuracy of 93.6%, 92.2%, and 91.8% at the bending angles of 0°, 119°, and 165° *via* the pre-trained neural network. Moreover, it is essential for event-driven information communication to design a self-powered patterned display. As a solution, Sun *et al.* presented a TENG-based MXene enhanced alternating current electroluminescence (ACEL) device array with stretchability and transparency.[292] Meanwhile, a patterned ACEL device was fabricated and implemented as a self-powered display for human health monitoring.

The sensitivity of TENGs can also be enhanced by using novel materials, which promotes a more sensitive tactile interface based on the sliding mode. Considering the issues of the large volume and narrow detection range of commercial acceleration sensors, Wang *et al.* designed a TENG-based miniaturized acceleration sensor with high accuracy, large detection scale, and eco-friendliness.[293] Experiments demonstrated that accelerations ranging from 0.1 m s^{-2} to 50 m s^{-2} were identified according to the relationship of response time and accelerations in the horizontal direction. Furthermore, no obvious decrease of output voltage was observed after 2000 operating cycles, exhibiting outstanding robustness and reliability. As shown in Fig. 13d, Ba *et al.* reported a novel TENG-based array with the electrode-miniaturized strategy.[294] Through comprehensive experimental measurements it was demonstrated that two-third reduction in the electrode area only presented a slight effect on the electrical output of the TENG. Moreover, a microsystem for trajectory tracking was successfully fabricated to demonstrate that the proposed strategy endows TENG with two more significant advantages, including higher light transmittance and lower signal interference.

5.3 Other types of interfaces

Besides the above typical methods of interface with human fingers, low-power TENG-based sensors can also be employed as HMI applications by attaching them to many human body parts, such as muscle,[295] foot,[296] eye,[168,185] ear,[297] and throat.[298,299] Inspired by the croaking behaviour of frogs, Zhou *et al.* designed a self-powered TENG-based bionic sensor with high ultra-sensitivity (54.6 mV mm^{-1}), a high-intensity signal (±700 mV), and a wide sensing range (0–5 mm), which functioned as a muscle-triggered communication aid device for the disabled.[295] The signal intensity was 206 times higher than that of traditional biopotential electromyography methods. The proposed bionic sensor provided a promising research direction for HMI applications for the disabled. Guo *et al.* developed an intriguing auditory system integrated with a triboelectric auditory sensor (TAS) based on a contact–separation mode TENG for an auxiliary hearing aid, which exhibited an ultrahigh sensitivity of 110 mV dB^{-1}.[297] The prepared TAS was integrated into smart robotics to achieve intelligent interaction with humans *via* wireless communication, such as voice recognition and music recording. The auditory system, as one of the most effective and straightforward communication strategies between humans and robots, was expected to have potential applications in the field of HMI.

Moreover, various types of wireless transmission have demonstrated their feasibility of being applied to the human–machine interface. Zou *et al.* proposed a bionic stretchable nanogenerator for human body multi-position motion sensing. It was employed to monitor the human motion during swimming for training and safety *via* the integrated wireless module.[300] Chen *et al.* presented a TENG-based wireless sensing system, consisting of a microswitch, a capacitor–inductor oscillating circuit, and a wireless transmission module.[301] Summarily, the recent developments in wireless communication foster the development of a WBAN, enabling the human–machine interface to be widely distributed in biomedical fields.[302,303] The aforementioned representative studies are summarized in Table 4.

6. Discussion

Recent years have witnessed many leading teams in this field making a series of innovative advances and achieving substantive progress in the aspects of output improvement and application extension of TENGs. The development status of TENGs in human body IoT systems has been more and more acknowledged based on the previous studies above. Here, statistic-based discussions (Fig. 14) about these studies are presented for further research on focused aspects of the development trends, materials, and integration approaches.

6.1 Development statistics

After sorting out the above studies, we conduct data-oriented discussions of interest from statistical perspectives. We collect

Table 4 Summary of the studies on HMIs based on various TENGs

Type	Material	Description/highlight	Year	Ref.
Gesture	PI encapsulation, Au, IZO nano-membrane	An ultrathin TENG which proved the feasibility of a closed-loop gesture-based HMI system	2019	252
	Silicone rubber, Cu, PDMS	A glove-based HMI with a bending-angle TENG for gesture sensing	2021	253
	PTFE, TPU, Al	A glove-based HMI with a TENG-based haptic-feedback ring for monitoring the bending of fingers	2021	254
	Silicone rubber, Spiral steel wire	A tailored TENG woven on a glove for finger motion sensing	2019	256
	PAN, Cu, Parylene	A TENG-based textile pressure sensor with outstanding breathability and washability	2020	257
	Ag NWs, PDMS/Mxene	A system can simulate the learning process of nerves by a field effect synaptic transistor	2021	259
Tactile (C–S mode)	PTFE, PMMA, Al	A facial mask-based TENG which is harmless to skin can serve as a touch sensor	2021	273
	PTFE, PE, Au, Cu	A TENG-based sensor by simulating the ampulla of fish to perceive an external micro-vibration	2019	274
	Glue, PTFE, Alg-M, Cu	A multifunctional TENG by synthesizing the alginate complexes with different metal ions	2020	275
	PVDF-TrFE/MXene, nylon-11	A sandwich-structured fabric-TENG with high flexibility for real-time biometric authentication	2021	276
	PTFE, CNT, Ag	A novel TENG demonstrated as a self-powered switch for controller of smart home appliances	2021	277
	FEP, Cu, PET, nylon	A tactile interactive system through an optical communicator triggered by a TENG	2020	278
	VHB, TPU, Ag NWs	A skin-inspired TENG with washability, which can conformally attach on human skin	2020	279
	PDMS foam, Ag NWs	An ultrathin TENG-based sensor integrated on a glove to magnify the capabilities of sensing	2021	280
Tactile (sliding mode)	PTFE, PET, Cu	A TENG-based electro-tactile system with high sensitivity *via* the ball-shaped electrode array	2021	288
	PTFE, Cu	A control disk interface based on a sliding mode TENG	2020	290
	FEP, Al, ITO, PET	A triboelectricity-based touchpad (TTP) with a TENG array (49 pixels)	2020	291
	ZnS, SWCNT	A TENG-based MXene enhanced alternating current electroluminescence (ACEL) device array	2021	292
	PTFE, Cu, steel	A TENG-based miniaturized acceleration sensor with high accuracy	2021	293
	PET, ITO, silicone rubber	A novel TENG-based array with the electrode-miniaturized strategy	2021	294
Others	Ag NWs, carbon	A TENG-based bionic sensor as a muscle-triggered communication aid device for the disabled	2021	295
	Kapton, Cu, FEP	An auditory system integrated with a triboelectric auditory sensor for an auxiliary hearing aid	2021	297

a total of 187 published papers which are elaborated in this review ranging from the year of 2017 to 2021, including 38 papers in ''TENG-based human energy harvesting (EH)'', 104 papers in ''TENG-based human motion and physiological signals monitoring'', and 45 papers in ''TENG-based human–machine interface (HMI)''. Meanwhile, 104 papers in ''TENG-based human motion and physiological signals monitoring'' are divided into three categories, including 49 papers in ''TENG-based wearable human motion signals monitoring (WHMS)'', 38 papers in ''TENG-based wearable human physiological signals monitoring (WHPS)'', and 19 papers in ''TENG-based implantable human physiological signals monitoring (IHPS)''. The relevant statistics are shown in Fig. 14a.

Fig. 14a reveals that the related studies show an overall rapid growth during these years, while a slight trough period is observed in 2019. The potential reason for the downturn is the bottleneck of materials and structures, resulting in a narrow scope of research. Subsequently, combining 5G technology with the novel materials and innovative structures, various studies related to TENG-based human body IoT systems are increasingly prevailingly reported leading to a distinctly rapid growth period after a few years. Furthermore, more intriguing materials and structures will be employed for performance enhancement of TENGs to improve the reliability and stability of human body IoT systems.

6.2 Statistics of triboelectric materials

The material, as one of the crucial factors for the enhancement of energy conversion efficiency in the process of the triboelectrification effect, plays a major role in improving the output performance of TENGs. Here, we present a statistical discussion on triboelectric materials in this review to offer inspirational angles.

With regard to the non-metallic triboelectric materials, Fig. 14b and c demonstrate that the most mainstream materials of TENGs are PDMS and PTFE in the human body based TENG applications. In the early stage, considering the special demand of stretchability and flexibility for the human body, PDMS, as one of the typical flexible silicone rubber materials, exhibited excellent properties for working as a triboelectric layer of wearable TENGs. Subsequently, the superiorities of PTFE were gradually disclosed, which motivated a growing number of developments in PTFE-based TENGs. As the statistics show, PTFE has become one of the dominant electronegative materials.

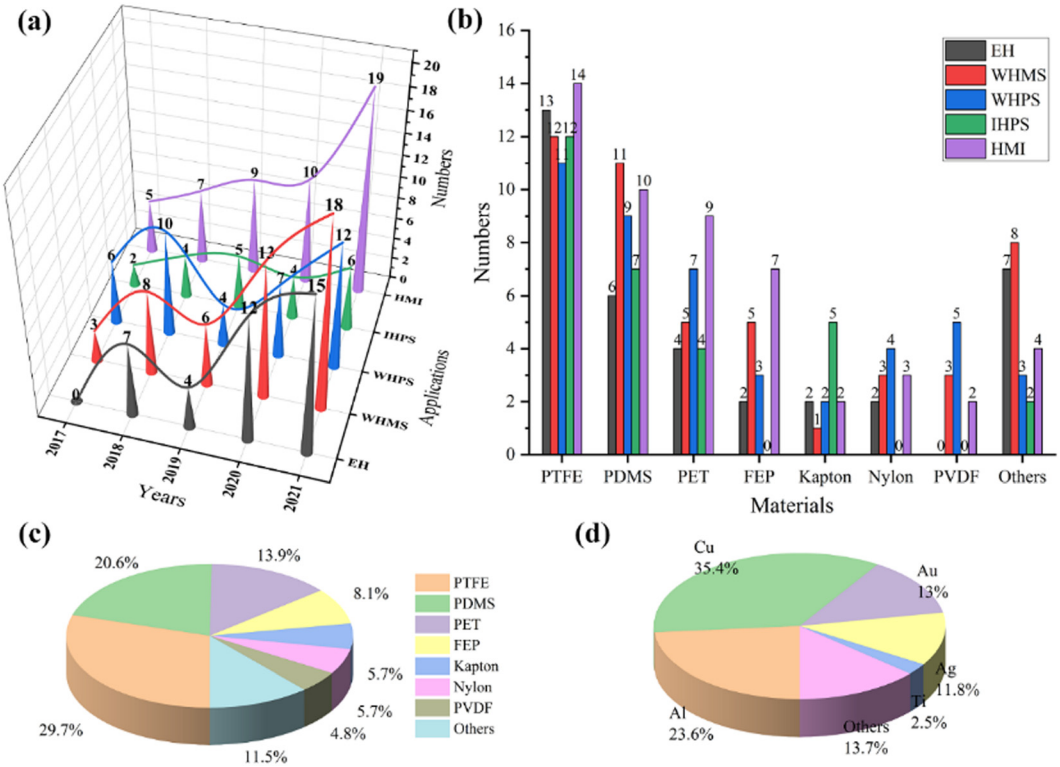

Fig. 14 Statistics of representative studies in this review. (a) The trend of representative published papers from 2017 to 2021 in this review. (b and c) The histogram of various non-metallic triboelectric materials of TENGs for different sceneries. (d) The proportion of various metallic triboelectric materials of TENGs.

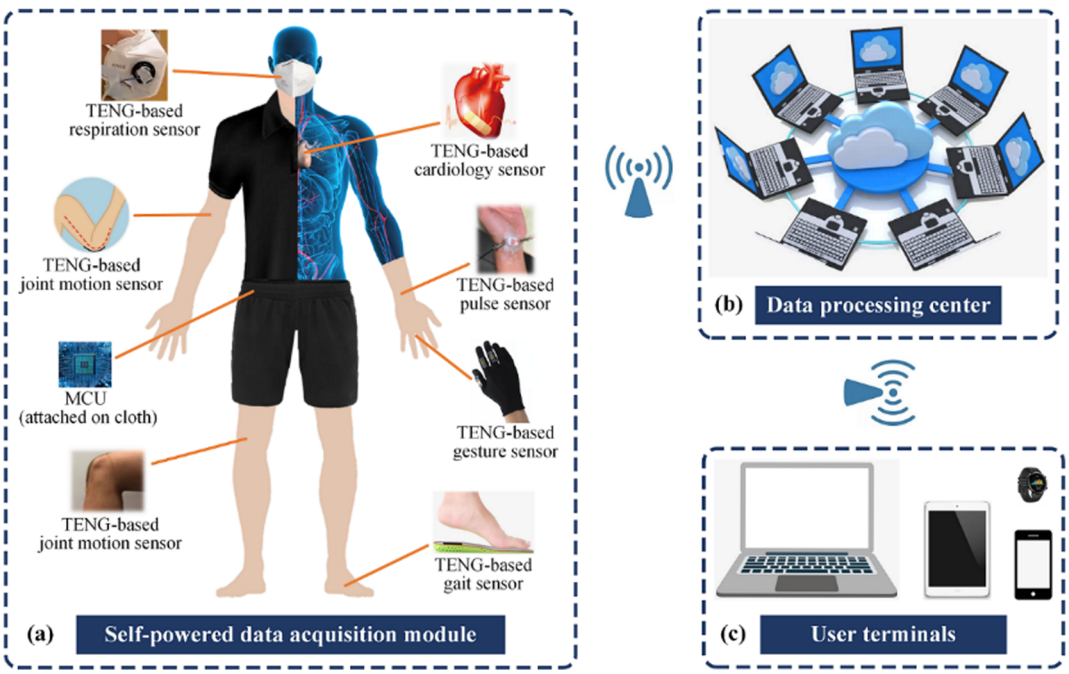

Fig. 15 Schematic illustration of the proposed TENG-based human body IoT system with three modules. (a) The self-powered data acquisition module with various wearable and implantable TENG-based sensors. The signals from these sensors can be processed by a MCU which is attached on cloth. (b) The data processing center with multiple functions can be employed to further process data from different individuals *via* wireless communication. (c) The data analysed and processed by the data processing center can be transmitted to the user terminals *via* wireless communication.

Meanwhile, researchers have never slowed down their exploration of other special materials which are capable of being applied in specific conditions, such as degradable materials in eco-friendliness, washable materials in textile, water-proof materials in humidity, and fire-proof materials in fire scenes.

Different from non-metallic materials, metal materials are employed as both electrodes and triboelectric layers. Fig. 14d presents that Al foil, as the most typical electropositive material, has been widely employed to fabricate the electrode because of its good conductivity and high surface cleanliness. Additionally, high-cost Cu foil is sometimes implemented as a substitute for Al foil to achieve higher outputs due to its higher conductivity. Compared with the former two metal materials, Au foil can further reduce the size of TENGs and extend the lifespan of TENGs owing to its high ductility and stability. Moreover, conventional metal electrode materials are not suitable for special occasions requiring specific materials, such as implantable TENGs with titanium (Ti) electrodes. Therefore, researchers are still attempting to synthesize new materials for various TENG-based human body IoT applications.

6.3 Integration of TENGs for human body IoT systems

In order to systematically monitor and manage human body status information *via* self-powered devices, it seems increasingly worthwhile to integrate the aforementioned three modules of harvesting, sensing and interfacing to the TENG-based human body IoT system. Such an IoT system can be applied for monitoring human motion and health status *via* TENG-based wearable/implantable devices with the properties of flexibility, compatibility, stability, and durability, powered by human mechanical motion and physiological activities.

The proposed concept of the TENG-based human body IoT system (Fig. 15) in this review can include a self-powered data acquisition module, a data processing center and various user terminals. Owing to smart cloth that is worn on the users, the self-powered data acquisition module can collect data *via* wearable and implantable TENG-based sensors for monitoring joint motion, finger gesture, respiration, pulse, *etc.* Besides, the data obtained by interaction with the external devices can also be collected in this module. Furthermore, the data processing center executes the multi-functions of data storage, data analysis, data management, physical status diagnosis and prediction, and control of data transmission. The data of exercise information, health diagnosis and medical records stored in the cloud are available for users to check *via* mobile terminals. The wireless communication technology is adopted between each module. Owing to the information sharing of individuals *via* the internet, such integrated systems will be expected to be promising prospects for medical diagnosis and health management in future.

7. Conclusions and perspectives

In this review, we have thoroughly discussed and summarized the recent studies towards the construction of the TENG-based human body IoT system, including energy harvesting, sensing, and interfacing. Firstly, as for human body energy harvesting, TENGs exhibit promising potential for smart wearables with the advantages of flexibility, comfortability, light weight, low cost, and high performance. Studies on harvesting human mechanical energy with TENGs have been summarized as two categories, *i.e.*, configurations and material synthesis and interface processing. Secondly, as for human body sensing, wearable and implantable TENG-based sensors have been proposed with capabilities to achieve posture recognition by sensing the human motion information, and to monitor human health status by analysing the human psychological signals. We have summarized most recent studies on TENG-based wearable sensors with the advantages of high sensitivity and stability which have been employed in human body status monitoring, such as monitoring of joint motions, hand gestures, and gaits, and monitoring of heart beat, pulse, and respiration. In addition, we have also summarized implantable TENGs with the properties of miniaturization and biocompatibility which have been applied in continuous monitoring of physiological signals to support disease diagnosis. Thirdly, researcher have realized information communication between the human body and external electronics by processing and analysing the collected electrical signals generated by TENGs. Such studies have been summarized based on various types of interfaces, including gesture interfaces and tactile interfaces based on the contact–separation and sliding mode. Finally, we have made a thorough statistical discussion of studies on TENG-based human body IoT systems in recent years. Discussions about the developmental trend and research hotspot have also been performed in detail. Integration of TENGs and the working mechanism of different modules have also been comprehensively illustrated to further achieve the integration and systematization of human body IoT systems for human health management.

Summarily, the current advances of TENGs shed light on the feasibility of digitized and integrated systems featured with wireless sensing, exhibiting promising prospects in the revolution of electronics in the future. Nonetheless, as an emerging technology, the TENG presents limitations including low durability and stability that need to be further explored for more progressive human body IoT systems. To promote the development of smart sensing and IoT fields, the main areas where future research may need to concentrate are proposed below.

(1) Stability and durability of TENGs. The output stability and durability of TENGs are critical factors for robustness in lifespan and electric outputs. An obvious issue is that the outputs of TENGs fluctuate due to the change of surroundings, such as the humidity[304] and temperature.[305,306] Considering that the human body will be exposed to various liquids, such as rain and sweat, it is a potential solution to use hydrophobic materials with humidity resistance such as improved polydimethylsiloxane (PDMS) with a nanostructure. Additionally, triboelectric layers of TENGs are worn after working for thousands of cycles, which leads to an inferior output.[307,308] Therefore, synthesizing a novel triboelectric layer featured with

corrosion resistance and wear resistance is essential for TENGs, especially implantable TENGs that demand long lifespan.

(2) Wearability and comfort of TENGs. To meet the comfort of wearing, it is essential to design lightweight, shape-adaptable, and skin-breathable TENGs while maintaining their high output performance simultaneously.[309] As potential solutions, textile materials, including carbon-based materials and natural products like wool and cotton, can be possibly implemented as the elements of triboelectric layers to improve air permeability. Developing materials with buffer function such as liquid metal may be a significant direction for protecting TENG-based sensors which are attached or woven on cloth.

(3) Biocompatibility of TENGs. Human skin, which covers the whole human body, plays a significant role in interacting with the external objects. Inspired by human skin, e-skin provides the possibility to achieve non-invasive medical diagnosis, human–machine interface, and prosthetics. As a potential solution, the chitosan (CS) membrane, with chitosan being a natural polymer with the properties of biocompatibility and biodegradability, is suitable to function as the triboelectric material of TENG-based e-skin. However, its high water vapor penetration ability and unsatisfactory mechanical properties are major challenges. The biocompatibility and other properties of the CS membrane can be effectively improved *via* interface processing, centrifugation, and other operations. Thus, from the perspective of material properties, choosing appropriate materials for synthesis and interface processing may effectively improve the biocompatibility of TENGs in future.

(4) TENG packaging: developing effective packaging technology for TENGs. The packaging of TENGs will be vitally important to make them commercialized products especially for application in a variety of hash environments, because moisture or any surface contaminant can largely affect the performance of the TENG. However, packaging of TENGs may be more difficult than that of the traditional micro electromechanical system devices, since TENGs contain parts in motion and possible air gaps to separate surface charges. To ensure the portability and stability of TENG-based devices, lightweight waterproof materials such as polyurethane will be suggested for employing as the shell for TENG packaging.

(5) Power management. Versatile TENGs, which are featured with high voltage, low current, and large internal impedance, usually yield AC outputs which need to be converted, transmitted, and finally stored for reutilization. Conventional power management approaches produce a large dissipation in the above processes. Thus, efficient power management strategies and energy storage units are desirable to effectively improve the energy conversion, transmission, and storage efficiency for constitution of stable and sustainable integrated systems. Specifically, as an alternative solution of the traditional impedance-matching approach, energy conversion efficiency can be enhanced effectively by minimizing the capacitive load of the improved energy extraction enhancement circuit. Furthermore, the design of the power management circuit suitable for the TENG network remains to be further studied.

(6) Communication and networking. As 5G wireless communication technology is rapidly getting integrated into the IoT systems, an increasing number of TENG-based smart devices are equipped with capabilities to access and collect information conveniently, analyse and process data precisely, and transmit messages rapidly.[310] It is worth mentioning that wireless communication between human body IoT systems, which are adopted for continuously monitoring the human body status by integrating with various wearable/implantable TENG-based sensors, can be realized *via* the internet. For *in vitro* monitoring, including human motion status and health monitoring, the human motion posture and medium-long distance transmission are a challenge for WBAN. Therefore, it can be considered to design a communication protocol that can be dynamically adjusted according to the possible human motion posture and transmission distance while ensuring anti signal interference. Meanwhile, clothing made from conductive fabrics can be used to transmit signals through radio surface plasmons propagating on metamaterial textiles, which can provide wireless transmission for textile-based wireless tactile sensing. Furthermore, the stability of long-distance data transmission is a direction worthy of further studies.

(7) AI technology. The majority of researchers focus on the monitoring and diagnosis of human body conditions. Studies on the prediction of individuals' potential diseases *via* TENGs have not been reported. Therefore, by combining with AI technologies, such as machine learning[311] and deep learning,[312] a long-term prediction of potential life-threatening diseases can be explored by analyzing the disease-related physiological indicators which are monitored by TENGs. Subsequently, personalized medical guidance and suggestions can be offered to prevent diseases in their early stages. Furthermore, combined with AI technology, we can effectively monitor and predict the physical status that can be monitored by TENG-based sensors, so as to focus on our physical state at all times.

(8) Fundamental theory of TENGs. The expanded Maxwell's equations, as the fundamental theory of TENGs, implied that physical contact among the moving media creates electrostatic charges on their surfaces in the mechano-driven slow moving media system due to the triboelectrification effect. The term $\boldsymbol{P}_S$ in eqn (8) is mainly due to the surface electrostatic charges, and the terms $\nu \times \boldsymbol{B}$ and $\nu \times (\boldsymbol{D}' + \boldsymbol{P}_S)$ in eqn (14) and (15) are the sources of electromagnetic waves generated by moving media. The current theory may be applied to explain the electromagnetic wave generation, transmission, scattering and reflection behaviour of TENGs due to additional contributions to such behaviour introduced by the electrostatic charges on the surfaces of TENGs.[70] Starting from the expanded Maxwell's equations, the influence of the magnetic field on the performance of TENGs remains to be further studied. Additionally, further research on electromagnetic waves emitted from TENGs may contribute to the development of wireless communication, signal processing, and imaging.

Conflicts of interest

There are no conflicts to declare.

Acknowledgements

This work is supported and funded by The National Natural Science Foundation of China (No.: U1813217, 62001281), "Shuguang" Program of Shanghai Education Commission (No.:20SG40) and the Shanghai Sailing Program (No.: 20YF1412700).

References

1 S. Li, Q. Ni, Y. Sun, G. Min and S. Al-Rubaye, *IEEE Trans. Ind. Inform.*, 2018, **14**, 2618–2628.
2 F. Hussain, S. G. Abbas, G. A. Shah, I. M. Pires, U. U. Fayyaz, F. Shahzad, N. M. Garcia and E. Zdravevski, *Sensors*, 2021, **21**, 3025.
3 A. Al-Fuqaha, M. Guizani, M. Mohammadi, M. Aledhari and M. Ayyash, *IEEE Commun. Surveys Tutorials*, 2015, **17**, 2347–2376.
4 M. Frustaci, P. Pace, G. Aloi and G. Fortino, *IEEE Internet Things J.*, 2018, **5**, 2483–2495.
5 A. Tewari and B. B. Gupta, *Future Gen. Comput. Syst.*, 2020, **108**, 909–920.
6 Internet of Things (IoT) Connected Devices Installed Base Worldwide from 2015 to 2025, **https://www.statista.com/statistics/471264/iot-number-of-connected-devices-worldwide/**.
7 L. Chettri and R. Bera, *IEEE Internet Things J.*, 2020, **7**, 16–32.
8 Z. L. Wang and W. Wu, *Angew. Chem., Int. Ed.*, 2012, **51**, 11700–11721.
9 Z. L. Wang, J. Chen and L. Lin, *Energy Environ. Sci.*, 2015, **8**, 2250–2282.
10 Y. Tang, H. Zhou, X. Sun, N. Diao, J. Wang, B. Zhang, C. Qin, E. Liang and Y. Mao, *Adv. Funct. Mater.*, 2019, **30**, 1907893.
11 Z. Lv, R. Lou, J. Li, A. K. Singh and H. Song, *IEEE Internet Things J.*, 2021, **8**, 5350–5359.
12 J. Duan, T. Hu, Y. Zhao, B. He and Q. Tang, *Angew. Chem., Int. Ed.*, 2018, **57**, 5746–5749.
13 M. T. Rahman, M. Salauddin, P. Maharjan, M. S. Rasel, H. Cho and J. Y. Park, *Nano Energy*, 2019, **57**, 256–268.
14 Z. Li, X. Jiang, P. Yin, L. Tang, H. Wu, Y. Peng, J. Luo, S. Xie, H. Pu and D. Wang, *Appl. Energy*, 2021, **302**, 117569.
15 G. Miao, S. Fang, S. Wang and S. Zhou, *Appl. Energy*, 2022, **305**, 117838.
16 Y. Peng, L. Zhang, Z. Li, S. Zhong, Y. Liu, S. Xie and J. Luo, *Int. J. Precis. Eng. Manuf.-Green Technol.*, 2022, DOI: **10.1007/s40684-022-00446-8**.
17 Z. Li, Y. Liu, P. Yin, Y. Peng, J. Luo, S. Xie and H. Pu, *Int. J. Mech. Sci.*, 2021, **198**, 106363.
18 J. Wang, D. Yurchenko, G. Hu, L. Zhao, L. Tang and Y. Yang, *Appl. Phys. Lett.*, 2021, **119**, 100502.
19 B. Yan, N. Yu, H. Ma and C. Wu, *Mech. Syst. Signal Process.*, 2022, **167**, 108507.
20 Z. Lin, B. Zhang, H. Zou, Z. Wu, H. Guo, Y. Zhang, J. Yang and Z. L. Wang, *Nano Energy*, 2020, **68**, 104378.
21 K. Fan, M. Cai, F. Wang, L. Tang, J. Liang, Y. Wu, H. Qu and Q. Tan, *Energy Convers. Manage.*, 2019, **198**, 111820.
22 Z. Li, J. Luo, S. Xie, L. Xin, H. Guo, H. Pu, P. Yin, Z. Xu, D. Zhang, Y. Peng, Z. Yang and H. Naguib, *Nano Energy*, 2021, **81**, 105629.
23 L. Q. Machado, D. Yurchenko, J. Wang, G. Clementi, S. Margueron and A. Bartasyte, *iScience*, 2021, **24**, 102749.
24 J. Wang and L. Zhao, *IEEE/ASME Trans. Mechatron.*, 2021, 1–12, DOI: **10.1109/tmech.2021.3121881**.
25 B. Yan, X. Pan, R. Su and C. Wu, *J. Sound Vib.*, 2022, **525**, 116810.
26 A. C. Wang, C. Wu, D. Pisignano, Z. L. Wang and L. Persano, *J. Appl. Polym. Sci.*, 2018, **135**, 45674.
27 F. Ershad, K. Sim, A. Thukral, Y. S. Zhang and C. Yu, *APL Mater.*, 2019, **7**, 031301.
28 K. Dong, X. Peng and Z. L. Wang, *Adv. Mater.*, 2020, **32**, 1902549.
29 F.-R. Fan, Z.-Q. Tian and Z. Lin Wang, *Nano Energy*, 2012, **1**, 328–334.
30 A. Chen, C. Zhang, G. Zhu and Z. L. Wang, *Adv. Sci.*, 2020, **7**, 2000186.
31 I. Aazem, D. T. Mathew, S. Radhakrishnan, K. V. Vijoy, H. John, D. M. Mulvihill and S. C. Pillai, *RSC Adv.*, 2022, **12**, 10545–10572.
32 P. Bai, G. Zhu, Z. H. Lin and Z. L. Wang, *ACS Nano*, 2013, **7**, 3713–3719.
33 W. Tang, C. B. Han, C. Zhang and Z. L. Wang, *Nano Energy*, 2014, **9**, 121–127.
34 Y. Kang, B. Wang, S. Dai, G. Liu, Y. Pu and C. Hu, *ACS Appl. Mater. Interfaces*, 2015, **7**, 20469–20476.
35 A. Chandrasekhar, N. R. Alluri, M. S. P. Sudhakaran, Y. S. Mok and S. J. Kim, *Nanoscale*, 2017, **9**, 9818–9824.
36 G. Q. Gu, C. B. Han, J. J. Tian, C. X. Lu, C. He, T. Jiang, Z. Li and Z. L. Wang, *ACS Appl. Mater. Interfaces*, 2017, **9**, 11882–11888.
37 M.-K. Kim, M.-S. Kim, H.-B. Kwon, S.-E. Jo and Y.-J. Kim, *RSC Adv.*, 2017, **7**, 48368–48373.
38 C. He, W. Zhu, B. Chen, L. Xu, T. Jiang, C. B. Han, G. Q. Gu, D. Li and Z. L. Wang, *ACS Appl. Mater. Interfaces*, 2017, **9**, 26126–26133.
39 A. Chandrasekhar, N. R. Alluri, V. Vivekananthan, J. H. Park and S.-J. Kim, *ACS Sustainable Chem. Eng.*, 2017, **5**, 7310–7316.
40 Z. W. Yang, Y. Pang, L. Zhang, C. Lu, J. Chen, T. Zhou, C. Zhang and Z. L. Wang, *ACS Nano*, 2016, **10**, 10912–10920.
41 P.-K. Yang, L. Lin, F. Yi, X. Li, K. C. Pradel, Y. Zi, C.-I. Wu, J.-H. He, Y. Zhang and Z. L. Wang, *Adv. Mater.*, 2015, **27**, 3817–3824.
42 L. Dhakar, S. Gudla, X. Shan, Z. Wang, F. E. Tay, C. H. Heng and C. Lee, *Sci. Rep.*, 2016, **6**, 22253.
43 M. Salauddin, M. S. Rasel, J. W. Kim and J. Y. Park, *Energy Convers. Manage.*, 2017, **153**, 1–11.
44 A. S. Uddin, U. Yaqoob and G. S. Chung, *ACS Appl. Mater. Interfaces*, 2016, **8**, 30079–30089.

45 P. Bai, G. Zhu, Q. Jing, J. Yang, J. Chen, Y. Su, J. Ma, G. Zhang and Z. L. Wang, *Adv. Funct. Mater.*, 2014, **24**, 5807–5813.
46 T. Q. Trung and N. E. Lee, *Adv. Mater.*, 2016, **28**, 4338–4372.
47 F. Yi, L. Lin, S. Niu, P. K. Yang, Z. Wang, J. Chen, Y. Zhou, Y. Zi, J. Wang, Q. Liao, Y. Zhang and Z. L. Wang, *Adv. Funct. Mater.*, 2015, **25**, 3688–3696.
48 W. Ding, A. C. Wang, C. Wu, H. Guo and Z. L. Wang, *Adv. Mater. Technol.*, 2019, **4**, 1800487.
49 L. Liu, X. Guo and C. Lee, *Nano Energy*, 2021, **88**, 106304.
50 W. He, X. Fu, D. Zhang, Q. Zhang, K. Zhuo, Z. Yuan and R. Ma, *Nano Energy*, 2021, **84**, 105880.
51 W. Wang, A. Yu, J. Zhai and Z. L. Wang, *Adv. Fiber Mater.*, 2021, **3**, 394–412.
52 A. A. Mathew, A. Chandrasekhar and S. Vivekanandan, *Nano Energy*, 2021, **80**, 105566.
53 M. Zhu, Z. Yi, B. Yang and C. Lee, *Nano Today*, 2021, **36**, 101016.
54 K. Venugopal, P. Panchatcharam, A. Chandrasekhar and V. Shanmugasundaram, *ACS Sens.*, 2021, **6**, 1681–1694.
55 X. Pu, S. An, Q. Tang, H. Guo and C. Hu, *iScience*, 2021, **24**, 102027.
56 Z. L. Wang, *Rep. Prog. Phys.*, 2021, **84**, 096502.
57 K. Sayfidinov, S. D. Cezan, B. Baytekin and H. T. Baytekin, *Sci. Adv.*, 2018, **4**, eaau3808.
58 Y. Fu, H. He, Y. Liu, Q. Wang, L. Xing and X. Xue, *J. Mater. Chem. C*, 2017, **5**, 1231–1239.
59 C. Shan, W. Liu, Z. Wang, X. Pu, W. He, Q. Tang, S. Fu, G. Li, L. Long, H. Guo, J. Sun, A. Liu and C. Hu, *Energy Environ. Sci.*, 2021, **14**, 5395–5405.
60 Z. L. Wang, *Mater. Today*, 2017, **20**, 74–82.
61 G. Khandelwal, A. Chandrasekhar, N. P. Maria Joseph Raj and S. J. Kim, *Adv. Energy Mater.*, 2019, **9**, 1803581.
62 R. K. Cheedarala and J. I. Song, *Int. J. Smart Nano Mater.*, 2020, **11**, 38–46.
63 A. C. Wang, B. Zhang, C. Xu, H. Zou, Z. Lin and Z. L. Wang, *Adv. Funct. Mater.*, 2020, **30**, 1909384.
64 J. Wu, X. Wang, J. He, Z. Li and L. Li, *J. Mater. Chem. A*, 2021, **9**, 6583–6590.
65 J. Park, A. Y. Choi, C. J. Lee, D. Kim and Y. T. Kim, *RSC Adv.*, 2017, **7**, 54829–54834.
66 Y. Lin, S. Duan, D. Zhu, Y. Li, B. Wang and J. Wu, *Adv. Intell. Syst.*, 2022, 2100120, DOI: **10.1002/aisy.202100120**.
67 S. Wang, Y. Xie, S. Niu, L. Lin and Z. L. Wang, *Adv. Mater.*, 2014, **26**, 2818–2824.
68 W. Paosangthong, R. Torah and S. Beeby, *J. Phys.: Conf. Ser.*, 2019, **1407**, 012124.
69 J. C. Maxwell, *London, Edinburgh Dublin Philos. Mag. J. Sci.*, 1861, **21**, 338–348.
70 Z. L. Wang, *Mater. Today*, 2022, **52**, 348–363.
71 Z. L. Wang, *arXiv e-prints*, 2022, DOI: **10.48550/arXiv.2202.13768**.
72 Z. L. Wang, *Nano Energy*, 2020, **68**, 104272.
73 J. Wang, S. Li, F. Yi, Y. Zi, J. Lin, X. Wang, Y. Xu and Z. L. Wang, *Nat. Commun.*, 2016, **7**, 12744.
74 Y. Zi, H. Guo, Z. Wen, M. H. Yeh, C. Hu and Z. L. Wang, *ACS Nano*, 2016, **10**, 4797–4805.
75 F. Shen, Z. Li, C. Xin, H. Guo, Y. Peng and K. Li, *ACS Appl. Mater. Interfaces*, 2022, **14**, 3437–3445.
76 J. Wu, Y. Xi and Y. Shi, *Nano Energy*, 2020, **72**, 104659.
77 R. Cao, Y. Xia, J. Wang, X. Jia, C. Jia, S. Zhu, W. Zhang, X. Gao and X. Zhang, *ACS Appl. Mater. Interfaces*, 2021, **13**, 41657–41668.
78 M. B. Khan, D. H. Kim, J. H. Han, H. Saif, H. Lee, Y. Lee, M. Kim, E. Jang, S. K. Hong, D. J. Joe, T.-I. Lee, T.-S. Kim, K. J. Lee and Y. Lee, *Nano Energy*, 2019, **58**, 211–219.
79 C. Xin, Z. Li, Q. Zhang, Y. Peng, H. Guo and S. Xie, *Nano Energy*, 2022, **100**, 107448.
80 S. Zhou and L. Zuo, *Commun. Nonliner Sci. Number Simulat.*, 2018, **61**, 271–284.
81 X. Ma, H. Li, S. Zhou, Z. Yang and G. Litak, *Mech. Syst. Signal Process.*, 2022, **168**, 108612.
82 Y. Peng, Z. Xu, M. Wang, Z. Li, J. Peng, J. Luo, S. Xie, H. Pu and Z. Yang, *Appl. Energy*, 2021, **172**, 551–563.
83 B. Y. Lee, D. H. Kim, J. Park, K. I. Park, K. J. Lee and C. K. Jeong, *Sci. Technol. Adv. Mater.*, 2019, **20**, 758–773.
84 P. Yin, K. C. Aw, X. Jiang, C. Xin, H. Guo, L. Tang, Y. Peng and Z. Li, *Nano Energy*, 2022, 106976.
85 S. M. S. Rana, M. T. Rahman, M. Salauddin, P. Maharjan, T. Bhatta, H. Cho and J. Y. Park, *Nano Energy*, 2020, **76**, 105025.
86 M. Toyabur Rahman, S. M. Sohel Rana, M. Salauddin, P. Maharjan, T. Bhatta, H. Kim, H. Cho and J. Y. Park, *Appl. Energy*, 2020, **279**, 115799.
87 S. Jung, J. Oh, U. J. Yang, S. M. Lee, J. Lee, M. Jeong, Y. Cho, S. Kim, J. M. Baik and C. Yang, *Nano Energy*, 2020, **77**, 105271.
88 H. Li, Y. Zhang, Y. Wu, H. Zhao, W. Wang, X. He and H. Zheng, *Beilstein J. Nanotechnol.*, 2021, **12**, 402–412.
89 S. Zargari, Z. Daie Koozehkanani, H. Veladi, J. Sobhi and A. Rezania, *Energy Convers. Manage.*, 2021, **244**, 114489.
90 Y. Yang, L. Chen, J. He, X. Hou, X. Qiao, J. Xiong and X. Chou, *Adv. Mater. Technol.*, 2021, **7**, 2100702.
91 X. Guan, B. Xu, M. Wu, T. Jing, Y. Yang and Y. Gao, *Nano Energy*, 2021, **80**, 105549.
92 Z. Ren, Q. Zheng, H. Wang, H. Guo, L. Miao, J. Wan, C. Xu, S. Cheng and H. Zhang, *Nano Energy*, 2020, **67**, 104243.
93 J. S. Y. Tan, J. H. Park, J. Li, Y. Dong, K. H. Chan, G. W. Ho and J. Yoo, *IEEE, J. Solid State Circ.*, 2021, **56**, 2913–2923.
94 Y. Yun, S. Jang, S. Cho, S. H. Lee, H. J. Hwang and D. Choi, *Nano Energy*, 2021, **80**, 105525.
95 C. Zhou, Y. Yang, N. Sun, Z. Wen, P. Cheng, X. Xie, H. Shao, Q. Shen, X. Chen, Y. Liu, Z. L. Wang and X. Sun, *Nano Res.*, 2018, **11**, 4313–4322.
96 K. Dong, J. Deng, W. Ding, A. C. Wang, P. Wang, C. Cheng, Y. Wang, L. Jin, B. Gu, B. Sun and Z. L. Wang, *Adv. Energy Mater.*, 2018, **8**, 1801114.
97 H. Chen, Q. Lu, X. Cao, N. Wang and Z. Wang, *Nano Res.*, 2021, **15**, 2505–2511.
98 Y. Kim, X. Wu, C. Lee and J. H. Oh, *ACS Appl. Mater. Interfaces*, 2021, **13**, 36967–36975.
99 Z. You, S. Wang, Z. Li, Y. Zou, T. Lu, F. Wang, B. Hu, X. Wang, L. Li, W. Fang and Y. Liu, *Nano Energy*, 2022, **91**, 106667.

100 Z. Zhang and J. Cai, *Curr. Appl. Phys.*, 2021, **22**, 1–5.
101 Y. Han, Y. Han, X. Zhang, L. Li, C. Zhang, J. Liu, G. Lu, H. D. Yu and W. Huang, *ACS Appl. Mater. Interfaces*, 2020, **12**, 16442–16450.
102 J. Liu, L. Zhang, N. Wang and C. Li, *Nano Energy*, 2020, **78**, 105385.
103 M. Su, J. Brugger and B. Kim, *Int. J. Precis. Eng. Manuf.-Green Technol.*, 2020, **7**, 683–698.
104 J. Zhao, Y. Wang, X. Song, A. Zhou, Y. Ma and X. Wang, *Nanoscale*, 2021, **13**, 18363–18373.
105 Z. Peng, J. Song, Y. Gao, J. Liu, C. Lee, G. Chen, Z. Wang, J. Chen and M. K. H. Leung, *Nano Energy*, 2021, **85**, 106021.
106 N. Zheng, J. Xue, Y. Jie, X. Cao and Z. L. Wang, *Nano Res.*, 2022, **15**, 6213–6219.
107 M. Mariello, E. Scarpa, L. Algieri, F. Guido, V. M. Mastronardi, A. Qualtieri and M. De Vittorio, *Energies*, 2020, **13**, 1625.
108 S. Pyo, M.-O. Kim, D.-S. Kwon, W. Kim, J.-H. Yang, H. S. Cho, J. H. Lee and J. Kim, *Smart Mater. Struct.*, 2020, **29**, 055026.
109 X. Liang, T. Zhao, W. Jiang, X. Yu, Y. Hu, P. Zhu, H. Zheng, R. Sun and C.-P. Wong, *Nano Energy*, 2019, **59**, 508–516.
110 Z. j Li, X. z PENG and G. b Hu, *Energy Convers. Manage.*, 2022, **258**, 115466.
111 A. Atalay, V. Sanchez, O. Atalay, D. M. Vogt, F. Haufe, R. J. Wood and C. J. Walsh, *Adv. Mater. Technol.*, 2017, **2**, 1700136.
112 H. Lee, S. J. Kim, H. Chang and J. Kim, *Mechatronics*, 2018, **52**, 90–101.
113 T. Han, A. Nag, R. Simorangkir, N. Afsarimanesh, H. Liu, S. C. Mukhopadhyay, Y. Xu, M. Zhadobov and R. Sauleau, *Sensors*, 2019, **19**, 3477.
114 Y. Feng, X. Chen, Q. Wu, G. Cao, D. McCoul, B. Huang and J. Zhao, *IEEE Sens. J.*, 2021, **21**, 20943–20950.
115 X. Li, Z. H. Lin, G. Cheng and Z. L. Wang, *ACS Nano*, 2014, **8**, 10674–10681.
116 L. Jin, J. Tao, R. Bao, L. Sun and C. Pan, *Sci. Rep.*, 2017, **7**, 10521.
117 K. Moran, C. Richter, E. Farrell, E. Mitchell, A. Ahmadi and N. E. O'Connor, *Procedia Eng.*, 2015, **112**, 180–183.
118 H. Chander, R. F. Burch, P. Talegaonkar, D. Saucier, T. Luczak, J. E. Ball, A. Turner, S. N. K. Kodithuwakku Arachchige, W. Carroll, B. K. Smith, A. Knight and R. K. Prabhu, *Int. J. Environ. Res. Public Health*, 2020, **17**, 3554.
119 R. Orji and K. Moffatt, *Health Informatics J.*, 2018, **24**, 66–91.
120 W. Qi, P. Markopoulos and B. Yu, *J. Neuroeng. Rehabil.*, 2017, **14**, 20.
121 S. An, A. Sankaran and A. L. Yarin, *ACS Appl. Mater. Interfaces*, 2018, **10**, 37749–37759.
122 L. Valentini, M. Cardinali and J. Kenny, *J. Polym. Sci., Part B: Polym. Phys.*, 2014, **52**, 859–863.
123 M. M. Alam, S. Lee, M. Kim, K. S. Han, V. A. Cao and J. Nah, *Nano Energy*, 2020, **72**, 104672.
124 Y. Liu, K. He, G. Chen, W. R. Leow and X. Chen, *Chem. Rev.*, 2017, **117**, 12893–12941.
125 N. Gogurla, B. Roy, J.-Y. Park and S. Kim, *Nano Energy*, 2019, **62**, 674–681.
126 Y.-C. Lai, J. Deng, S. L. Zhang, S. Niu, H. Guo and Z. L. Wang, *Adv. Funct. Mater.*, 2017, **27**, 1604462.
127 J. Yu, X. Hou, M. Cui, S. Shi, J. He, Y. Sun, C. Wang and X. Chou, *Sci. China Mater.*, 2019, **62**, 1423–1432.
128 J. Wang, S. Qian, J. Yu, Q. Zhang, Z. Yuan, S. Sang, X. Zhou and L. Sun, *Nanomaterials*, 2019, **9**, 1304.
129 Y.-T. Jao, P.-K. Yang, C.-M. Chiu, Y.-J. Lin, S.-W. Chen, D. Choi and Z.-H. Lin, *Nano Energy*, 2018, **50**, 513–520.
130 Q. Ju, H. Li and Y. Zhang, *IEEE Sens. J.*, 2018, **18**, 4336–4345.
131 Y.-E. Shin, J.-E. Lee, Y. Park, S.-H. Hwang, H. G. Chae and H. Ko, *J. Mater. Chem. A*, 2018, **6**, 22879–22888.
132 Z. Wen, Y. Yang, N. Sun, G. Li, Y. Liu, C. Chen, J. Shi, L. Xie, H. Jiang, D. Bao, Q. Zhuo and X. Sun, *Adv. Funct. Mater.*, 2018, **28**, 1803684.
133 F. He, X. You, H. Gong, Y. Yang, T. Bai, W. Wang, W. Guo, X. Liu and M. Ye, *ACS Appl. Mater. Interfaces*, 2020, **12**, 6442–6450.
134 J. Huang, Y. Hao, M. Zhao, H. Qiao, F. Huang, D. Li and Q. Wei, *Composites, Part A*, 2021, **146**, 106412.
135 Y. Yang, T. Jing and B. Xu, *Macromol. Mater. Eng.*, 2020, **305**, 2000276.
136 P. Sun, N. Cai, X. Zhong, X. Zhao, L. Zhang and S. Jiang, *Nano Energy*, 2021, **89**, 106492.
137 C. Chen, L. Chen, Z. Wu, H. Guo, W. Yu, Z. Du and Z. L. Wang, *Mater. Today*, 2020, **32**, 84–93.
138 F. Sheng, J. Yi, S. Shen, R. Cheng, C. Ning, L. Ma, X. Peng, W. Deng, K. Dong and Z. L. Wang, *ACS Appl. Mater. Interfaces*, 2021, **13**, 44868–44877.
139 Z. Ma, W. Wang and D. Yu, *Energy Technol.*, 2020, **8**, 2000164.
140 S. Liu, H. Wang, T. He, S. Dong and C. Lee, *Nano Energy*, 2020, **69**, 104462.
141 Y. Li, N. Yang, L. Li, L. Liu, Y. Yang, Z. Zhang, L. Liu, L. Li and X. Zhang, *Web Intelligence*, 2018, **16**, 123–129.
142 X. Pu, H. Guo, Q. Tang, J. Chen, L. Feng, G. Liu, X. Wang, Y. Xi, C. Hu and Z. L. Wang, *Nano Energy*, 2018, **54**, 453–460.
143 Y. Xue, Z. Ju, K. Xiang, J. Chen and H. Liu, *IEEE Trans. Cogn. Dev. Syst.*, 2019, **11**, 162–175.
144 B. G. Lee and S. M. Lee, *IEEE Sens. J.*, 2018, **18**, 1224–1232.
145 Z. Zhou, K. Chen, X. Li, S. Zhang, Y. Wu, Y. Zhou, K. Meng, C. Sun, Q. He, W. Fan, E. Fan, Z. Lin, X. Tan, W. Deng, J. Yang and J. Chen, *Nat. Electron.*, 2020, **3**, 571–578.
146 C. M. Chiu, S. W. Chen, Y. P. Pao, M. Z. Huang, S. W. Chan and Z. H. Lin, *Sci. Technol. Adv. Mater.*, 2019, **20**, 964–971.
147 J. Zhu, X. Wang, Y. Xing and J. Li, *Nanoscale Res. Lett.*, 2019, **14**, 247.
148 C. Sukumaran, P. Viswanathan, P. Munirathinam and A. Chandrasekhar, *Int. J. Nanotechnol.*, 2021, **18**, 697–704.
149 S. Wang, F. Yuan, S. Liu, J. Zhou, S. Xuan, Y. Wang and X. Gong, *J. Mater. Chem. C*, 2020, **8**, 3715–3723.
150 W. Lu, Y. Xu, Y. Zou, L.-A. Zhang, J. Zhang, W. Wu and G. Song, *Nano Energy*, 2020, **69**, 104430.

151 L. B. Huang, W. Xu, C. Zhao, Y. L. Zhang, K. L. Yung, D. Diao, K. H. Fung and J. Hao, *ACS Appl. Mater. Interfaces*, 2020, **12**, 24030–24038.
152 H.-T. Deng, X.-R. Zhang, Z.-Y. Wang, D.-L. Wen, Y.-Y. Ba, B. Kim, M.-D. Han, H.-X. Zhang and X.-S. Zhang, *Nano Energy*, 2021, **83**, 105823.
153 L. Ren, *Mater. Technol.*, 2021, **3**, 1–6.
154 L. Wang, W. Liu, Z. Yan, F. Wang and X. Wang, *Adv. Funct. Mater.*, 2020, **31**, 2007221.
155 S. Shin, H. U. Yoon and B. Yoo, *Sensors*, 2021, **21**, 3204.
156 D. Zhang, Z. Xu, Z. Yang and X. Song, *Nano Energy*, 2020, **67**, 104251.
157 F. Yuan, S. Liu, J. Zhou, X. Fan, S. Wang and X. Gong, *Smart Mater. Struct.*, 2020, **29**, 125007.
158 K. Dong, X. Peng, J. An, A. C. Wang, J. Luo, B. Sun, J. Wang and Z. L. Wang, *Nat. Commun.*, 2020, **11**, 2868.
159 J. Zhou, S. Wang, F. Yuan, J. Zhang, S. Liu, C. Zhao, Y. Wang and X. Gong, *ACS Appl. Mater. Interfaces*, 2021, **13**, 6575–6584.
160 Y. Mao, Y. Zhu, T. Zhao, C. Jia, X. Wang and Q. Wang, *Energies*, 2021, **14**, 4996.
161 Z. Zhang, T. He, M. Zhu, Z. Sun, Q. Shi, J. Zhu, B. Dong, M. R. Yuce and C. Lee, *npj Flexible Electron.*, 2020, **4**, 12.
162 P. Zhang, Z. Zhang and J. Cai, *Microsyst. Technol.*, 2021, **27**, 3507–3512.
163 L. Liu, Q. Shi and C. Lee, *Nano Res.*, 2021, **14**, 4227–4235.
164 S. Gao, T. He, Z. Zhang, H. Ao, H. Jiang and C. Lee, *Adv. Sci.*, 2021, **8**, e2101834.
165 Q. Zhang, T. Jin, J. Cai, L. Xu, T. He, T. Wang, Y. Tian, L. Li, Y. Peng and C. Lee, *Adv. Sci.*, 2022, **9**, e2103694.
166 H. Zhang, P. Zhang and W. Zhang, *Nano Energy*, 2021, **84**, 105933.
167 J. Wang, Z. Zhao, X. Zeng, X. Liu and Y. Hu, *Sensors*, 2021, **21**, 3634.
168 D. Vera Anaya, T. He, C. Lee and M. R. Yuce, *Nano Energy*, 2020, **72**, 104675.
169 J. Fu, K. Xia and Z. Xu, *Sens. Actuators, A*, 2021, **323**, 112650.
170 S. Zhao, *J. Electron. Mater.*, 2021, **50**, 6836–6843.
171 Q. Zheng, Y. Zou, Y. Zhang, Z. Liu, B. Shi, X. Wang, Y. Jin, H. Ouyang, Z. Li and Z. L. Wang, *Biomed. Eng.*, 2016, **2**, e1501478.
172 J. Li and X. Wang, *APL Mater.*, 2017, **5**, 073801.
173 G. Y. Bae, S. W. Pak, D. Kim, G. Lee, H. Kim do, Y. Chung and K. Cho, *Adv. Mater.*, 2016, **28**, 5300–5306.
174 T. Ohkuma, T. Ninomiya, H. Tomiyama, K. Kario, S. Hoshide, Y. Kita, T. Inoguchi, Y. Maeda, K. Kohara, Y. Tabara, M. Nakamura, T. Ohkubo, H. Watada, M. Munakata, M. Ohishi, N. Ito, M. Nakamura, T. Shoji, C. Vlachopoulos and A. Yamashina, *Hypertension*, 2017, **69**, 1045–1052.
175 M. A. Said, R. N. Eppinga, E. Lipsic, N. Verweij and P. van der Harst, *J. Am. Heart Assoc.*, 2018, **7**, e007621.
176 Y. Ma, J. Choi, A. Hourlier-Fargette, Y. Xue, H. U. Chung, J. Y. Lee, X. Wang, Z. Xie, D. Kang, H. Wang, S. Han, S. K. Kang, Y. Kang, X. Yu, M. J. Slepian, M. S. Raj, J. B. Model, X. Feng, R. Ghaffari, J. A. Rogers and Y. Huang, *Proc. Natl. Acad. Sci. U. S. A.*, 2018, **115**, 11144–11149.
177 C. L. Shen, T. H. Huang, P. C. Hsu, Y. C. Ko, F. L. Chen, W. C. Wang, T. Kao and C. T. Chan, *J. Med. Biol. Eng.*, 2017, **37**, 826–842.
178 Y. Koyama, M. Nishiyama and K. Watanabe, *IEEE Sens. J.*, 2018, **18**, 6175–6180.
179 S. G. C. Chikkaramanna and V. ST, *Biomed. Res.*, 2019, **30**, 538–545.
180 R. Yan, M. Zhou, W. Sun and J. Meng, *Analyzing Wrist Pulse Signals Measured with Polyvinylidene Fluoride Film for Hypertension Identification*, Nanjing, China, 2017.
181 W. Jiang, H. Li, Z. Liu, Z. Li, J. Tian, B. Shi, Z. L. Wang and Z. Li, *Adv. Mater.*, 2018, **30**, 1801895.
182 Y. Zhang, Z. Zhou and T. H. Tao, Presented in part at the 32nd IEEE International Conference on Micro Electro Mechanical Systems (IEEE MEMS), Seoul, SOUTH KOREA, 2019.
183 Q. Zheng, B. Shi, F. Fan, X. Wang, L. Yan, W. Yuan, S. Wang, H. Liu, Z. Li and Z. L. Wang, *Adv. Mater.*, 2014, **26**, 5851–5856.
184 X. Guo, W. Pei, Y. Wang, Y. Chen, H. Zhang, X. Wu, X. Yang, H. Chen, Y. Liu and R. Liu, *Biomed. Signal Process. Control*, 2016, **30**, 98–105.
185 X. Pu, H. Guo, J. Chen, X. Wang, Y. Xi, C. Hu and Z. L. Wang, *Sci. Adv.*, 2017, **3**, e1700694.
186 T. Okano, S. Izumi, T. Katsuura, H. Kawaguchi and M. Yoshimoto, *J. Signal Process. Syst.*, 2018, **91**, 1053–1062.
187 Y. Si, F. Li, K. Duan, Q. Tao, C. Li, Z. Cao, Y. Zhang, B. Biswal, P. Li, D. Yao and P. Xu, *NeuroImage*, 2020, **206**, 116333.
188 Z. Lin, J. Chen, X. Li, Z. Zhou, K. Meng, W. Wei, J. Yang and Z. L. Wang, *ACS Nano*, 2017, **11**, 8830–8837.
189 C. Pang, G. Y. Lee, T. I. Kim, S. M. Kim, H. N. Kim, S. H. Ahn and K. Y. Suh, *Nat. Mater.*, 2012, **11**, 795–801.
190 S. K. Ghosh and D. Mandal, *ACS Sustainable Chem. Eng.*, 2017, **5**, 8836–8843.
191 P. Fayyaz Shahandashti, H. Pourkheyrollah, A. Jahanshahi and H. Ghafoorifard, *Sens. Actuators, A*, 2019, **295**, 678–686.
192 M. Lou, I. Abdalla, M. Zhu, X. Wei, J. Yu, Z. Li and B. Ding, *ACS Appl. Mater. Interfaces*, 2020, **12**, 19965–19973.
193 M. Lou, I. Abdalla, M. Zhu, J. Yu, Z. Li and B. Ding, *ACS Appl. Mater. Interfaces*, 2020, **12**, 1597–1605.
194 P. Maharjan, R. M. Toyabur and J. Y. Park, *Nano Energy*, 2018, **46**, 383–395.
195 M.-F. Lin, J. Xiong, J. Wang, K. Parida and P. S. Lee, *Nano Energy*, 2018, **44**, 248–255.
196 X. Cui, C. Zhang, W. Liu, Y. Zhang, J. Zhang, X. Li, L. Geng and X. Wang, *Sens. Actuators, A*, 2018, **280**, 326–331.
197 J. Park, D. Kim and Y. T. Kim, Presented in part at the 2021 IEEE 21st International Conference on Nanotechnology (NANO), 2021.
198 R. Wang, L. Mu, Y. Bao, H. Lin, T. Ji, Y. Shi, J. Zhu and W. Wu, *Adv. Mater.*, 2020, **32**, e2002878.
199 K. Fu, J. Zhou, H. Wu and Z. Su, *Nano Energy*, 2021, **88**, 106258.

200 W. Zhang, Q. Liu, S. Chao, R. Liu, X. Cui, Y. Sun, H. Ouyang and Z. Li, *ACS Appl. Mater. Interfaces*, 2021, **13**, 42966–42976.
201 K. T. Mills, A. Stefanescu and J. He, *Nat. Rev. Nephrol.*, 2020, **16**, 223–237.
202 K. Meng, J. Chen, X. Li, Y. Wu, W. Fan, Z. Zhou, Q. He, X. Wang, X. Fan, Y. Zhang, J. Yang and Z. L. Wang, *Adv. Funct. Mater.*, 2018, **29**, 1806388.
203 H. Chen, W. Yang, C. Zhang, M. Wu, W. Li, Y. Zou, L. Lv, H. Yu, H. Ke, R. Liu, Y. Xu, J. Wang and Z. Li, *Nano Res.*, 2021, **15**, 2465–2471.
204 K. Bazaka and M. Jacob, *Electronics*, 2012, **2**, 1–34.
205 J. Li and X. Wang, *Acc. Mater. Res.*, 2021, **2**, 739–750.
206 J. C. Miller, D. Skoll and L. A. Saxon, *Curr. Cardiol. Rep.*, 2020, **23**, 1.
207 Q. Zheng, H. Zhang, B. Shi, X. Xue, Z. Liu, Y. Jin, Y. Ma, Y. Zou, X. Wang, Z. An, W. Tang, W. Zhang, F. Yang, Y. Liu, X. Lang, Z. Xu, Z. Li and Z. L. Wang, *ACS Nano*, 2016, **10**, 6510–6518.
208 R. J. Kuang, J. Pirakalathanan, T. Lau, D. Koh, E. Kotschet, B. Ko and K. K. Lau, *J. Med. Imaging Radiat. Oncol.*, 2021, **65**, 896–903.
209 H. Ryu, H. M. Park, M. K. Kim, B. Kim, H. S. Myoung, T. Y. Kim, H. J. Yoon, S. S. Kwak, J. Kim, T. H. Hwang, E. K. Choi and S. W. Kim, *Nat. Commun.*, 2021, **12**, 4374.
210 H. Ouyang, Z. Liu, N. Li, B. Shi, Y. Zou, F. Xie, Y. Ma, Z. Li, H. Li, Q. Zheng, X. Qu, Y. Fan, Z. L. Wang, H. Zhang and Z. Li, *Nat. Commun.*, 2019, **10**, 1821.
211 Z. Liu, Y. Ma, H. Ouyang, B. Shi, N. Li, D. Jiang, F. Xie, D. Qu, Y. Zou, Y. Huang, H. Li, C. Zhao, P. Tan, M. Yu, Y. Fan, H. Zhang, Z. L. Wang and Z. Li, *Adv. Funct. Mater.*, 2019, **29**, 1807560.
212 Y. Ma, Q. Zheng, Y. Liu, B. Shi, X. Xue, W. Ji, Z. Liu, Y. Jin, Y. Zou, Z. An, W. Zhang, X. Wang, W. Jiang, Z. Xu, Z. L. Wang, Z. Li and H. Zhang, *Nano Lett.*, 2016, **16**, 6042–6051.
213 D. Zhao, J. Zhuo, Z. Chen, J. Wu, R. Ma, X. Zhang, Y. Zhang, X. Wang, X. Wei, L. Liu, C. Pan, J. Wang, J. Yang, F. Yi and G. Yang, *Nano Energy*, 2021, **90**, 106580.
214 O. Atalay, W. R. Kennon and E. Demirok, *IEEE Sens. J.*, 2015, **15**, 110–122.
215 C. Massaroni, C. Venanzi, A. P. Silvatti, D. Lo Presti, P. Saccomandi, D. Formica, F. Giurazza, M. A. Caponero and E. Schena, *J. Biophotonics*, 2018, **11**, e201700263.
216 Z. Zhao, C. Yan, Z. Liu, X. Fu, L. M. Peng, Y. Hu and Z. Zheng, *Adv. Mater.*, 2016, **28**, 10267–10274.
217 R. Cao, J. Wang, S. Zhao, W. Yang, Z. Yuan, Y. Yin, X. Du, N.-W. Li, X. Zhang, X. Li, Z. L. Wang and C. Li, *Nano Res.*, 2018, **11**, 3771–3779.
218 X. He, H. Zou, Z. Geng, X. Wang, W. Ding, F. Hu, Y. Zi, C. Xu, S. L. Zhang, H. Yu, M. Xu, W. Zhang, C. Lu and Z. L. Wang, *Adv. Funct. Mater.*, 2018, **28**, 1805540.
219 W. Fan, Q. He, K. Meng, X. Tan, Z. Zhou, G. Zhang, J. Yang and Z. L. Wang, *Sci. Adv.*, 2020, **6**, eaay2840.
220 Y. Khan, A. E. Ostfeld, C. M. Lochner, A. Pierre and A. C. Arias, *Adv. Mater.*, 2016, **28**, 4373–4395.
221 M. Wang, J. Zhang, Y. Tang, J. Li, B. Zhang, E. Liang, Y. Mao and X. Wang, *ACS Nano*, 2018, **12**, 6156–6162.
222 H. Zhang, J. Zhang, Z. Hu, L. Quan, L. Shi, J. Chen, W. Xuan, Z. Zhang, S. Dong and J. Luo, *Nano Energy*, 2019, **59**, 75–83.
223 H.-J. Qiu, W.-Z. Song, X.-X. Wang, J. Zhang, Z. Fan, M. Yu, S. Ramakrishna and Y.-Z. Long, *Nano Energy*, 2019, **58**, 536–542.
224 Y. Su, T. Yang, X. Zhao, Z. Cai, G. Chen, M. Yao, K. Chen, M. Bick, J. Wang, S. Li, G. Xie, H. Tai, X. Du, Y. Jiang and J. Chen, *Nano Energy*, 2020, **74**, 104941.
225 A. Rajabi-Abhari, J. N. Kim, J. Lee, R. Tabassian, M. Mahato, H. J. Youn, H. Lee and I. K. Oh, *ACS Appl. Mater. Interfaces*, 2021, **13**, 219–232.
226 H. He, J. Guo, B. Illés, A. Géczy, B. Istók, V. Hliva, D. Török, J. G. Kovács, I. Harmati and K. Molnár, *Nano Energy*, 2021, **89**, 106418.
227 D. Wang, D. Zhang, J. Guo, Y. Hu, Y. Yang, T. Sun, H. Zhang and X. Liu, *Nano Energy*, 2021, **89**, 106410.
228 H. Li, Y. Sun, Y. Su, R. Li, H. Jiang, Y. Xie, X. Ding, X. Wu and Y. Tang, *Nano Energy*, 2021, **89**, 106423.
229 X. Peng, K. Dong, C. Ning, R. Cheng, J. Yi, Y. Zhang, F. Sheng, Z. Wu and Z. L. Wang, *Adv. Funct. Mater.*, 2021, **31**, 2103559.
230 W. Song, B. Gan, T. Jiang, Y. Zhang, A. Yu, H. Yuan, N. Chen, C. Sun and Z. L. Wang, *ACS Nano*, 2016, **10**, 8097–8103.
231 Z. Zhou, S. Padgett, Z. Cai, G. Conta, Y. Wu, Q. He, S. Zhang, C. Sun, J. Liu, E. Fan, K. Meng, Z. Lin, C. Uy, J. Yang and J. Chen, *Biosens. Bioelectron.*, 2020, **155**, 112064.
232 J. Li, L. Kang, Y. Long, H. Wei, Y. Yu, Y. Wang, C. A. Ferreira, G. Yao, Z. Zhang, C. Carlos, L. German, X. Lan, W. Cai and X. Wang, *ACS Appl. Mater. Interfaces*, 2018, **10**, 42030–42038.
233 J. Cai and Z. Zhang, *Mater. Technol.*, 2021, 1–8, DOI: 10.1080/10667857.2021.1959157.
234 D. Yang, Y. Ni, X. Kong, S. Li, X. Chen, L. Zhang and Z. L. Wang, *ACS Nano*, 2021, **15**, 14653–14661.
235 Y.-W. Cai, X.-N. Zhang, G.-G. Wang, G.-Z. Li, D.-Q. Zhao, N. Sun, F. Li, H.-Y. Zhang, J.-C. Han and Y. Yang, *Nano Energy*, 2021, **81**, 105663.
236 S. Lee, H. Wang, W. Y. Xian Peh, T. He, S.-C. Yen, N. V. Thakor and C. Lee, *Nano Energy*, 2019, **60**, 449–456.
237 R. Shi, J. Zhang, J. Tian, C. Zhao, Z. Li, Y. Zhang, Y. Li, C. Wu, W. Tian and Z. Li, *Nano Energy*, 2020, **77**, 105201.
238 I. Shlomy, S. Divald, K. Tadmor, Y. Leichtmann-Bardoogo, A. Arami and B. M. Maoz, *ACS Nano*, 2021, **15**, 11087–11098.
239 G. Conta, A. Libanori, T. Tat, G. Chen and J. Chen, *Adv. Mater.*, 2021, **33**, e2007502.
240 C. M. Apovian, S. N. Shah, B. M. Wolfe, S. Ikramuddin, C. J. Miller, K. S. Tweden, C. J. Billington and S. A. Shikora, *Obes. Surg.*, 2017, **27**, 169–176.
241 F. Arab Hassani, R. P. Mogan, G. G. L. Gammad, H. Wang, S. C. Yen, N. V. Thakor and C. Lee, *ACS Nano*, 2018, **12**, 3487–3501.
242 G. Yao, L. Kang, J. Li, Y. Long, H. Wei, C. A. Ferreira, J. J. Jeffery, Y. Lin, W. Cai and X. Wang, *Nat. Commun.*, 2018, **9**, 5349.

243 J. Wang, H. Wang, T. He, B. He, N. V. Thakor and C. Lee, *Adv. Sci.*, 2019, **6**, 1900149.
244 X. Wang, Y. Zhang, X. Zhang, Z. Huo, X. Li, M. Que, Z. Peng, H. Wang and C. Pan, *Adv. Mater.*, 2018, **30**, e1706738.
245 T. Chen, M. Zhao, Q. Shi, Z. Yang, H. Liu, L. Sun, J. Ouyang and C. Lee, *Nano Energy*, 2018, **51**, 162–172.
246 X. Yu, Z. Xie, Y. Yu, J. Lee, A. Vazquez-Guardado, H. Luan, J. Ruban, X. Ning, A. Akhtar, D. Li, B. Ji, Y. Liu, R. Sun, J. Cao, Q. Huo, Y. Zhong, C. Lee, S. Kim, P. Gutruf, C. Zhang, Y. Xue, Q. Guo, A. Chempakasseril, P. Tian, W. Lu, J. Jeong, Y. Yu, J. Cornman, C. Tan, B. Kim, K. Lee, X. Feng, Y. Huang and J. A. Rogers, *Nature*, 2019, **575**, 473–479.
247 B. Mallika, H. Y. Y. Nyein and A. Javey, *Nat. Electron.*, 2018, **1**, 160–171.
248 C. M. Boutry, L. Beker, Y. Kaizawa, C. Vassos, H. Tran, A. C. Hinckley, R. Pfattner, S. Niu, J. Li, J. Claverie, Z. Wang, J. Chang, P. M. Fox and Z. Bao, *Nat. Biomed. Eng.*, 2019, **3**, 47–57.
249 L. Li, F. Xie, T. Wang, G. Wang, Y. Tian, T. Jin and Q. Zhang, *Soft Robot.*, 2022, DOI: **10.1089/soro.2021.0025**.
250 M. Han, H. Wang, Y. Yang, C. Liang, W. Bai, Z. Yan, H. Li, Y. Xue, X. Wang, B. Akar, H. Zhao, H. Luan, J. Lim, I. Kandela, G. A. Ameer, Y. Zhang, Y. Huang and J. A. Rogers, *Nat. Electron.*, 2019, **2**, 26–35.
251 V. C. Ferreira, C. Albuquerque and D. C. Muchaluat-Saade, *IEEE Sens. J.*, 2022, **22**, 10009–10017.
252 K. Sim, Z. Rao, Z. Zou, F. Ershad, J. Lei, A. Thukral, J. Chen, Q.-A. Huang, J. Xiao and C. Yu, *Sci. Adv.*, 2019, **5**, eaav9653.
253 Y. Luo, Z. Wang, J. Wang, X. Xiao, Q. Li, W. Ding and H. Y. Fu, *Nano Energy*, 2021, **89**, 106330.
254 Z. Sun, M. Zhu, Z. Chen, X. Shan and C. Lee, Presented in part at the 2021 21st International Conference on Solid-State Sensors, Actuators and Microsystems (Transducers), Orlando, FL, USA, 2021.
255 T. He, Z. Sun, Q. Shi, M. Zhu, D. V. Anaya, M. Xu, T. Chen, M. R. Yuce, A. V.-Y. Thean and C. Lee, *Nano Energy*, 2019, **58**, 641–651.
256 L. Xie, X. Chen, Z. Wen, Y. Yang, J. Shi, C. Chen, M. Peng, Y. Liu and X. Sun, *Nanomicro Lett.*, 2019, **11**, 39.
257 Z. Zhao, Q. Huang, C. Yan, Y. Liu, X. Zeng, X. Wei, Y. Hu and Z. Zheng, *Nano Energy*, 2020, **70**, 104528.
258 M. Gao, H. Wu, R. Plamthottam, Z. Xie, Y. Liu, J. Hu, S. Wu, L. Wu, X. He and Q. Pei, *Matter*, 2021, **4**, 1962–1974.
259 L. Shan, Y. Liu, X. Zhang, E. Li, R. Yu, Q. Lian, X. Chen, H. Chen and T. Guo, *Nano Energy*, 2021, **88**, 106283.
260 F. R. Fan, L. Lin, G. Zhu, W. Wu, R. Zhang and Z. L. Wang, *Nano Lett.*, 2012, **12**, 3109–3114.
261 Y. Yang, H. Zhang, Z.-H. Lin, Y. S. Zhou, Q. Jing, Y. Su, J. Yang, J. Chen, C. Hu and Z. L. Wang, *ACS Nano*, 2013, **7**, 9213–9222.
262 L. Lin, Y. Xie, S. Wang, W. Wu, S. Niu, X. Wen and Z. L. Wang, *ACS Nano*, 2013, **7**, 8266–8274.
263 G. Zhu, W. Q. Yang, T. Zhang, Q. Jing, J. Chen, Y. S. Zhou, P. Bai and Z. L. Wang, *Nano Lett.*, 2014, **14**, 3208–3213.
264 A. Ahmed, S. L. Zhang, I. Hassan, Z. Saadatnia, Y. Zi, J. Zu and Z. L. Wang, *Extreme Mech. Lett.*, 2017, **13**, 25–35.
265 S. W. Chen, X. Cao, N. Wang, L. Ma, H. R. Zhu, M. Willander, Y. Jie and Z. L. Wang, *Adv. Energy Mater.*, 2017, **7**, 1601255.
266 Y. Pang, J. Li, T. Zhou, Z. Yang, J. Luo, L. Zhang, G. Dong, C. Zhang and Z. L. Wang, *Nano Energy*, 2017, **31**, 533–540.
267 X. Pu, M. Liu, X. Chen, J. Sun, C. Du, Y. Zhang, J. Zhai, W. Hu and Z. L. Wang, *Sci. Adv.*, 2017, **3**, e1700015.
268 M. Shi, J. Zhang, H. Chen, M. Han, S. A. Shankaregowda, Z. Su, B. Meng, X. Cheng and H. Zhang, *ACS Nano*, 2016, **10**, 4083–4091.
269 T. Li, J. Zou, F. Xing, M. Zhang, X. Cao, N. Wang and Z. L. Wang, *ACS Nano*, 2017, **11**, 3950–3956.
270 T. Chen, Q. Shi, K. Li, Z. Yang, H. Liu, L. Sun, J. A. Dziuban and C. Lee, *Nanomaterials*, 2018, **8**, 613.
271 J. Chen, G. Zhu, J. Yang, Q. Jing, P. Bai, W. Yang, X. Qi, Y. Su and Z. L. Wang, *ACS Nano*, 2015, **9**, 105–116.
272 W. Yin, Y. Xie, J. Long, P. Zhao, J. Chen, J. Luo, X. Wang and S. Dong, *Nano Energy*, 2018, **50**, 16–24.
273 K. Xia and Z. Xu, *Sens. Actuators, A*, 2021, **331**, 112710.
274 Q. He, Y. Wu, Z. Feng, C. Sun, W. Fan, Z. Zhou, K. Meng, E. Fan and J. Yang, *Nano Energy*, 2019, **59**, 689–696.
275 K. Xia, D. Wu, J. Fu, N. A. Hoque, Y. Ye and Z. Xu, *Nano Energy*, 2020, **78**, 105263.
276 J. Yi, K. Dong, S. Shen, Y. Jiang, X. Peng, C. Ye and Z. L. Wang, *Nanomicro Lett.*, 2021, **13**, 103.
277 S. M. S. Rana, M. T. Rahman, M. Salauddin, S. Sharma, P. Maharjan, T. Bhatta, H. Cho, C. Park and J. Y. Park, *ACS Appl. Mater. Interfaces*, 2021, **13**, 4955–4967.
278 J. Huang, X. Yang, J. Yu, J. Han, C. Jia, M. Ding, J. Sun, X. Cao, Q. Sun and Z. L. Wang, *Nano Energy*, 2020, **69**, 104419.
279 Y. Jiang, K. Dong, X. Li, J. An, D. Wu, X. Peng, J. Yi, C. Ning, R. Cheng, P. Yu and Z. L. Wang, *Adv. Funct. Mater.*, 2020, **31**, 2005584.
280 M. Wu, Z. Gao, K. Yao, S. Hou, Y. Liu, D. Li, J. He, X. Huang, E. Song, J. Yu and X. Yu, *Mater. Today Energy*, 2021, **20**, 100657.
281 J. Wang, J. He, L. Ma, Y. Yao, X. Zhu, L. Peng, X. Liu, K. Li and M. Qu, *Chem. Eng. J.*, 2021, **423**, 130200.
282 J. Zhang, S. Hu, Z. Shi, Y. Wang, Y. Lei, J. Han, Y. Xiong, J. Sun, L. Zheng, Q. Sun, G. Yang and Z. L. Wang, *Nano Energy*, 2021, **89**, 106354.
283 Q. Shi, Z. Zhang, T. Chen and C. Lee, *Nano Energy*, 2019, **62**, 355–366.
284 Y. Liu, W. Yang, Y. Yan, X. Wu, X. Wang, Y. Zhou, Y. Hu, H. Chen and T. Guo, *Nano Energy*, 2020, **75**, 104930.
285 C. Qiu, F. Wu, Q. Shi, C. Lee and M. R. Yuce, *IEEE Access*, 2019, **7**, 92745–92757.
286 Q. Shi, C. Qiu, T. He, F. Wu, M. Zhu, J. A. Dziuban, R. Walczak, M. R. Yuce and C. Lee, *Nano Energy*, 2019, **60**, 545–556.
287 X. Zhao, Z. Zhang, L. Xu, F. Gao, B. Zhao, T. Ouyang, Z. Kang, Q. Liao and Y. Zhang, *Nano Energy*, 2021, **85**, 106001.

288 Y. Shi, F. Wang, J. Tian, S. Li, E. Fu, J. Nie, R. Lei, Y. Ding, X. Chen and Z. L. Wang, *Sci. Adv.*, 2021, **7**, eabe2943.
289 Y. Yu, J. Nassar, C. Xu, J. Min, Y. Yang, A. Dai, R. Doshi, A. Huang, Y. Song, R. Gehlhar, A. D. Ames and W. Gao, *Sci. Robot.*, 2020, **5**, eaaz7946.
290 C. Qiu, F. Wu, C. Lee and M. R. Yuce, *Nano Energy*, 2020, **70**, 104456.
291 J. Yun, N. Jayababu and D. Kim, *Nano Energy*, 2020, **78**, 105325.
292 J. Sun, Y. Chang, L. Dong, K. Zhang, Q. Hua, J. Zang, Q. Chen, Y. Shang, C. Pan and C. Shan, *Nano Energy*, 2021, **86**, 106077.
293 B. Wang, X. Wei, J. Chen, Z. Yuan, Y. Shi, Z. Wu and Z. L. Wang, *IEEE Open J. Nanotechnol.*, 2021, **2**, 78–85.
294 Y.-Y. Ba, J.-F. Bao, Z.-Y. Wang, H.-T. Deng, D.-L. Wen, X.-R. Zhang, C. Tu and X.-S. Zhang, *Nano Energy*, 2021, **82**, 105730.
295 H. Zhou, D. Li, X. He, X. Hui, H. Guo, C. Hu, X. Mu and Z. L. Wang, *Adv. Sci.*, 2021, **8**, e2101020.
296 L. Liu, Q. Shi, Z. Sun and C. Lee, *Nano Energy*, 2021, **86**, 106154.
297 H. Guo, X. Pu, J. Chen, Y. Meng, M.-H. Yeh, G. Liu, Q. Tang, B. Chen, D. Liu, S. Qi, C. Wu, C. Hu, J. Wang and Z. L. Wang, *Sci. Robot.*, 2018, **3**, eaat2516.
298 H. Liu, W. Dong, Y. Li, F. Li, J. Geng, M. Zhu, T. Chen, H. Zhang, L. Sun and C. Lee, *Microsyst. Nanoeng.*, 2020, **6**, 16.
299 X. Ji, T. Zhao, X. Zhao, X. Lu and T. Li, *Adv. Mater. Technol.*, 2020, **5**, 1900921.
300 Y. Zou, P. Tan, B. Shi, H. Ouyang, D. Jiang, Z. Liu, H. Li, M. Yu, C. Wang, X. Qu, L. Zhao, Y. Fan, Z. L. Wang and Z. Li, *Nat. Commun.*, 2019, **10**, 2695.
301 J. Chen, W. Xuan, P. Zhao, U. Farooq, P. Ding, W. Yin, H. Jin, X. Wang, Y. Fu, S. Dong and J. Luo, *Nano Energy*, 2018, **51**, 1–9.
302 B. Abidi, A. Jilbab and E. H. Mohamed, *J. Med. Eng. Technol.*, 2019, **43**, 124–132.
303 X. Tian, P. M. Lee, Y. J. Tan, T. L. Y. Wu, H. Yao, M. Zhang, Z. Li, K. A. Ng, B. C. K. Tee and J. S. Ho, *Nat. Electron.*, 2019, **2**, 243–251.
304 Y. Liu, W. Liu, Z. Wang, W. He, Q. Tang, Y. Xi, X. Wang, H. Guo and C. Hu, *Nat. Commun.*, 2020, **11**, 1599.
305 P. Zhang, W. Zhang, L. Deng and H. Zhang, *Nano Energy*, 2021, **87**, 106176.
306 F. Shen, D. Zhang, Q. Zhang, Z. Li, H. Guo, Y. Gong and Y. Peng, *Nano Energy*, 2022, **99**, 107431.
307 K. Wang, J. Li, J. Li, C. Wu, S. Yi, Y. Liu and J. Luo, *Nano Energy*, 2021, **87**, 106198.
308 H. S. Kim, D. Y. Kim, J. E. Kim, J. H. Kim, D. S. Kong, G. Murillo, G. H. Lee, J. Y. Park and J. H. Jung, *Adv. Funct. Mater.*, 2019, **29**, 1905816.
309 G. Chen, Y. Li, M. Bick and J. Chen, *Chem. Rev.*, 2020, **120**, 3668–3720.
310 Q. Zhang, L. Li, T. Wang, Y. Jiang, Y. Tian, T. Jin, T. Yue and C. Lee, *Nano Energy*, 2021, **90**, 106501.
311 G. Manogaran, P. M. Shakeel, H. Fouad, Y. Nam, S. Baskar, N. Chilamkurti and R. Sundarasekar, *Sensors*, 2019, **19**, 3030.
312 M. Kachuee, M. M. Kiani, H. Mohammadzade and M. Shabany, *IEEE Trans. Biomed. Eng.*, 2017, **64**, 859–869.

